PhD degree in Molecular Medicine

European School of Molecular Medicine (SEMM),

University of Milan and University of Naples "Federico II"

Faculty of Medicine

Settore disciplinare: MED/04

FUNCTIONAL CHARACTERISATION OF THE ADAPTOR PROTEIN SHCD/RALP

Margherita Yayoi Turco

IFOM-IEO Campus, Milan

Matricola n. R07391

Supervisor: Dr. Luisa Lanfrancone

IFOM-IEO Campus, Milan

Added co-Supervisor: Dr. Giuseppe Testa

IFOM-IEO Campus, Milan

Anno accademico 2009-2010

Abstract

Development requires the strict coordination of signalling pathways driving proliferation, differentiation and migration. Adaptor proteins play an important role in the regulation of specific signalling pathways by linking activated cell-surface receptors to their downstream intracellular targets and mediating crosstalk mechanisms between pathways. ShcD/RaLP, the latest identified member of the Shc family of adaptor proteins showed a unique expression pattern from the other members of the family. It is expressed early during embryogenesis in the pluripotent epiblast and is re-expressed in the developing central and peripheral nervous system and its expression is confined to the brain in the adult. In the pathological context, RaLP is expressed in melanomas and its expression level correlates with disease progression. The physiological role of this protein is still largely uncharacterised. The aim of this PhD project was to characterise the function of RaLP and to understand how this family of adaptor proteins have evolved to modulate distinct signal transduction within different cell types. This could also provide insight on how its deregulation could contribute to pathogenesis.

RaLP knockout (KO) and heterozygote (HT) embryonic stem cells (ESCs) were used as the *in vitro* model system to dissect the role and signalling pathway of RaLP in development. We found that RaLP expression was recapitulated *in vitro* as *in vivo* as it was tightly regulated during the formation of the epiblast in several differentiation programs and then re-expressed when neuronal commitment initiated. Using the recent protocol that allows the transition of pluripotent ESCs to another pluripotent stem cell type, epiblast stem cells (EpiSCs), we specifically investigated the role of RaLP in the establishment of this cell identity. We found that the genetic deletion of RaLP resulted in an impairment of the establishment and maintenance of EpiSCs due to defective proliferation capacity upon differentiation. Furthermore, we have also described for the first time, the emergence of

Cdx2 expressing cells during ESC commitment to EpiSC fate and we observed that the absence of RaLP results in an enrichment of this population and enhanced levels of MAPK/Erk1/2 activation. Our data suggests that RaLP plays an important role in the switch of key pathway/s involved in determining EpiSC identity and that the absence of RaLP perturbs the commitment process.

RaLP is also implicated in the differentiation of neural stem cells to neuronal fate. As RaLP is highly expressed in the brain, we sought to understand whether it plays a role in this commitment process. We found that the RaLP KO NSCs showed severe defects in neuronal formation and we are currently analysing our RaLP KO mouse model to obtain a further understanding of the physiological role of RaLP.

In summary, our studies showed that RaLP is involved in EpiSC formation and maintenance as well as neurogenesis, and this dual role is unique for this member of the Shc family, providing an interesting insight into the mechanisms that the cell has evolved to regulate signalling pathways through adaptor proteins in a cell specific manner.

Table of Contents

Introduction

1. Signalling through adaptor proteins

Cells are continuously subjected to multiple stimuli from both external and internal environments. They must integrate a wide range of input and generate an appropriate response that can vary from proliferation to cell-cycle arrest and differentiation. During evolution, several mechanisms that confer specificity, timing and the directionality of signal transduction as well as the cross-talk between them have developed, and the class of adaptor or scaffolding proteins represents one of them. Adaptor proteins operate downstream to many receptors of the cell surface and in response to their activation, couple the receptors to their intracellular targets, amplify and propagate the signal [1]. This mechanism allows the organisation of the plethora of protein kinases and protein phosphatases that have relatively broad substrate specificity into specific signalling pathways in a controlled and efficient manner. Therefore adaptor proteins through their selective protein-protein interactions play a crucial role in organising the processes within the cell in a spatial and temporal manner.

The identification and emergence of the class of adaptor proteins closely followed the first studies on protein structures by Michael G. Rossman that identified the presence of structural domains and associated these domains to the protein function [2]. This study gave way to the idea that protein domains could be defined based on the comparison with homologous sequences in other proteins, their structure, their spatial separation within the protein, their function and their active center. This idea then was succeeded by Pawson and colleagues who performed bioinformatic screening for domains present within a protein through amino acid sequence comparison. In this way, one of the now most characterised protein-protein interaction domain, the src-homology 2 (SH2) domain, was identified

within the amino terminus of the Src non-receptor tyrosine kinase [3,4]. The presence of this domain was then characterised in many other proteins and not long afterward, a large number of other types of conserved non-catalytic modules was identified, such as the src-homology 3 (SH3) domain [1], pleckstrin homology (PH) domain [5] and phosphotyrosine binding domain (PTB) [6], developing the idea of common protein binding modules used in different combinations within signalling transducers. It was found that the combination, arrangement and number of these domains contained within the protein determine its specific biological function. Biochemical analysis of different types of adaptor proteins containing these protein binding modules demonstrated that these domains are important for their function and evidenced the crucial role of this class of proteins in signal transduction.

The modular interaction domains that constitute adaptor proteins define their function by selectively recognising and binding to specific regions of their target proteins, thereby mediating the formation of signalling complexes. The formation of these multiprotein complexes plays an important role in regulating the transduction of specific pathways in two manners: (i) increasing the efficiency by bringing in proximity the components of a signalling pathway or (ii) disrupting or inhibiting a pathway by sequestering activation elements so that they cannot propagate the signal. Furthermore, adaptor proteins are not simply coupling devices that bring together the components of signalling pathways. This system is highly dynamic, as many of the regions that are recognised by the modules contain amino acids that are subjected to a diverse set of post-translational modifications (PTMs). Currently the list of protein modifications has risen to well over 200, such as phosphorylation, ubiquitination, acetylation and methylation. These PTMs reflect the cellular state, as the cell responds to its environment by activating and silencing specific pathways by placing reversible covalent modification on specific residues or by modifying chemical groups on existing molecules. Therefore, as the adaptor proteins can recognise

and mediate signalling pathways according to the PTM of effector proteins, the current view is that the cell uses modular protein-interaction domains as a device to decode the state of its protein and lipid modifications, thereby coupling PTMs to cellular organization [7].

2. The Shc family of adaptor proteins

2.1. Gene ontology

The Shc (Src homologue and collagen homologue) family of adaptor proteins is a crucial linker of receptors such as the tyrosine kinase receptors, cytokine receptors, G-protein coupled receptors and integrins, to their downstream effectors. The Shc family members are involved in several important cellular processes, such as the regulation of proliferation, survival and differentiation. ShcA (formally Shc) was the first member of the family to be identified, and was discovered in 1992 by a low-stringency hybridisation to human cDNA libraries using an SH2-coding sequence as a probe [8]. The transcript that was isolated possessed two in-frame ATGs and encoded two polypeptides: the p52Shc and p46Shc [8]. Then a few years later, a third isoform was characterised, the p66Shc [9]. Subsequently, two other members of the family, ShcB (Sli/SCK) and ShcC (Rai/N-Shc) were identified [10] and *in silico* reconstruction of the genomic organization of the Shc locus across species showed that despite considerable differences in length, they possessed an almost identical exonic organization for the human, the mouse, the *Fugu rupripes* and the single Shc in *Drosophila melanogaster* and *Caenorhabiditis elegans* [11]. This suggested the existence of a common ancestor and that the Shc gene expanded during evolution between insects and mammals. Furthermore, it suggests for a conserved role for the Shc proteins across species. Recently, a fourth member of the family the ShcD/RaLP (for *Rai Like*

Protein) was identified by our laboratory using the TBLASSTn analysis of the human and mouse genome with ShcA, ShcB and ShcC [12].

A feature of this family of adaptors, is the encoding of several isoforms for each member due to alternative intiation codon usage and splicing patterns. As mentioned earlier, the Shc gene encodes three isoforms, two proteins of 46 and 52 kDa that are translated from two different intiation sites [8], while the third isoform of 66 kDa is a spliced variant [13] resulting in an extended region at the amino-terminal portion of the protein. There are two ShcB isoforms, 52 kDa and 47 kDa, as well as two ShcC isoforms of 52 kDa and 64 kDa. These isoforms are encoded by the same transcript for each gene with alternative usage of in-frame ATGs [14].

2.2. Biochemical characteristics

The Shc proteins identified in mammals all share a conserved, modular organisation (Figure 1) [10]. They possess two independent protein binding domains: the PTB at the amino-terminal and the carboxy-terminal SH2 domain. The PTB domain was first described in Shc and it binds to specific pTyr-containing motifs on activated receptor tyrosine kinases [6]. The PTB based binding to its target is influenced by residues N-terminal to the pTyr and the consensus sequence on its target proteins recognised by this domain is Asn-Pro-X-Tyr motif (X is any amino acid) [15]. However, recent studies have shown that the majority of PTB domains can also recognise non-phosphorylated peptide ligands or phosphoinositides [16], suggesting also the possibility that the proteins can anchor to the membrane through this domain. The SH2 domain represents one of the largest classes of pTyr-recognition domains and in contrast to the PTB, its binding requirements are less stringent. It recognises short phospho-peptide motifs composed of pTyr followed by three to five carboxy-terminal residues [17]. These two domains are linked by a central stretch of amino acids that is glycine and proline rich, the Collagen

homology 1 (CH1) region that contains important tyrosine consensus sequences that are phosphorylated upon its engagement by an activated receptor. Sequence alignment revealed the conservation of the tyrosine residues 239 and 240 also in the *Drosophila*, suggesting a crucial and conserved role for the CH1 domain in signalling [18]. These phosphorylated tyrosine residues on Shc then in turn become target for downstream signalling molecules that bind and propagates the signal, such the Growth factor receptor bound protein 2 (Grb2) adaptor through the binding to these residues by its SH2 region. The CH1 region also contains an adaptin-binding motif, which has been shown to interact with adaptins, proteins involved in the formation of clathrin-coated pits [19]. An additional stretch of amino acids similar to the CH1, the Collagen homology 2 (CH2), is positioned in the amino-terminal portion of the protein. The long isoforms of the ShcA, ShcB, ShcC and RaLP contain the CH2 and this region can mediate interaction with proteins containing SH3 domains as well as serving as a substrate for serine kinases, as it contains important regulatory serine residues. The CH2-PTB-CH1-SH2 modularity together with the sequence of these domains, is a unique feature of this protein family [11].

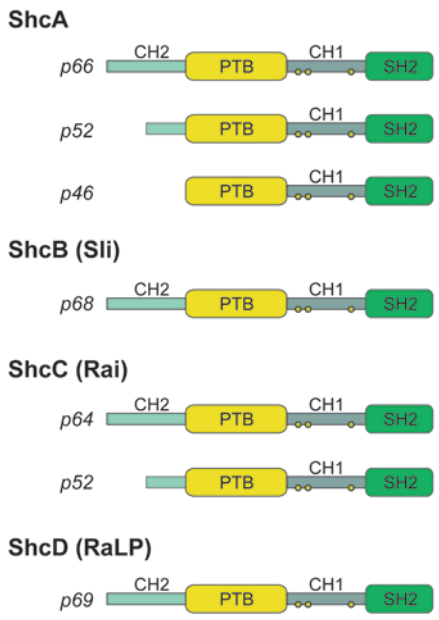

Figure 1. The Shc family members and their modular organisation. Shc proteins contain an SH2 protein binding domain at their C-terminus, a central proline and glycine rich region CH1 and the PTB domain at the N-terminus. The CH1 region contains three conserved tyrosine residues that are phosphorylated upon their

recruitment to signalling pathways (indicated as yellow dots). The longer isoforms contain an extra CH2 region at their N-terminus.

2.3. Expression pattern of the Shc members

The Shc family members have distinct expression patterns, reflecting their specific functions. The p52ShcA and p46ShcA isoforms are expressed at the same levels, ubiquitously during development and also in the adult, where it is expressed in the majority of the tissues except for the brain where its mRNA remains present only in the proliferative areas of the ventricular zone, the region of adult neurogenesis [8,20]. The expression of the third isoform on the other hand, p66ShcA, is restricted to certain tissues and cell lines, being mainly found in epithelial cells, in most haematopoietic cell lines and in peripheral blood lymphocytes [8].

ShcB is expressed throughout the developing embryo at the level of the developing central nervous system (CNS) and the peripheral ganglia such as the dorsal root ganglia and superior cervical ganglion [21]. ShcC on the other hand, is expressed at very low levels during development and is then strongly upregulated within the CNS around the time of birth [21]. And in the adult mouse, unlike ShcA, both ShcB and ShcC expression become confined to the nervous system in post-mitotic and mature neurons [20,21]. Analysis of ShcA and ShcC in the brain revealed that there is a transition of the levels of these two members during the proliferation and differentiation of neural stem cells (NSCs)/neuroblasts to neurons. As the NSCs cease to proliferate and terminally differentiate to post-mitotic neurons, ShcA is downregulated and is replaced by ShcC. This suggests that one possible mechanism that the cells have adopted to regulate pathways, is the differential expression of proteins so that their variation in the availability influences the response of the cell to the same external stimuli [20].

Detailed characterisation of RaLP expression was part of this study and will be discussed in the results (see results section 1). It is expressed in the epiblast of the preimplantation

and peri-implantation embryo, in the developing CNS and peripheral nervous sytem, the adult brain and in the skeletal muscle [22].

2.4. Signalling via the Shc proteins

Despite their high homology in structure, the different family members are implicated in distinct signalling pathways that lead to a variety of cellular events. The most characterised role of p52 and p46 isoforms of ShcA is its implication in mitogenic and motogenic signalling through the Ras activation downstream to several tyrosine as well as non tyrosine kinase receptors. ShcA phosphorylation can be induced by a plethora of stimuli, such as epidermal growth factor (EGF) [8] platelet-derived growth factor (PDGF) [23], hepatocyte growth factor (HGF) [24], insulin growth factor (IGF) [25], fibroblast growth factor (FGF) [26], nerve growth factor (NGF) [27], transforming growth factor β (TGF-β) [28], as well as interleukins [29] and integrins [30]. ShcA is phosphorylated on its tyrosine residues of the CH1 region by the activated tyrosine kinase receptor and this leads to the formation of a complex with Grb2, which in turn through its SH3 domain binds to the Ras guanine nucleotide exchange factor, Sos1. ShcA is still associated to the receptor and so the Shc-Grb2-Sos complex is localised to the membrane in this way, ultimately leading to mitogen activated protein kinase (MAPK) and phosphatidyl inositol 3' kinase (PI3K) activation (Figure 2). A similar mechanism of MAPK activation was seen upon the activation of several other types of receptors such as integrins and G-protein coupled receptor. Interestingly, the p66ShcA isoform is implicated in a completely different pathway. It mediates stress induced response of the cell through the regulation of reactive oxygen species metabolism and apoptosis as well as exerting a negative effect on MAPK activation [13]. This particular role of the p66 isoform is mediated through its amino-terminal CH2 region in which the serine residue is phosphorylated upon environmental stresses such as ultraviolet light or reactive oxygen species (ROS) [9]. In this way,

p66ShcA mediates p53 dependent apoptotic responses through its production of ROS, the regulation of mitochondrial permeability and hence Cytochrome C release [31,32].

ShcC isoforms are specific substrates of the c-RET receptor, a tyrosine kinase receptor for the glial cell line derived neurotrophic factor family, as well as the EGF receptor and Trk receptors, in a similar fashion to ShcA [14]. They are implicated in the signalling via the PI3K activation that plays an important role in sustaining neuronal cell survival [33]. Notably, ShcC can be activated and propagate the signal to PI3K directly after hypoxia or oxidation insults, even in the absence of growth factors [34], suggesting an interesting mechanism of the recruitment of these adaptors not only upon growth factor stimulation. The signalling pathway in which ShcB is implicated in is still unknown, although to some extent, genetic studies that will be discussed further on, seem to suggest they have overlapping functions.

The signalling pathway/s in which RaLP is implicated are still largely unknown. So far, it was seen to associate to the muscle-specific kinase (MuSK) receptor at the neuromuscular junction, primarily through its PTB domain [22]. This interaction could contribute to the early Src-dependent phase of agrin-induced MuSK signalling which is important for the regulation of the stability of Acetylecholine receptor (AChR) clusters. The biological relevance of this finding remains to be understood. In the human system, RaLP was reported to be expressed in melanocytes and it mediates MAPK through association with Grb2 [12].

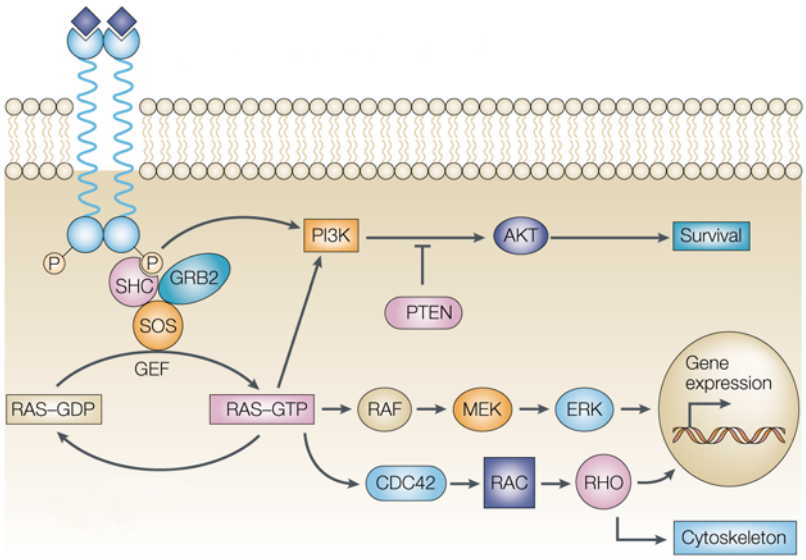

Figure 2. Signalling pathways mediated by growth factor receptor tyrosine kinase and Shc adaptor proteins. Upon growth factor binding to the receptor, the receptor dimerizes and undergoes autophosphorylation on its intracellular portion. The Shc family of adaptor proteins are recruited to the now phosphorylated tyrosine residues on the receptor, which are recognised by its protein binding domain. This results in the activation of various downstream effectors such as MAPK/Erk1/2 and PI3K/Akt signalling which then leads to the regulation of the expression of its target genes, leading to different outcomes such as the promotion of survival and cytoskeleton regulation. Adapted from [35].

One of the most interesting aspects of the Shc adaptor family is its versatility in signalling. Despite their similarity in structure, they are involved in a broad range of signalling pathways and furthermore, they are tyrosine phosphorylated and recruited upon the activation of many types of receptors and other stimuli. In fact, one of the central issues that surround Shc function that remains unsolved is why Shc is recruited upon in so many signalling receptor systems and how the members have evolved to mediate distinct functions.

2.5. The Shc knockout mouse models

The important role of Shc *in vivo* has been demonstrated a few years ago by Lai and Pawson by the generation of a knockout mouse model for the ShcA gene [36]. All three isoforms, p66, p52 and p46 were ablated by gene targeting of exons two and three, which encode for the entire PTB domain. The homozygous mutants died at embryonic day 11.5 (E11.5) due to severe defects in heart development and the formation of mature blood

vessels. The depletion of ShcA resulted impaired sensitivity to growth factors and a loss of MAPK activation. Furthermore, ShcA mutant embryos exhibited adhesion defects in the heart, yolk sac and major blood vessels due to aberrant focal contact organisation and actin stress fibres, due to the additional role of Shc in cytoskeleton organisation, as they are substrates of the focal adhesion kinase. In contrast, the single knockout for the p66ShcA isoform generated mice with higher tolerance to oxidative stress that has a longer lifespan [13]. This was found to be due to the decreased accumulation of oxidative damage to mitochondrial DNA, which is one of the critical events during the ageing process, in tissues of p66ShcA null mice.

The genetic deletion of ShcB, ShcC or both genes results in mice that are viable and fertile. ShcC null mice appear to show no gross anatomical abnormalities, while the ShcB knockout (KO) mice as well as the double mutant ShcB/ShcC null mice showed a partial loss of peptidergic and non-peptidergic nociceptive sensory neurons that did not influence their physiological functions [21]. Furthermore, the double mutants demonstrated a reduction in neuronal number within the sympathetic nervous system, while the single mutants did not. However, the single mutants as well as the double mutants did not show gross alterations in auditory, olfactory or visual functions, despite their high expression in the brain and sensory ganglia [21]. Taken together, these studies suggested that ShcB plays a role in the survival of sensory neurons and acts together with ShcC in supporting sympathetic development and survival mainly through the TrkA receptor signalling and also through some other receptors, which have not yet been identifed.

The RaLP KO mouse has been generated by our laboratory in collaboration with Genoway. The characterisation of the mutant mouse is currently ongoing and will be partly discussed in the results in this thesis (see results section 5).

2.6. The fourth Shc member, RaLP, what is known so far

The characterisation of the fourth member of the Shc family of adaptor proteins, ShcD/RaLP is still in its infancy. It has been identified only a few years ago and there is very little information on its biological function as well as the signalling pathway it is regulating. The mouse RaLP gene is located on the chromosome 2F1 and the longest open reading frame of the homology-based reconstructed cDNA predicts a protein of 69 kDa. Several shorter isoforms have been predicted for RaLP, due to multiple potential initiator methionine residues present in the region encoding for the CH2 as well as due to alternative splicing. These isoforms are predicted to have molecular weights of 38 kDa and 24 kDa.

The comparison of the amino acid sequences of mammalian Shc members evidenced the highest similarity between RaLP and ShcA [22]. The highest homology between RaLP and the other members was seen in regions of the PTB and SH2, but with more divergence in the CH1 and CH2 regions. The RaLP protein possesses several biochemical characteristics that render it unique from the other family members. The CH2 region is extended in RaLP and it contains several unique proline-rich motifs that could be recognised by proteins containing SH3 domains. It also possesses a non-conventional Shc PTB domain that contains an unusual histidine residue at the 5' position relative to the Tyr, not present in the other family members. The carboxy-terminal sequence also differs from the corresponding sequences of the other members and the peptide of this region was used to raise antibodies against RaLP in collaboration with Giuseppe Ossolengo of the Biochemistry Unit at the IFOM-IEO campus (for detailed description, see materials and methods section 2.1). RaLP also has specific characteristics in the CH1 region: (i) the absence of the adaptin-binding motif which is present in all the other members and, (ii) an additional tyrosine residue that can also mediate binding to Grb2, resulting in three Grb2 binding sites compared to two found in the other members. Although the part of the expression pattern of RaLP overlaps

with that of ShcB and ShcC, its unique structural characteristics together with its specific expression in the early embryo, suggests a non-redundant and specific role of this protein and merits further investigation.

Deregulated levels of RaLP have been shown to be implicated in tumourigenesis. In particular, it is highly expressed in aggressive and metastatic human melanomas. [12]. RaLP is a substrate of IGF-1 and EGF receptors and its overexpression in melanoma cell lines resulted in the increase of Ras-MAPK signalling which led to the induction of cell migration. On the other hand, RaLP silencing did not affect MAPK signalling, suggesting that RaLP may be involved in both Ras-dependent and independent pathways.

The characterisation of this family member would provide further insight into how this family of adaptor proteins have evolved to modulate distinct signal transduction within different cell types and would provide important information on how adaptor proteins play an important role in the fine-tuning and regulation of different signalling pathways. Furthermore, understanding the physiological function of this protein might shed some light in understanding how deregulated levels of the protein can be involved in disease.

3. Early embryonic development and pluripotent lineages

As will be discussed in more detail in the results, the characterisation of RaLP expression in the mouse, evidenced its bi-phasic expression during development: its expression in the epiblast of the early embryo, the developing central and peripheral nervous sytem, and the adult brain (see results section 1). This led to the development of the project to understand what role RaLP plays during embryogenesis and which signalling pathways are regulated by it during these two time-windows. Both these aspects could be addressed by using mouse embryonic stem cells as they represent the ideal model to study pluripotency and differentiation *in vitro,* in parallel with the characterisation of our RaLP KO mouse model.

3.1. ESCs as a tool to study development *in vitro*

Ever since the isolation and the characterisation of mouse embryonic stem cells (ESCs) in 1981 by Evans, Kaufman and Martin [37,38], these cells have represented both an essential tool to address developmental questions but also an entity that has intrigued researchers since decades because of their remarkable properties. The discovery of ESCs was preceded in the 70's by the isolation of a similar pluripotent cell type that was first isolated from teratocarcinomas from the mouse testis, the embryonic carcinoma cells (ECs). Teratomas are tumours that contain in a disorganised manner, a mixture of differentiated cell populations that derive from the three germ layers. They were seen to arise spontaneously in mice of the 129 strain and the ECs isolated from these tumours showed clonal ability, pluripotency and when reintroduced into a blastocyst they could sometimes contribute to the developing fetus [39], suggesting an identity similar to that of early embryonic lineages. ECs were derived and maintained efficiently *in vitro* by the co-culture with fibroblasts [40] and because they recapitulated many features of normal development, they provided the first system to study embryogenesis *in vitro*. The unique characteristics of these cells then led to the idea of the possibility to isolate cells directly from the preimplantation embryo and this proved possible, generating cells that are now known as ESCs.

What makes ESCs so remarkable and now a powerful instrument that is routinely used to generate genetically modified mouse models, are two main characteristics: their pluripotency, in other words, their ability to differentiate into all cell types deriving from the germ layers and their self-renewal capacities. Their pluripotency confers them the ability to contribute to all the tissues of the adult mouse including the germline, when introduced into host blastocysts and they can pass their genetic inheritance to the following generation [41,42]. This opened the possibility to study gene function *in vivo* by generating ESCs with the desired genetic mutation and then reintroducing these cells into the

blastocyst to generate chimeras to obtain genetically manipulated mouse models. The second defining feature of ESCs is their ability to undergo symmetrical cell division called self-renewal, to generate identical pluripotent progeny without differentiating. Therefore, these cells can be maintained and expanded indefinitely *in vitro.*

In addition to their developmental potential *in vivo*, ESCs are also used as a model to study embryogenesis *in vitro*, as they are able to undergo differentiation to different cell types in culture. Studies over the past 20 years have led to the development of specific culture conditions and protocols for the generation of a variety of cell lineages from ESCs. Also for this reason, the discovery of ESCs has caused excitement for its huge potential in cell replacement therapy, especially when human ESCs were first isolated in 1998 [43]. Furthermore, several protocols have now been characterised at the molecular level and have shown that the events that occur during the differentiation *in vitro* mimic those *in vivo*. For example, one of the first differentiation protocols that were implemented for studying developmental processes is the embryoid body formation. This was first introduced by Evans and co-workers using ECs and it was adapted for ESCs by Doetschman [44]. When ESCs are grown in the absence of feeder cells in culture dishes that do not allow their adherence and in the absence of the self-renewal factor leukemia inhibitory factor (LIF), they spontaneously differentiate by aggregating into spheres called embryoid bodies (EBs). The cells then start to undergo a differentiation program that mimics the preimplantation embryo stage up to the postimplantation gastrulation stages, generating intermediate cell types such as the primitive ectoderm, endoderm and mesoderm, and subsequently more differentiated cells, such as cardiomyocytes, neurons and endothelial cells. This process of ESC differentiation in EBs recapitulates quite accurately early embryonic development. Gene expression profiling and immunohistochemical studies have shown that the EBs progress through the specific stages of embryogenesis, starting from a morula-like stage and then progressing to form the

epiblast surrounded by primitive endoderm. The epiblast then starts to cavitate as well as differentiate, forming germ layer progenitors of the mesoderm, then progressing to form neuroectoderm. A recent study even showed the formation of a gradient driven by Wnt signalling, just like *in vivo*, is responsible for the determination of the apical-polar axis of the embryo [45], demonstrating a high degree of organisation in EBs than previously thought. These progenitor tissues then give rise to populations of differentiated cell types. Specific stages of development can be observed during EB differentiation, now characterised at the cellular and molecular level, rendering this protocol a valuable tool to study the role of developmental genes, *in vitro* (Figure 3).

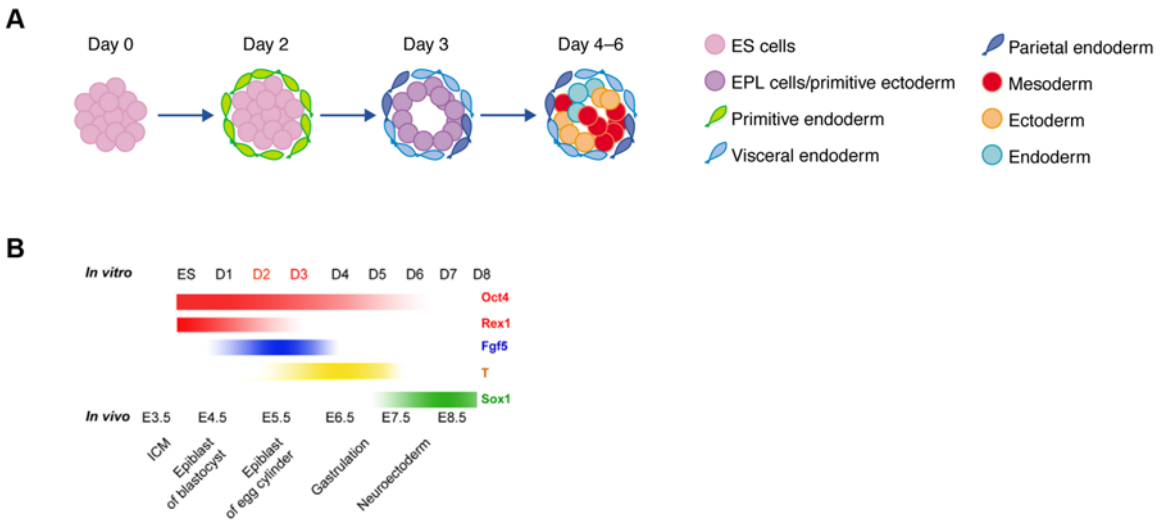

Figure 3. Embryoid body differentiation of ESCs mimic embryonic development. (A) Schematic representation of the different phases of EB formation and the cell types that are generated during the first few days of differentiation. From [46]. **(B)** Characterisation of the different phases of differentiation by global gene expression patterns. The temporal expression of marker genes is similar to the pattern *in vivo*, suggesting that the progeny of ESC differentiation *in vitro* can reflect the comparable states of cells *in vivo*. From [47].

In addition to the EB differentiation that generates simultaneously many cell types, there are currently several protocols that have been developed over the years that allow more specific differentiation towards certain cell lineages. One of the most widely used systems for studying the neural commitment of ESCs is the differentiation under defined monolayer culture conditions in the absence of serum and the addition of two growth

factors important for the self-renewal of neural progenitors, fibroblast growth factor 2 (FGF2) and the epidermal growth factor (EGF) [48]. This protocol induces the ESCs to undergo autoinductive signals to commit to a neural fate and then the neural progenitors/neural stem cell population is selected and enriched by culturing these committed cells in the presence of the growth factors. Studies have shown convincingly that these ESC-derived neural stem cells are *bona fide* radial glial cells, which are the neural stem cells found *in vivo*, as they are able to differentiate into the three lineages of the CNS, astrocytes, oligodendrocytes and neurons [49]. These cells also undergo symmetrical division in vitro, like other stem cell types and are capable of undergoing self-renewal indefinitely. Furthermore, these ESC-derived NS cells have been transplanted into brains of adult mice and were able to integrate into the host, proving their true stem cell capacity.

Like the EB differentiation, this protocol has been recently shown to closely mimic neurogenesis *in vivo*. Detailed characterisation by gene expression profiling (Figure 4) and immunochemistry techniques have demonstrated that the cells transit through all the intermediates states generated during development, providing not only an efficient protocol to obtain neural stem cells but also an invaluable *in vitro* model system to dissect mechanisms underlying neuronal commitment of ESCs [50,51].

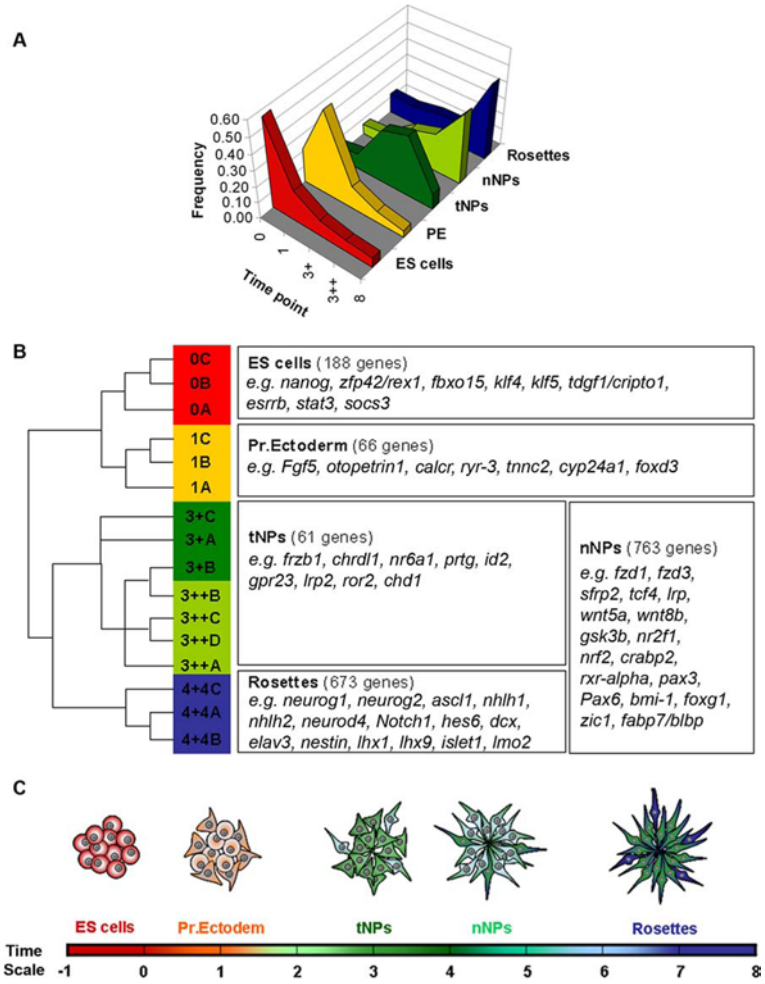

Figure 4. Clustering analysis of differentially expressed genes during ESC differentiation to neural fate. (A) Frequency distribution of the expression levels of the genes belonging to the five defined groups. **(B)** Dendogram of the relationship of expression of genes belonging to each group (with biological replicates being represented by the letters A, B, C and D) and examples of genes that are present in the five defined groups. **(C)** Schematic representation of the successive cellular states that occur along the path to neural differentiation**.** Abbreviations: embryonic stem cells (ES cells), Pr. Ectoderm (primitive ectoderm), transient neuroepithelial progenitors (tNPs), neurogenic neuroepithelial progenitors (nNPs). From [50].

These characteristics rendered the ESCs a valuable tool to dissect the mechanisms of self-renewal and differentiation, as well as dissecting the function of many proteins involved in the signalling pathways of these processes.

3.2. The formation of early embryonic lineages and derivation of stem cells

The first differentiation event that occurs during embryonic development is the segregation of the trophectoderm from the inner cell mass during the passage from the late morula stage to the blastocyst at E3.5 [52] (Figure 5). The trophectoderm gives rise to the chorion

and trophoblast, which will then form the placenta, a vital organ that will sustain the growth and survival of the fetus. The inner cell mass will give rise primarily to the embryonic lineages [53]. At the peri-implantation stage of the blastocyst, at E4.5, the inner cell mass has further segregated into the epiblast called also the primitive ectoderm and surrounded by a monolayer of primitive endoderm, also called the hypoblast, on its blastocoelic surface. The primitive endoderm constitutes another extraembryonic lineage to support fetal development, the yolk sac cavity and the exocoelom, as well as playing an important role in the establishment of the anterior/posterior axis. At this point, these three lineages are restricted in fate, demonstrated by extensive lineage tracing and chimera studies in the mouse. This is also reflected by their distinct transcriptional profile and epigenetic status. Upon implantation, the embryo undergoes rapid proliferation and at E5.5, it consists of an expanded epiblast surrounded by the extraembryonic endoderm which will then further segregate into the visceral and parietal endoderm, while the trophoblast has expanded and differentiated to contain self-renewing trophoblast stem cells, intermediate cells and giant cells. The major event that occurs is gastrulation during which the epiblast cells generate the three germ layers of the embryo, the ectoderm, mesoderm and definitive endoderm. The hallmark of this process is the formation of the primitive streak, which begins at E6.5. The endo-mesoderm precursors ingress through the primitive streak while the cells that will take on the ectodermal identity do not. These primary germ layers are the progenitors of all the tissues of the organism. These progenitors are further specified by the activation of tissue specific genes while genes involved in the pluripotency are gradually restricted. This process is tightly controlled by cellular interactions and cell signalling [54].

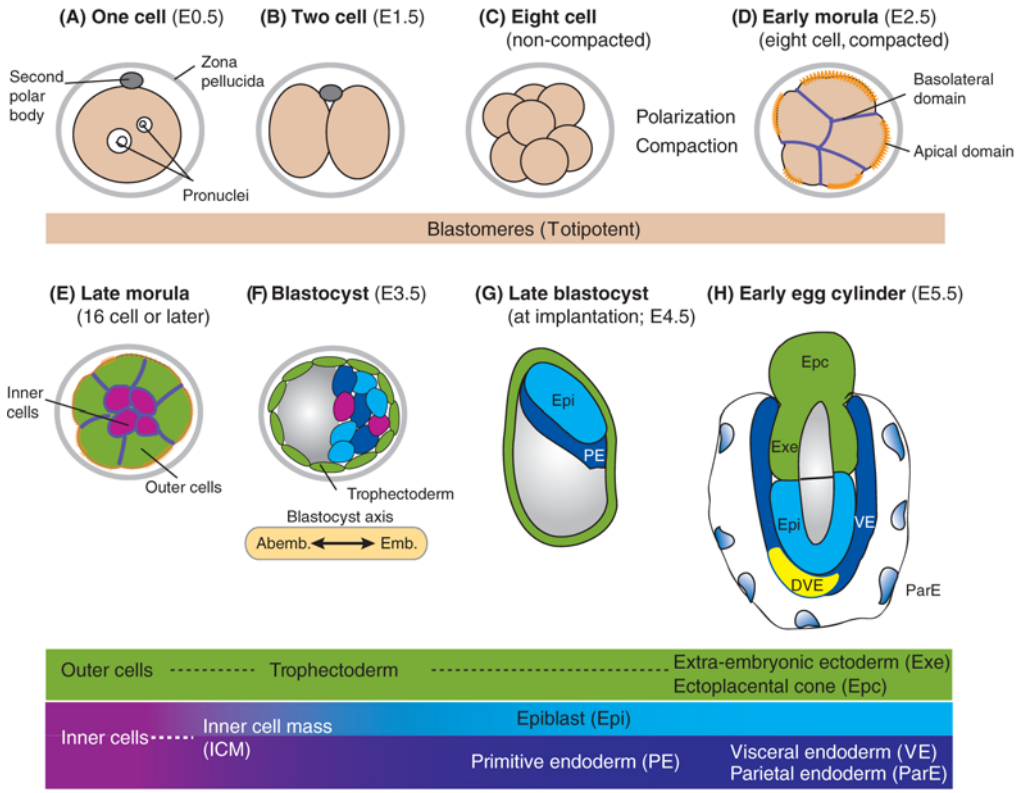

Figure 5. Cell lineage formation from egg to egg cylinder. (A to H) Schematics of the morphological changes and cell lineage specification that occur in a mouse embryo, from its fertilization at embryonic day (E) 0.5 to the early egg cylinder stage (E5.5). The coloured bars show the progressive allocation of totipotent blastomeres to outer and inner cells and to the trophectoderm and inner cell mass lineages. The cell types in the embryos are colour coded. Abbreviations: abembryonic-embryonic (Abemb Emb) axis of the blastocyst, distal visceral endoderm (DVE). From [55].

During the early stages of embryogenesis, several types of stem cells can be derived. ESCs [37,38], trophoblast stem cells (TSCs) [56] and extraembryonic endoderm cells (XEN) [57]. Each stem cell type, according to their gene expression and epigenetic profile, morphology and most importantly, their ability to recapitulate the behavior of their precursors when injected into blastocysts, reflects the lineage restriction of the tissue from which they were isolated.

ESCs can be derived from the embryos as early as the morula at E2.5 [58] to the late blastocyst E4.5 [37,38]. They are dependent on the expression of key transcription factors, Oct4, Sox2 and Nanog for the maintenance of their pluripotent state and rely on LIF and BMP4 signalling for their self-renewal. In 2007, stable, pluripotent stem cell lines, the epiblast stem cells (EpiSCs) were isolated from the postimplantation embryo epiblast

between E5.5 to E7.5 [59,60]. These pluripotent cells provide a robust and invaluable system *in vitro* to study the mechanisms underlying the transition from pluripotency to differentiation, which cannot be done using embryos at these stages. Furthermore, they share some characteristics with ESCs but also possess specific features that renders them biochemically and functionally distinct from ESCs. Stem cells can also be derived from the extraembryonic compartment. Trophoblast stem cells (TSCs) can be derived from the trophoblast of the blastocyst and can only contribute to trophectodermal cell lineages *in vivo* and *in vitro* as they are restricted in their potency, differentiating only to their lineages, the intermediate and giant cells [56,61]. TSCs rely on the FGF and activin/nodal signalling for self-renewal and they require the expression of Cdx2, Eomes and other TS-specific transcription factors. A third type of stem cell has been recently isolated from the extraembryonic endoderm, the extraembryonic endoderm (XEN) cells [57]. They are morphologically and molecularly similar to the primitive endoderm derivative. They depend on Gata6, Sox7 transcription factors.

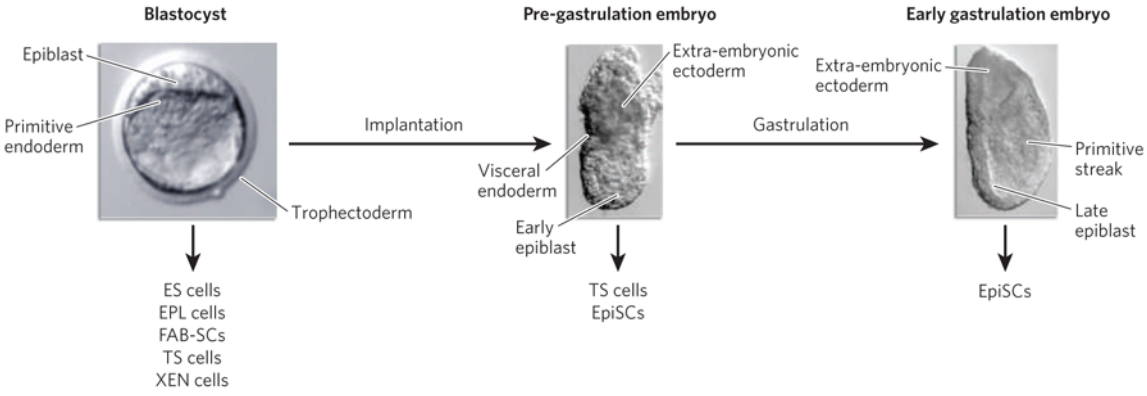

Figure 6. Stem cell types derived from mouse embryos around the time of implantation. At implantation, mouse blastocysts comprise three distinct cell types: the trophectoderm; the inner cell mass, the primitive endoderm and the early pre-implantation epiblast. Under appropriate *in vitro* culture conditions, three types of stem cell with a comparable potential for differentiation to each of the cell types of the blastocyst can be derived: ES cells, trophoblast stem (TS) cells and extraembryonic endoderm (XEN) stem cells. Pluripotent stem cells can be derived from the epiblast of the early post-implantation embryo at 5.5 up to 7.5 days post coitum. From [62]**.**

Recent studies have provided interesting insight on how the the culture growth factor environment and cell to cell interaction can play a critical role in defining the stem cell identity during its derivation [63].

3.3. The key signalling pathways underlying lineage determination and identity

There are several key pathways governing lineage determination during development and the same pathways that underlie lineage segregation *in vivo* have been found to be responsible for the regulation of pluripotency and differentiation of stem cells *in vitro*. The dissection of the signalling mechanisms underlying cell fate decisions is not only important in understanding the development of the embryo but also for developing techniques that allow the propagation and differentiation of stem cells into pure populations of progenitors or functional and mature differentiated cell types under defined conditions *in vitro* for stem cell based therapies.

3.3.1. JAK/STAT pathway

The most well known factor that promotes self-renewal is LIF, a member of the interleukin 6 family of cytokines. Historically, ESCs were derived on a feeder layer of MEFs, however it was found that the conditioned medium of MEFs is enough to support the self-renewal of ESCs. Subsequently, it was found that MEFs sustain ESCs by secreting LIF [64]. LIF binds to the heteromeric complex receptor that consists of the LIF receptor and the glycoprotein receptor, gp130. Upon LIF binding, the tyrosine kinase Janus kinase (JAK) phosphorylates the tyrosine residues in the intracellular portion of both receptors. This results in the recruitment of the signal transducer and activator of transcription (STAT3) through its SH2 domain, which in turn is activated by JAK mediated phosphorylation. STAT3 then dimerizes and then translocates to the nucleus to activate the transcription of its target genes [65], such as c-Myc. LIF signalling can also induce other pathways such as the Ras/Erk and PI3 kinase through the JAK activation of a SH2 domain containing

phosphatase (SHP2). However, LIF by itself is not sufficient to sustain the self-renewal of ESCs, as it cannot sustain the expansion of these cells in the absence of serum, suggesting that there are other factors contained in serum that are important for ESC maintainance and proliferation.

Although LIF is required *in vitro* to derive and maintain pluripotent mouse ESCs, this signalling was not required *in vivo* for early embryonic stages, as embryos lacking LIF can develop to stages later than the blastocyst. Interestingly, mouse EpiSCs and human ESCs do not rely on this signalling for their self-renewal and it is unknown whether LIF has different effects on these cell types.

3.3.2. TGF-β superfamily

In the mouse embryo, signalling by bone morphogenetic protein (BMPs), members of the transforming growth factor β superfamily, has been shown to be crucial for the proliferation of the epiblast, as the genetic deletion of BMP4, BMPR1a or Smad4 leads to a reduction in cell proliferation in the epiblast and precocious neural induction. Furthermore, BMPs play also an important role gastrulation for mesoderm formation and patterning [66,67].

In mouse ESCs, BMP4 can replace the requirement of serum in culture for their self-renewal by maintaining the expression of a family of negative transcriptional modulators, the Inhibitor of differentiation (Id) genes, in this way suppressing their differentiation in to neural cell types [68]. The binding of BMP triggers the formation of receptor complexes, which leads to the phosphorylation of the transcription factors Smads. The effect of BMP4 on ESC maintenance depends on the activation of the JAK/STAT pathway by LIF, as in its absence. BMP4 drives non-neural differentiation of ESCs. Therefore it is thought that instead of directly promoting self-renewal, BMP prevents the differentiation of ESCs. BMP4 treatment of ESCs together with LIF is sufficient to sustain ESC self-renewal

without the addition of serum or feeders. This led to the view that differentiation is the default pathway for ESCs [69].

The response to BMP4 of human ESCs and mouse EpiSCs on the other hand are completely different. BMP4 promotes trophoblast differentiation of human ESCs [70] while in mouse EpiSCs, it promotes the differentiation to non-neural lineages [47]. However in these two stem cell types, another member of the TGF-β superfamily, Nodal, plays a role in sustaining their self-renewal. Nodal is an important regulator of many processes during embryonic development. It is important for the maintenance and growth of the epiblast, as embryos without Nodal are detrimental due to loss of expression of Oct4 and premature differentiation of epiblast into neuroectoderm. Activin, another member of the family, also signals through the same receptor as Nodal and is often used in cell culture as a substitute for Nodal due its wider availability and comparable activity. In contrast to mouse ESCs, Nodal/activin signalling is important for sustaining the self-renewal of mouse EpiSCs and human ESCs, as it suppresses their differentiation by regulating the expression of another key pluripotency transcription factor, Nanog [71,72].

3.3.3. Wnt family

Wnts are secreted glycoproteins that have many roles in organogenesis. Canoncal Wnt signalling is activated upon Wnt binding to the Frizzled receptor on the cell membrane. This results in the inhibition of glycogen-synthase kinase 3 (GSK-3) and a subsequent accumulation of β-catenin in the nucleus, allowing transcriptional regulation of its target genes. For mouse embryonic development, there is no evidence that Wnt signalling has a role in the maintenance of the pluripotent epiblast *in vivo*, as the depletion of Wnt3 does not show any effect on the epiblast of the mutants, however in later stages it is crucial for the development of the primitive streak, mesoderm and node [73].

In mouse ESCs, it was shown that the effect of Wnt mediated signalling depends on the balance between the association of β-catenin with p300 and CBP, two transcriptional co-

activators. It is thought that the association of β-catenin with p300 drives stem cell maintenance at the expense of differentiation, however, the exact mechanisms are not clear. It seems that in general mimicking the activation of this pathway has beneficial effects on ESC self-renewal. The role of Wnt signalling in the maintenance of human ESCs and mouse EpiSCs remains uncertain up to date.

3.3.4. FGF/Erk pathway

Recent studies showed that ESCs have an autocrine signalling through the fibroblast growth factor (FGF) that activates the MAPK pathway, which is important for promoting exit from self-renewal and commitment to differentiation [74]. FGF signalling is initiated by its binding to the tyrosine kinase receptor FGF-R. There are several FGF ligands and they are implicated in different pathways. In particular, FGF4 is produced by ESCs in an autocrine manner and it is needed to exit from self-renewal to start the differentiation program [74].

Until recently, the prevailing view of the molecular basis of ESC self-renewal was that they rely on extrinsic determinants for the maintenance of this state. However, recent studies have demonstrated that it is sufficient to shield the ESCs from differentiation factors to promote their self-renewal, leading to the view that ESCs represent a “ground state”. ESCs retain pluripotency and undergo self-renewal by blocking FGF4 mediated signalling by chemical inhibitor of MEK to inhibit the activation of Erk1/2 downstream [69]. In line with these studies, the use of small molecule inhibitors for MEK and the suppression of GSK-3 of the Wnt signalling pathway, which increases the viability of the cells, together with LIF, are sufficient to stabilise and sustain mouse ESCs in their pluripotent and self-renewing state.

Interestingly, the same FGF signalling that induces the exit of ESCs from self-renewal becomes part of the circuit that sustains self-renewal of mouse EpiSCs and human ESCs. In mouse EpiSCs, FGF2 signalling was demonstrated to act by inhibiting the

differentiation of these cells to neural fate while at the same time, blocking its reversion to an ESC like state [75]. Following studies showed that FGF signalling is crucial for the transition from ESC to EpiSC, but the further differentiation to neuroectoderm state is actually inhibited by this pathway [76].

It is interesting that the same pathways mediate different functions within the different types of stem cells, such as the transition of the role of FGF signalling from one pluripotent state to another. FGF signalling is regulated at multiple levels and one of the mechanisms that have been proposed to allow the differential response of cells to the same stimuli, is by expressing negative regulators to attenuate the signal, such as the Sprouty-related protein with an EVH1 (Ena/VASP [vasodilator-stimulated phosphoprotein] homology domain 1) domain (Spred1) of the MAPK/Erk pathway [77] and adaptor proteins that can recircuit the pathway to compartmentalise signalling or mediate cross-talk with other pathways, creating completely different outputs from the same stimulus. These regulatory mechanisms have profound effects on the downstream signalling of receptors that in turn regulate the transcriptional activity of genes. In fact, studies have shown that the manipulation of these pathways through the addition or withdrawl of specific cytochines and growth factors can even allow the interconversion of one stem cell type to another [62,78,79].

3.4. Pluripotent stem cell lines and their relation to embryonic lineages

When studying developmental processes *in vitro*, one must always keep in mind the events and the corresponding stages *in vivo*. Although the predominant view of the identity of ESCs were thought to be unequivocally representing the inner cell mass of the blastocyst, recent studies are challenging this notion, as recently, other types of pluripotent stem cell lines that share properties with ESCs have been derived from different developmental stages and mammalian species, as well as from the reprogramming of adult cells by the

introduction of transcription factors [80]. The relationship of these cell lines to the lineages from which they are established and their relation to one another is still a matter of intense debate.

Pluripotency is a transitory state that exists only during brief and specific time-windows of development. When cells are isolated from the embryo during these time-windows, they are "captured" in their self-renewing state and by *in vitro* culture conditions, this transitory state becomes permanent as the cells acquire the capacity to undergo self-renewal indefinitely. When cells are isolated from the inner cell mass of the blastocyst, the epiblast of the post-implantation embryo and the primitive streak and cultured *in vitro* to derive ESCs, EpiSCs and embryonic germ cells (EGCs) respectively, they retain their pluripotency and undergo self-renewal indefinitely under their ideal culture conditions. On the other hand, the corresponding cells *in vivo* continue their developmental program and differentiate. This suggests that there are signalling pathways that sustain this self-renewal ability that must be continuously activated and differentiation programs that must be silenced in order for these cells to maintain their identity. These are events that do not occur *in vivo* and so to some extent it is difficult to say with precision the exact identity of these cells with the *in vivo* counterpart. In depth analysis of transcriptional profile, epigenetic profile and proteome studies have given some insight to this, however, the exact identities are still open questions.

Over the past few years, several types of pluripotent stem cells have been derived from the embryo and although it seems that these cells have a common genetic network of transcription factors that is responsible for their pluripotency, several studies have shown that they also possess unique properties. Intriguingly, these cells are highly plastic and certain cell types can readily convert into other stem cell types upon extracellular stimuli (Figure 7). This has lead to the view that each type of pluripotent cell has reached a different developmental potential and that the pluripotent state is a continuum of states

[81]. Extrinsic regulation of cells play a crucial part in this regulation, as their activation is intricately linked to intrinsic mechanisms that determine the state of the cell. Understanding how the stem cell types are related to one another and how they can interconvert in response to extracellular signals is one of the challenging questions in this field today.

The properties of these various stem cell types are believed to reflect their embryonic cell of origin *in vivo*, although some characteristics must be acquired as adaptive changes made in response to propagation and establishment *in vitro*.

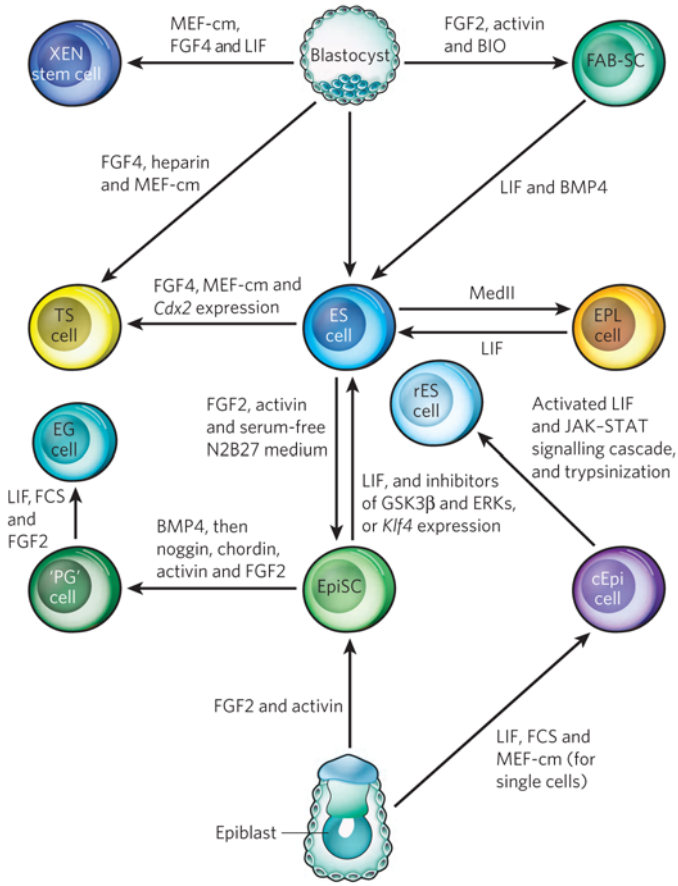

Figure 7. The interconversion of stem cells derived from the mouse embryo. Stem cells with different characteristics can be derived from the mouse blastocyst or from the early postimplantation embryo. The stem cells can be converted to each other through the manipulation of culture conditions and/or enforcing the expression of certain genes. Three types of stem cell can be derived from the blastocyst: ES cells, TS cells, XEN cells. FAB-SC are a particular type of stem cells that initially are unable to differentiate and they can be converted to pluripotency with BMP4 and LIF. ES cells can be converted into TS cells by culturing them in MEF-cm containing FGF4, together the expression of the transcription factor Cdx2. ES cells can be turned into EPL cells by culturing them in MedII. EpiSCs are derived from postimplanation epiblast in presence of FGF2 and activin. EpiSCs cultured in MEF-cm, LIF and FBS become cEpi cells that can be converted into ES cells (rES). EpiSCs can also be converted into ES cells by culturing them with LIF and GSK3β and ERK inhibitors or by enforced Klf4 expression. ES cells can be turned into EpiSCs by culturing them with activin

and FGF2. EpiSCs can differentiate to PG cells with BMP4, noggin, chordin, activin and FGF2. PG cells can be converted into EG cells by culturing with LIF, FBS and FGF2. Abbreviations: bFGF, Activin and BIO-derived stem cells (FAB-SCs), mouse embryonic-fibroblast-conditioned medium (MEF-cm), primitive ectoderm-like (EPL) cells, MedII (medium conditioned by the human hepatocarcinoma cell line HepG2), fetal bovine serum (FBS), cultured epiblast cells (cEpi), reversed ES cells (rES), primordial germ cells (PG), embryonic germ (EG) cells. From [62].

The relationship between mouse ESCs and EpiSCs represents an interesting example of this interconversion between pluripotent states. Although they are both pluripotent, they are functionally and biochemically distinct (Figure 8). As described previously, EpiSCs share the expression of the core pluripotent transcriptional factors, Oct4, Nanog and Sox2 but their overall transcriptional profile and epigenetic status are strikingly different from that of ESCs [59,60]. EpiSCs also have a morphology different to that of ESCs, as they grow as flattened 2-D colonies rather than the 3-D ESC colonies. Furthermore, EpiSCs rely on FGF2 and activin signalling for the maintenance of pluripotency and self-renewal in culture, whereas ESCs rely on LIF and BMP4. When mouse EpiSCs are cultured under stringent ESC conditions of 2i, they are unable to self-renew and they undergo cell death. These characteristics are very similar to human ESCs, in fact this has led to the idea that human ESCs and mouse EpiSCs might reflect the same origin of derivation. However, although human ESCs are derived from the preimplantation blastocyst, the corresponding origin is still unclear.

EpiSCs are pluripotent, as they are able to generate the derivatives of all three germ layers during *in vitro* differentiation and *in vivo*, in the teratoma assay. However, when they are injected into the recipient blastocyst, they are unable to contribute to chimera formation probably due to the fact that they represent a different developmental stage. EpiSCs also manifest a major epigenetic modification that occurs *in vivo* after the formation of the post-implantation epiblast, one copy of the X chromosome is silenced in female embryos.

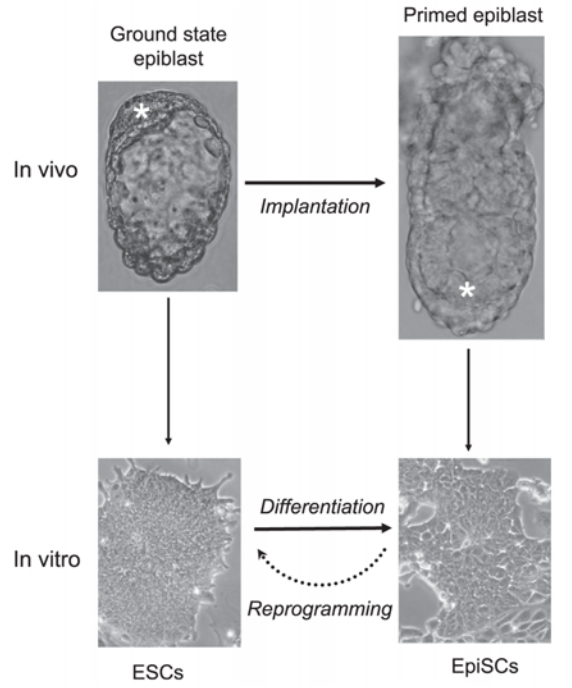

Property	Ground State	Primed State
Embryonic tissue	early epiblast	egg cylinder or embryonic disc
Culture stem cell	rodent ESCs	rodent EpiSCs; primate "ESCs"
Blastocyst chimaeras	yes	no[a]
Teratomas	yes	yes
Differentiation bias	none	variable
Pluripotency factors	Oct4, Nanog, Sox2, Klf2, Klf4	Oct4, Sox2, Nanog
Naive markers[b]	Rex1, NrOb1, Fgf4	absent
Specification markers	absent	Fgf5, T
Response to Lif/Stat3	self-renewal	none
Response to Fgf/Erk	differentiation	self-renewal
Clonogenicity	high	low
XX status	XaXa	XaXi
Response to 2i	self-renewal	differentiation/death

[a] Not applied to primate cells.
[b] Representative examples.

Figure 8. Two phases of pluripotency. ESCs can be induced to differentiate into EpiSCs by exposure to activin A and Fgf2. The reverse transition can be made by the overexpression of a pluripotency factor Klf4 or in response to LIF-STAT3 signalling.The white asterisks indicate the epiblast. Adapted from [82]. The table summarises the biochemical and functional properties of ESCs (ground state) and EpiSCs (primed state).

ESCs can be converted into EpiSCs *in vitro*, by culturing them in the presence of FGF2 and activin [78]. EpiSCs can be converted back into ESCs by the exogenous expression of Klf4 [78] or as demonstrated recently, by passaging ESCs under the stimulation of LIF-STAT3 signalling [79].

These studies have lead to the idea that ESCs and probably also other pluripotent cells although this has not been investigated yet, exist in different metastable states that are determined by fluctuations in the expression of pluripotency and differentiation related genes. This property might represent "noise" that allows the cells to fluctuate between more pluripotent/multipotent state and more poised or biased states, generating the plasticity of the cells to readily respond to environment signals. Taken together, the regulation of extrinsic signals plays a fundamental role in determining the self-renewal and differentiation of pluripotent stem cells and the characterisation of these pathways will be very important not only in understanding the biology of these cells but for future application in stem cell therapy.

4. Aim of the PhD project

The aim of this PhD project is to understand the physiological role and dissect the signalling pathway of a previously uncharacterised family member of the Shc adaptor proteins, ShcD/RaLP. Based on the expression pattern of RaLP during mouse embryonic development and in the adult, we decided to use as a model system, mouse ESCs. This system would allow us to investigate the role of RaLP in the pluripotency of mouse ESCs and EpiSCs and in the induction of their differentiation. In parallel, our RaLP knockout mouse model, which up to present is the first to be generated, was characterised.

The study of the function of RaLP would provide insight into the intricate signalling pathways governing ESC self-renewal and differentiation, as well as how this family of adaptor proteins have evolved to take on distinct functional roles in the organism. Furthermore, understanding the physiological function of this protein might provide insight into how deregulated levels of this protein is involved in the metastasis of tumours.

Materials and Methods

1. Cell culture methods

1.1. Preparation of mouse embryonic fibroblasts for feeder layer

Wild type mice were set up for timed matings. Pregnant females were sacrificed between embryonic days E11.5 and E13.5 following standard procedures. The intact uterus was carefully extracted and transferred to a 100-mm dish containing sterile phosphate buffered saline (PBS). The uterus was sectioned to release the embryos and each one was placed in a 60-mm plate with PBS. The fetal membranes, umbilical cord, head and organs were removed and the remaining tissues were collectively transferred to a 100-mm plate containing 5 mL trypsin-EDTA (Lonza). The tissues were further dissociated with forceps and scissors and incubated at 37°C for 5 to 10 min. The cells and tissue pieces were triturated by pipetting up and down and collected in mouse embryonic fibroblast (MEF) medium which consists of Dulbecco's modified Eagle's Medium (DMEM with high glucose, with sodium pyruvate and without L-glutamine; Lonza), 10% North American foetal bovine serum (FBS; Gibco), 2 mM L-glutamine (Gibco), 0.1 mM non-essential aminoacids (NEAA; Gibco), 50 U/mL penicillin and 50 μg/mL streptomycin (Lonza) and 0.1 mM β-mercaptoethanol (Gibco). The digested tissue was centrifuged at 280 × *g* for 5 min. The pellet was resuspended in MEF medium and cells were plated onto 100-mm plates. Cells were cultured in a humidified incubator at 37°C with 5% CO_2 and were passaged every two days at a 1 to 4 ratio. When cells almost reached confluency, some 100-mm dishes were frozen in 90% FBS with 10% dymethylsulfoxide (DMSO) to create stocks of MEFs.

For the preparation of feeder layers, MEFs at a maximum of passage three after isolation were used. When MEFs reached confluency they were incubated in MEF medium

containing 10 μg/mL mitomycin C (Sigma) for 4 h in a humidified incubator at 37°C with 5% CO_2. Cells were then washed with PBS, trypsinised and seeded at a density of 6×10^4 cells/cm^2 onto culture dishes. MEF medium was replaced with ESC medium at least 2 h before using them for ESC culture.

1.2. Derivation of mouse embryonic stem cells

RaLP knockout (KO) males and RaLP heterozygote (HT) females were mated and the latter were sacrificed at days postcoitus (dpc) 2.5 and uteri were flushed to collect the embryos at the morula stage. They were cultured *in vitro* in drop cultures of KSOM medium (95 mM NaCl, 2.5 mM KCl, 0.35 mM KH_2PO_4, 0.20 mM $MgSO_4 \bullet 7H_20$, 0.20 mM glucose, 10 mM sodium lactate, 25 mM $NaHCO_3$ phenol red, 0.2 mM sodium pyruvate, 1.71 mM $CaCl_2 \bullet 2H_20$, 0.01 mM EDTA, 1 mM L-glutamine and 1 mg/mL BSA) covered in embryo-tested mineral oil (Sigma) for 24 h in a humidified atmosphere of 5% CO_2 at 37°C. The blastocysts were transferred individually to 48-wells previously plated with mitotically inactivated MEFs. The medium for embryonic stem cell (ESC) derivation consists of DMEM, 15% ESC screened FBS (PAN), 0.1 mM NEAA, 2 mM L-glutamine, 25 mM HEPES and 0.1 mM β-mercaptoethanol, 1000 U/mL Leukemia Inhibitory Factor (LIF; prepared by the Transgenic facility, IFOM-IEO campus) supplemented with 50 μM mitogen-activated protein kinase/extracellular signal-regulated kinase (MEK1) inhibitor PD98059 (Cell Signaling) to facilitate the derivation process by suppressing differentiation cues and enhancing the effect of LIF on self-renewal [83,84]. After five to six days, blastocyst outgrowths were passaged in trypsin-EDTA containing 1% chicken serum (Gibco) following a wash in Ca^{2+}/Mg^{2+}-free PBS (Lonza). Cells were expanded onto 24-wells plated with inactivated MEFs and allowed to grow for three to five days. After this period, the cells were no longer cultured in the presence of the MEK inhibitor. The growing cultures were passaged onto progressively larger areas with feeder, for the

expansion of the ESC population. Medium was replaced daily and cultures were monitored for the appearance of distinct ESC colonies. Usually by the 12-well format, ESC colonies could be seen. When they reached 80 to 90% confluency, they were trypsinised and transferred onto 6-well plates with feeder for three to four days. Each well was then trypsinised and 75% of the cell population was frozen in freezing medium consisting of 90% FBS and 10% DMSO to have the first stock. The derived ESCs were grown on MEFs for two more passages and then adapted to feeder free conditions.

1.3. Culturing of ESCs

1.3.1. Passaging of ESCs

Established wild-type ESCs ETg2a.4 (BayGenomics), 46C ESCs [85] and derived RaLP HT and KO ESCs were cultured routinely in ESC medium. Medium was replenished daily. Cells were passaged at 70 to 80% confluency, every two days. For passaging, cells were washed once in PBS and then incubated in trypsin-EDTA for 5 min at 37°C. Cell suspension was gently pipetted to have single cells and trypsin was inactivated by the addition of the ESC medium. The cells were centrifuged at 280 × *g* for 5 min and resuspended in fresh medium and plated at a density of 2-4 × 10^5 cells/cm^2 (corresponding to a splitting ratio of about 1:10) in feeder free conditions.

ESCs can also be efficiently maintained in culture under defined culture conditions containing small molecule inhibitors that block extrinsic differentiation inducing signals, the mitogen-activated protein kinase (MAPK/ERK1/2) and glycogen synthase kinase 3 (GSK3), in the presence of LIF [69]. This medium is called 2i/LIF medium which consists of N2B27 medium [DMEM/F-12 + Glutamax™ (Invitrogen) and Neurobasal medium without L-glutamine (Invitrogen) at a 1:1 mixture, N-2 (Invitrogen), B-27 (Invitrogen), 0.1 mM β-mercaptoethanol, 2 mM L-glutamine, 25 mM HEPES] supplemented with 1 μM MEK inhibitor PD0325901 (ABCR), 3 μM GSK3 inihibitor CHIR99021 (ABCR) and LIF

(prepared by the transgenic facility). Under these culture conditions, cells were passaged every three days by detaching them in Accutase® (Sigma) incubated for 5 min at 37°C and colonies were dissociated into single cells by pipetting. Cells were collected in 2i/LIF medium and centrifuged at 280 × *g* for 5 min. The cell pellet was resuspended in fresh 2i/LIF medium and cells were seeded onto 0.1% gelatinised plates at a density of 2-4 × 10^5 cells/cm^2.

1.3.2. Freezing and thawing of ESCs

For the cryopreservation of ESCs cultured in ESC medium, ESCs were detached from dishes as described in section 1.3.1 and the pellet was resuspended in freezing medium consiting of 90% FBS and 10% DMSO. Approximately 3 × 10^6 cells were frozen per cryovial. For ESCs cultured in 2i/LIF medium, the freezing medium consisted of 70% 2i/LIF medium, 20% knockout serum replacement (KSR; Gibco) and 10% DMSO. For the thawing of cells under both culture conditions, the cryovials were quickly warmed in a water bath set at 37°C and the contents were transferred to a conical tube containing 10 mL medium. The cells were centrifuged at 280 × *g* for 5 min and seeded in the corresponding medium.

1.4. Differentiation of mouse ESCs

1.4.1. Embryoid body differentiation

Embryoid bodies were generated using the hanging drop method [44] in order to obtain a homogenous and reproducibile differentiation. The embryoid body (EB) differentation medium consisted of ESC medium without LIF. ESCs were resuspended in this medium at a concentration of 5 × 10^4 cells/mL and 20 μL drops of this cell suspension were placed on the lid of 100-mm plates that contains PBS at the bottom to prevent evaporation of the medium. Cells were allowed to aggregate for two days and then the EBs were transferred to bacterial dishes in EB medium for a further nine days. Medium was changed every two

days by allowing the EBs to sediment after collecting them into conical tubes. Embryoid bodies were collected at different timepoints: day two, three, four, six and nine of differentiation for analysis.

1.4.2. Teratoma assay

One million RaLP HT and KO ESCs cultured in 2i/LIF medium were injected subcutaneously into the hind flanks of (non-obese diabetic severe combined immunodeficiency) NOD/SCID (interleukin-2 receptor gamma) IL2R γ chain knockout mice. At three, four and five weeks after injection, teratomas were recovered and the major and minor axes were measured using a caliper. Tumours were briefly washed in PBS and then divided into two pieces, one half of the tumour was fixed in formaldehyde for immunohistochemical analysis (section 2.3) and the other half was flash frozen in liquid nitrogen for RNA (section 4) and protein analysis (section 2.2).

1.5. Culturing of embryonic stem cell derived neural stem cells

1.5.1. Derivation of embryonic stem cell derived neural stem cells

ESCs were differentiated to neural stem cells (ES-NSCs) following the monolayer differentiation protocol established by Ying and Smith [48,49]. ESCs were seeded on 0.1% gelatinised culture dishes at low density (0.5-1.5 × 10^4 cells/cm^2) in N2B27 medium. Medium was replaced daily. Cells were allowed to commit to neural fate under these conditions for eight days, after which they were detached in accutase® for 5 min at 37°C, resuspended in N2B27 and centrifuged at 280 × *g* for 5 min. Cells were resuspended in NS expansion medium, which consists of Euromed (Euroclone) supplemented with 2 mM L-glutamine, N-2, 20 ng/mL of Fibroblast growth factor 2 (FGF2; Peprotech) and 20 ng/mL Epidermal growth factor (EGF; Peprotech), in T25 flasks (Iwaki). Typically, cells from a 100-mm plate were replated into two T25 flasks. After two to three days, numerous floating aggregates were present in the culture and were harvested by mild centrifugation.

The spheres were transferred in fresh NS expansion medium in T25 flasks to allow for the selection and expansion of ES-NSCs. After several days, the aggregates attached and characteristic bipolar neural progenitor cells outgrew from the spheres. The population was gently disaggregated in accutase® at 37°C for 3 min, collected in NS expansion medium and centrifuged. The cells were passaged onto T25 flasks at low splitting ratio of 1:2-3. After a further two to three passages, differentiated cells were eliminated and the cultures consisted of a homogenous population of ES-NSCs that could be maintained in culture indefinitely. ES-NSCs were passaged every three days at a splitting ratio of 1:4.

1.5.2. Freezing and thawing of ES-NSCS

ES-NSCs were cryopreserved in NS expansion medium and 10% DMSO. Typically, cells from a T25 were frozen into one cryovial and from a T75 into two cryovials. ES-NSCs were thawed rapidly by warming the cryovial to 37°C and cells were transferred to 10 mL of NS expansion media. Cells were centrifuged and then resuspended in fresh medium and plated.

1.5.3. Differentiation of ES-NSCs to neuronal lineages

ES-NSCs were differentiated to neurons following the protocol established by Conti and colleagues [49]. ES-NSCs were seeded at 5×10^4 cells/cm^2 onto 24-wells containing coverslips double coated with 50 μg/mL poly-ornithine (Sigma) and 5 μg/mL laminin (Sigma). Cells were grown for seven days in Euromed supplemented with FGF2, N-2 and B-27 and half the volume of medium was replaced every two to three days. After one week, the medium was switched to Euromed and Neurobasal (v:v 1:1) supplemented with 0.25 N-2 and B-27 for an additional three days. Cultures were then analysed by immunofluorescence.

1.5.4. Differentiation of ES-NSC to astrocytes

ES-NSCs were passaged at 1:4 onto gelatinised culture dishes containing glass coverslips. The cell density for this differentiation was not crucial. Cells were cultured in Euromed

containing N-2 and 1% FBS. Medium was changed every two days and after seven days of culture, coverslips were recovered for analysis of the differentiation by immunofluorescence.

1.5.5. Cell Sorting

46C ESCs were differentiated to NSCs following the protocol described in Section 1.5.2. Cells were collected with accutase® on day two, three and four of differentiation and resuspended in PBS containing 1% FBS. Cell suspension was passed through BD Falcon™ Cell Strainer nylon with 70 μm pores in order to remove cell clumps. Cells were sorted for green fluorescent protein (GFP) positive and negative populations with the appropriate controls.

1.6. Culturing of epiblast stem cells

1.6.1. Derivation of epiblast stem cells from ESCs

Epiblast stem cells were derived from ESCs (ES-EpiSCs) following the protocol established by Guo and colleagues [78]. ESCs were seeded onto 15 μg/mL fibronectin (Roche) coated 6-well plates at 1×10^5 cells per well in ESC medium. After 24 h, the medium was switched to EpiSC medium [N2B27 supplemented with 12 ng/mL Fgf2 (Peprotech) and 20 ng/mL Activin A (R&D systems)]. When the cells reached 80 to 90% confluency, they were passaged in accutase® at 37°C for 5 min, collected in EpiSC medium and centrifuged at 280 × *g* for 5 min. Cells were resuspended in fresh EpiSC medium and were seeded onto 6-well coated with fibronectin, at high density typically at 5×10^5, corresponding to a splitting ratio of 1:5. From around passage four or five, the cultures consisted of mainly ES-EpiSCs colonies.

1.6.2. Culturing postimplantation embryo derived EpiSCs

EpiSCs derived from the postimplantation embryo of mice carrying GFP gene under the promoter of Oct4 (Oct4-GFP EpiSC; from Prof. A. Smith, Cambridge [78]) were cultured

on fibronectin coated plates in EpiSC medium, as for the ES-EpiSCs. Puromycin (Sigma) was added to culture medium at 1 μg/mL to select for Oct4 expressing cells and medium was replaced daily. EpiSCs were passaged at low splitting ratio of 1:5 to 1:6 every two to three days.

1.6.3. Freezing and thawing of EpiSCs

Derived and established EpiSC lines were cryopreserved in EpiSC medium containing 20% KSR and 10% DMSO. Approximately 5×10^6 cells were frozen per cryovial. For the thawing of these cells, the cryovials were rapidly thawed to 37°C and the contents were transfered to 10 mL of EpiSC medium. The cells were centrifuged at 280 × *g* for 5 min. and the pellet was resuspended in fresh EpiSC medium. Cells were seeded onto fibronectin treated plates.

1.7. Culturing of adult neural stem cells

1.7.1. Derivation of adult neural stem cells

RaLP wild-type and KO mice were sacrificed according to standard procedures and the brains of the mice were carefully dissected and placed in ice cold PBS. Under the stereomicroscope, the brain was sectioned into three parts and the central slice was used to isolate the area surrounding the subventricular zone. The tissue was cut into small pieces with fine scissors and the pieces were placed into 60-mm plates with PBS containing 1 mg/mL Papain Lyo (Worthington), 0.2 mg/mL Disodium Ethylene Diamine Tetra-Acetate (EDTA) and 0.2 mg/mL cysteine (Sigma), and incubated at 37°C for 1 h. The digested tissue was collected by centrifugation at 233 × *g* for 10 min at 4°C. The supernatant was carefully discarded and the pellet was resuspended in 1 mL of Neurocult culture medium which consists of NeuroCult® NS-A (StemCell Technologies Inc) supplemented with 10% NeuroCult® NS-A Proliferation supplements (StemCell Technologies Inc), 10 ng/mL FGF2 (Peprotech), 20 ng/mL EGF (Peprotech) and 2 μg/mL Heparin (Sigma). The cell

suspension was transferred to 35-mm plates and cultured in a humidified atmosphere of 5% CO_2 at 37°C. Cultures were monitored daily for the appearance of characteristic aggregates called neurospheres.

1.7.2. Culturing NSCs

Neurospheres were routinely cultured in Neurocult culture medium and passaged every three to four days. Neurospheres were collected and centrifuged at 28 × *g* for 10 min at 4°C. The spheres were dissociated by gentle pipetting in a low volume of fresh medium. Single cells were passaged by seeding 2×10^5 cells in T25 flasks and 6×10^5 cells in T75 flasks.

1.7.3. Freezing and thawing of NSCs

For the cryopreservation of NSCs, the neurospheres were collected by centrifugation and resuspended directly in freezing medium (Neurocult culture medium and 10% DMSO) without disaggregation of the spheres. For the thawing of the cells, the contents of the cryovial were warmed to 37°C, transferred to 10 mL medium and centrifuged at 28 × *g* for 10 min at 4°C. The spheres were gently resuspended in fresh medium and seeded into T25 or T75 flasks.

1.7.4. Differentiation of NSCs

24-well plates containing glass coverslips were coated with Matrigel™ (BD Biosciences) diluted at 1:100 in PBS, and incubated at 37°C for 2 h. Single cells were plated at 6×10^4 cells per well in Neurocult medium. After 48 h, the medium was changed to Neurocult without FGF2 and EGF, and additioned with 2% FBS, to induce differentiation. Cells were analysed after a further three to five days of differentiation, by immunofluorescence.

2. Protein methods

2.1. RaLP antibody generation

The RaLP antibody was generated in collaboration with the Biochemistry Unit at the IFOM-IEO campus. Antibodies against the SH2 region of murine RaLP was raised using the peptide sequence of 16 amino acids: QPYRKYDNTGLLPPKK [22]. This synthesised peptide sequence corresponds to the most carboxy-terminal part of the protein, which is specific for RaLP and not present in the other three members of the family. The immunised sera was tested on RaLP overexpressing cell lines by Western blotting and the reactive sera was immunopurified by Sulfolink columns, according to the manufacturer's instructions.

2.2. Western blotting

2.2.1. Lysate preparation

Cells were washed in PBS and collected by centrifugation. Cell pellets were flash frozen in liquid nitrogen and stored at -80°C until use. Cell lysates were prepared on ice using Radio Immuno Precipitation Assay (RIPA) buffer (150 mM sodium chloride, 1% Triton X-100, 0.5% sodium deoxycholate, 0.1% SDS and 50 mM Tris pH8.0) or Laemmli Sample Buffer (62.5 mM Tris HCl pH 6.8, 2% SDS, 10% glycerol), freshly supplemented with protease inhibitor cocktail Complete Mini (Roche), phosphatase inhibitor mix PhosSTOP (Roche) and 50 mM Dithiothreitol (DTT). Benzonase nuclease (Sigma) was added at a final concentration of 0.05 units/μL of lysate and was incubated at 4°C for 10 min to digest genomic DNA and reduce viscosity. Samples were further lysed by sonication. After 20 min of incubation on ice, samples were centrifuged at maximum speed (16060 × *g*) for 15 min at 4°C to pellet cell debris and the supernatants were collected. Protein concentration was determined by the Bradford assay using BSA (Sigma) as a protein standard. Lysates were measured at 595 nm with the spectophotometer.

2.2.2. Immunoblotting

Depending on the antigen to be detected, 30 to 100 μg of protein lysate were mixed with 6× Laemmli Sample Buffer with 0.01% bromophenol blue and added freshly with DTT. Samples were denatured at 95°C for 5 min. Samples were electrophoresed on 8, 10 or 12% sodium dodecyl sulfate polyacrylamide (SDS-PAGE) gels and prestained and nonstained molecular weight markers (Biolabs) were also loaded on the gel for the determination of protein size and to monitor the run. The proteins were transferred onto nitrocellulose (Whatman) or poly-vinylidene fluoride (PVDF) Immobilon™-P transfer (Millipore) membranes in wet conditions using the Mini Trans-Blot® Electrophoretic Transfer Cell (BioRad) at 100 V for 1 h or 30 V overnight, at 4°C. The efficiency of protein transfer and even loading between the samples were checked by incubating the membrane for 5 min in Ponceau Red. Membranes were blocked in 5% skimmed milk powder (w/v) in Tris-buffered saline with 0.1% Tween 20 (TBST) or 5% BSA (w/v) in TBST for the detection of phosphorylated proteins, for 1 h at RT. Primary antibodies were diluted in 1 to 5% skimmed milk powder in TBST or 5% BSA in TBST (for working dilutions and supplier of antibodies see Table 1) and membranes were incubated at 4°C overnight with rocking. Blots were washed for 5 min at least three times in TBST. Membranes were incubated with secondary antibodies goat-anti-mouse IgG or goat anti-rabbit IgG conjugated with horseradish peroxidase (Bio-Rad) diluted at 1 to 10,000 in 5% skimmed milk powder in TBST for 1 h at RT. Membranes were washed three times for 10 min each in TSBT and bands were detected using Amersham ECL Plus Western Blotting Detection Reagents (GE Healthcare) following the manufacturer's instructions.

2.2.3. Membrane stripping and reblotting

Membranes were stripped of primary and secondary antibodies in Stripping Buffer (2% SDS, 62.5 mM Tris pH6.8 in water) freshly added with 100 mM β-mercaptoethanol (BDH) and incubated at 56°C for 30 min, with agitation every 10 min. Blots were washed

thoroughly in TBST for a total of 30 min and blocked and reprobed for another antigen, as described in Section 2.2.2.

Table 1. Primary antibodies used in Western blotting analysis.

Antigen	Working dilution	Supplier
RaLP	1:100	Home-made
Phospho-Erk1/2 (Thr202/Tyr204)	1:2000	Cell Signaling (9106)
Erk1/2	1:5000	Santa Cruz (sc-94)
Phospho-SMAD2 (Ser465/467)	1:1000	Cell Signaling (3108)
SMAD2	1:1000	Cell Signaling (3103)
Vinculin	1:15000	Sigma (V9131)

2.3. Immunohistochemistry

The teratomas were washed in PBS for 30 min to remove blood and fixed in 4% buffered formalin for 10 h. After paraffin embedding, consecutive 3 μm sections were mounted onto electrostatically charged glass slides. After heat drying, sections were deparaffinised in xylene two 5 min treatments and sequentially rehydrated in 100%, 70%, and 50% ethanol. Antigen unmasking pretreatments were performed according to the antibody and the sections were incubated in 3% aqueous hydrogen peroxide for 5 min to quench endogenous peroxidase activity. Primary antibodies for markers of differentiation (for working dilutions and supplier see Table 2) were diluted in Dako REAL™ Antibody diluent and immunostained using the Autoimmunostainer (DakoCytomation).

Table 2. Primary antibodies used for immunohistochemical analysis.

Antigen	Working dilution	Antigen unmasking	Supplier
GFAP	1:400	none	Dako (6F2)
Myogenin	1:800	none	Dako (F5D)
Keratin	1:400	pepsin 5 min 37°C	Dako (MNF 116)

Commercially available detection kit (Dako EnVision Plus-HRP) was used, according to the manufacturer's instructions. Peroxidase activity was developed with 3-3'-diaminobenzidine-copper sulfate (Sigma Chemical, St Louis, MO) to obtain a brown-black end product. Sections were then counterstained with 1% modified Harris hematoxylin, dehydrated in two times for 5 min each in 100% alcohol and twice for 5 min in xylene, and mounted with Eukitt™ (quick-hardening mounting medium for microscopy). Images were taken using the microscope Olympus Upright BX51 equipped with a Nikon colour camera.

2.4. Alkaline phosphase staining

ESCs were seeded onto 0.1% gelatinised 6-well plates and allowed to grow for five days. Staining for alkaline phosphase was done following the manufacture's instructions (Chemicon). Briefly, sodium nitrite solution and FRV alkaline solution was prepared and then the AS-BI alkaline solution was added to the mixture. The cells were rinsed with PBS and then fixed in formaldehyde, acetone and citrate solution containing fixative for 30 sec. The alkaline solution was added and reaction was allowed to develop at RT for 15 min in the dark. The stained wells were then rinsed in water. ESCs stain red for positivity of alkaline phosphatase and differentiated cells remain unstained.

2.5. Immunofluorescence

Cells grown on coverslips were fixed for 15 min in 4% PFA and washed three times in PBS for 5 min each. Cells were permealised for 10 min in 0.1% Triton X100. Aspecific binding was saturated by blocking in 5% goat serum (v/v; Euroclone) or 2% BSA (w/v) in PBS for 45 min at RT. Primary antibodies were diluted in blocking solution (for working dilutions and supplier, see Table 3) and cells were incubated for 1 h at RT. Cells were washed three times 5 min each in PBS and incubated with the appropriate fluorescently labelled secondary antibodies (Invitrogen and Jackson) diluted in PBS (for working

dilutions and supplier, see Table 1), for 1 h at RT. Unbound secondary antibody was removed by three washes of 5 min each in PBS. Nuclei were counterstained with 1 μg/mL 4',6-diamidino-2-phenylindole (DAPI; Sigma) in PBS for 30 min, coverslips were dipped in water, blotted to remove excess moisture and mounted onto slides in mowiol (Calbiochem). For combination with conjugated antibodies, following the three washes in PBS following the secondary antibody incubation, the primary-secondary complexes were post-fixed by 4% PFA treatment for 5 min. The cells were rinsed three times 5 min each in PBS and permealised for 10 min in 0.1% Triton X100 and blocked again in 2% BSA in PBS with 1:250 of mouse Gamma globulin IgG (Jackson) for 20 min at RT. Coverslips were incubated with antibodies directly conjugated with fluorochromes for 1 h at RT. Cells were washed three times 5 min each in PBS and incubated with 1 μg/mL DAPI in PBS for 30 min. Coverslips were dipped in water, blotted to remove excess moisture and mounted onto slides in mowiol. Images were acquired with an Olympus fluorescence microscope equippd with a CoolSNAP *EZ* CCD camera (photometrics), using the MetaMorph® imaging software (Molecular Devices). For clarity, images were adjusted for contrast and brightness, and merged using Adobe Photoshop.

Table 3. Antibodies used for immunofluorescence.

Antigen	Working dilution	Supplier
β-III-tubulin	1:2000	Covance (MMS-435P)
MAP2	1:200	Chemicon (MAB3418)
Nestin	1:200	Chemicon (MAB353)
Oct3/4	1:500	Santa Cruz (sc-5279)
Nanog	1:50	R&D systems (AF2729)
GFAP	1:500	Dako (6F2)
Sox1	1:50	Santa Cruz (sc-17318)
Phalloidin-TRITC	1:10	Sigma (P1951)

Cdx2	1:50	Biogenex (CDX2-88)
Oct3/4-Alexa Fluor 647	1:20	BD Pharmigen (560329)
Phospho-Erk1/2 (Thr202/Tyr204)	1:500	Cell Signaling (9106)
Goat anti-rabbit FITC	1:50	Invitrogen
Goat anti-mouse Cy5	1:400	Invitrogen
Donkey anti-mouse Alexa Fluor 488	1:100	Jackson

2.5.1. Image acquisition by confocal analysis

For immunofluorescence of EpiSC cultures, images were acquired using the Leica SP5 Confocal Microscope at a 40× 1.25 NA oil immersion objective. To preserve statistical significant sensitivity and resolution, large fields of view (>1.2 mm) were acquired with a mosaic approach using the Matrix Software (Leica Microsystems).

2.6. Flow cytometry analysis for intracellular antigens together with EdU detection

To measure the proliferation rate of the cells, a thymidine analogue, 5-ethynyl-2'deoxyuridine (EdU) was added to the cells in culture at a concentration of 10 μm for a pulse of 30 min. The supernatant of cells was collected together with the adherent cells, which were detached in accutase® at 37°C for 5 min. Cells were dissociated into single cell suspension by pipetting and centrifuged at 524 × *g* for 5 min. The pellet was resuspended in PBS and cell suspension was brought to a concentration of 10^6 cells/mL and distributed into tubes. Cells were spun down at 7000 × *g* for 5 min and resuspended in 500 μL of PBS and fixed by the addition of an equal volume of 2% formaldehyde and incubated on ice for 20 min. Cells were washed in 1 mL 1% BSA in PBS and were resuspended in 500 μL PBS and immediately processed for staining or stored at 4°C until use. Cells were permealised in 100 μL of Triton X-100 provided by the Click-iT® EdU Pacific Blue™ Flow Cytometry Assay Kit (Invitrogen A10034) for 15 min in ice. Cells were washed in 1 mL 1% BSA in PBS and resuspended in 100 μL 1% BSA in PBS for 30 min for blocking of unspecific

binding. Cells were resuspended in primary antibody diluted in 100 µL of 1% BSA in PBS, for 1 h at RT (for working dilutions and supplier, see Table 4). After washing in 500 µL of 1% BSA in PBS, cells were resuspended in 100 µL of 1% BSA in PBS containing secondary antibody and incubated for 1 h at RT (for working dilutions and supplier, see Table 4). After another wash in 1% BSA PBS, cells were then processed for EdU detection for 45 min at RT, following manufacturer's instructions. Cells were finally resuspended in PBS containing 2.5 µg/mL propidium iodide (PI; Sigma) and 250 µg/mL RNase (Roche) and were left at 4°C overnight before acquisition. Negative samples were prepared by incubating only with secondary antibody.

Table 4. Antibodies used for FACS analysis.

Antibody	Working concentration	Supplier
Oct3/4	1:100	Santa Cruz (sc-5279)
Cleaved caspase-3 (Asp175)	1:50	Cell Signaling (9664)
Goat anti-rabbit FITC	1:50	Invitrogen
Donkey anti-mouse A647	1:100	Jackson

Samples were acquired using the BD FACS Canto™ II equipped with laser 488 nm, 633 nm and 405 nm. Data was analysed by the BD FACS Diva software version 6.1.1. Aggregates were excluded from analysis by appropriate gating of PI fluorescence.

3. DNA methods

3.1. Genotyping for RaLP

Genomic DNA (gDNA) was extracted from ESCs cultured on 0.1% gelatin with the DNA extraction kit DNeasy Blood and Tissue (Qiagen) following manufacturer's instructions. GDNA was eluted in water. The genotyping strategy was set up in collaboration with

Genoway for the generation of the RaLP KO mouse (for details refer to results section 2). Two PCR reactions were set up using two sets of primer pairs, differing for the reverse primer. With the two PCR reactions, the RaLP allele WT, HT or KO can be distinguished. The sequences of the primers are (5'-3'):

GTRaLPF: AGATCAGATCCTCAGGAGCCAGAGG

GTRaLPR2: TACCCTCACAGACCTTCAGAGCTGG

GTRaLPR1: CCTTGGAGCAAAGTGGATCTGACTCTGG

PCR conditions: denaturation at 95°C for 15 min followed by 35 cycles of 94°C 15 sec, 65°C 1 min, 68°C 15 min, then 68°C for 10 min. The PCR products were run on a 1% agarose gel in Tris-acetate-EDTA (TAE) buffer with 0.5 μg/mL ethidium bromide with 1kb DNA ladder (Biolabs).

3.2. Genotyping for the presence of the Y chromosome

For assessing the sex of the ESCs, the PCR strategy for the Y-linked gene *Sry* was employed [86].

Sry F: TGACTGGGATGCAGTAGTTC

Sry R: TGTGCTAGAGAGAAACCCTG

PCR conditions: denaturation at 95°C for 5 min followed by 35 cycles of 95°C 30 sec, 65°C 30 min, 72°C 45 min, then 72°C for 10 min. The PCR products were run on a 1% agarose gel in TAE with 0.5 μg/mL ethidium bromide with 1kb DNA ladder (Biolabs).

3.3. Karyotyping

ESCs plated on 0.1% gelatin at 70% of confluency were cultured in the presence of 0.1 μg/mL KaryoMAX® colcemid (Gibco) for 1 h, to block the metaphases. Cells were then trypsinised, collected and centrifuged at 520 × *g* for 10 min. After discarding the supernatant, 0.075M KCl hypotonic solution was added drop by drop to the pellet and incubated at 37°C for 30 min. For pre-fixation, four to five drops of fixative consisting of

three parts methanol and one part acetic acid, were added to the solution, followed by centrifugation at 520 × *g* for 10 min. Cells were resuspended gently by adding drop by drop while vortexing, 10 mL of fixative and centrifuged at 520 × *g* for 10 min. The pellet was resuspended in 1 mL fixative and 60 μL of the solution was dropped onto each slide pre-warmed at 57°C from about 30 cm in height. The drop was allowed to spread over the surface and dried. Metaphases and nuclei were stained in 1 μg/mL DAPI in Saline Sodium Citrate (SSC) for 5 min and dried overnight and then mounted in mowiol. For each slide, ten metaphases were randomly picked and those that were well spread and intact were scored for the number of chromosomes. Images were acquired with an Olympus fluorescence microscope equipped with a CoolSNAP *EZ* CCD camera (Photometrics).

4. RNA methods

4.1. RNA extraction and quantification

Total RNAs were extracted from cells using the RNeasy Mini kit (Qiagen) following manufacturer's instructions. GDNA was digested by on column treatment with RNAse-Free DNAse (Qiagen) at RT for 15 min. RNA was eluted with RNAse free water. RNA was quantified with the Nanodrop ND-1000 Spectrophotometer (Thermo Scientific).

Total RNA was extracted from blastocysts using the RNA picopuro extraction kit (MDS Arctus) following manufacturer's instructions.

4.2. cDNA synthesis

For each sample, 1 μg of total RNA was reverse transcribed using Superscript III Reverse Transcriptase (Invitrogen) with 250 ng/μL random primers (Invitrogen) and 10 mM dNTPs (Invitrogen) in 20 μL of reaction volume, in the presence of 2U/μL of RNase inhibitor

RNase OUT™ (Invitrogen). Samples were incubated at 25°C for 5 min, 50°C for 1 h and 70°C for 15 min.

4.3. Quantitative real time PCR

Quantitative real-time PCR (qRT-PCR) was performed on 7900HT Fast Real-Time PCR system (Applied Biosystems) using Fast SYBR® Green PCR Master Mix or TaqMan® Gene expression assays (Applied Biosystems). Correct PCR products were confirmed by melting curve analysis. Each sample was analysed in triplicates and normalised to an endogenous control. Normalisation was used to correct sample-to-sample variations in RNA concentration and integrity. Relative mRNA amounts were calculated by the comparative cycle threshold (Ct) method using the formula $2^{-\Delta Ct}$. Primers that were designed in house were done when possible spanning two exons and amplified sequence between 100 to 120 bp, using the Primer 3 program.

Table 5. Primer sequences.

Gene	Primer sequence (5'-3')	Application
RaLP p69	F: GGGCCCATGGAGCCATTAAAA R: CTTTTGCCAAGAACCGTTGTCA Reporter: ACTTAACGGGAGCCTTTC	Custom Taqman gene expression assay
TBP	Applied Biosystems ID: Mm00446973_m1	Taqman gene expression assay
TBP	F: CTGGAATTGTACCGCAGCTT R: TCCTGTGCACACCATTTTTC	SYBR® green real-time PCR
Oct 3/4	F: CCAATCAGCTTGGGCTAGAG R: CTGGGAAAGGTGTCCCTGTA	SYBR® green real-time PCR
Nanog	F: AAGGATGAAGTGCAAGCGGTG R: GGATAGCTGCAATGGATGCTG	SYBR® green real-time PCR
Rex1	F: GGACTAAGAGCTGGGACACG R: GCGATCCTGCTTTCTTCTGT	SYBR® green real-time PCR
Klf4	F: CTCTGCTCCCGTCCTTCTC R: AGAGAGTTCCTCACGCCAAC	SYBR® green real-time PCR
Sox2	F: CTCTGCACATGAAGGAGCAC R: ATGTAGGTCTGCGAGCTGGT	SYBR® green real-time PCR

Sox1	F: AGATGCACAACTCGGAGATCAG R: GAGTACTTGTCCTTCTTGAGCAGC	SYBR® green real-time PCR
Fgf4	F: TGGGTGTGATGCTGTTTCAT R: CTCAGGGTCCTTCTCACTGC	SYBR® green real-time PCR
Fgf5	F: GCTGTGTCTCAGGGGATTGT R: CATCCGTAAATTTGGCACTTG	SYBR® green real-time PCR
Otx2	F: ACAAGTGGCCAGTTCAGTCC R: CTGGGTGGAAAGAGAAGCTG	SYBR® green real-time PCR
Nestin	F: AGGCTGAGAACTCTCGCTTGC R: GGTGCTGGTCCTCTGGTATCC	SYBR® green real-time PCR
Brachyury [87]	F: CCTCCCTTGTTGCCTTAGAGTAGTT R: GCAGATTGTCTTTGGCTACTTTGTC	SYBR® green real-time PCR
Gata 4	F: CTGTGCCAACTGCCAGACTA R: CCTGCTGGCGTCTTAGATTT	SYBR® green real-time PCR
Gata 6	F: ATGCTTGCGGGCTCTATATG R: TACCGGAGCAAGCTTTTGAC	SYBR® green real-time PCR
Cdx2	F: TCACCATCAGGAGGAAAAGTG R: CTGCTGCTGCTTCTTCTTGA	SYBR® green real-time PCR
Hand1 [87]	F: CCCCTCTTCCGTCCTCTTAC R: CTGCGAGTGGTCACACTGAT	SYBR® green real-time PCR
Tbx3	F: GAACCTACCTGTTCCCGGAAA R: CAATGCCCAATGTCTCGAAAAC	SYBR® green real-time PCR
Foxa2	F: TAGCGGAGGCAAGAAGACC R: CTTAGGCCACCTCGCTTGT	SYBR® green real-time PCR
Stella	F: TGTCGGTGCTGAAAGACCCTAT R: TTTCCTTCGAGCCTTTTTTGTC	SYBR® green real-time PCR
Cer1	F: CTCTGGGGAAGGCAGACCTAT R: CCACAAACAGATCCGGCTT	SYBR® green real-time PCR
Sox7	F: ATGCTGGGAAAGTCATGGAAG R: CGTGTTCTGGTCACGAGAGA	SYBR® green real-time PCR
Flk1	F: GGGTCGATTTCAAACCTCAATGT R: AGAGTAAAGCCTATCTCGCTGT	SYBR® green real-time PCR
Ck18	F: CAGCCAGCGTCTATGCAGG R: CTTTCTCGGTCTGGATTCCAC	SYBR® green real-time PCR
Ck19	F: GGGGTTCAGTACGCATTGG R: GAGGACGAGGTCACGAAGC	SYBR® green real-time PCR
Sox17	F: CGAGCCAAAGCGGAGTCTC R: TGCCAAGGTCAACGCCTTC	SYBR® green real-time PCR

4.4. RNA whole mount *in situ* hybridisation

Until the hybridisation step, all solutions for washing or incubating the specimens were prepared with diethyl pyrocarbonate (DEPC)-treated water or PBS. DEPC was added at a final concentration of 0.1% and solutions were autoclaved to hydrolyse any remaining DEPC.

4.4.1. Collection of embryos

Embryos were dissected away from the extraembryonic tissues in PBS with 1% FBS. Embryos were fixed in 4% paraformaldehyde in PBS at 4^{o}C overnight. Embryos were then washed in DEPC treated PBS containing 0.1% Tween-20 (PBT) three times, 5-10 min each. They were dehydrated in consecutive 5 min treatment in 25%, 50%, 75% methanol in PBT and two times in 100% methanol. Embryos were stored at -20^{O}C until use.

4.4.2. Probe preparation

For linearisation of the *in situ* plasmid (Figure 9), 10 µg of plasmid DNA was incubated with 10-20 units of the restriction enzyme, NotI for 1 h. An equal volume of phenol/chloroform/IAA (25:24:1) was used to extract the digest, followed with a chloroform/IAA (24:1) extraction. One µl of glycogen and 5 µl of 3M NaOAc (pH 5.2) were added to the extracted DNA and then 110 µl of cold 100% ethanol was added and stored at -20 ^{o}C for 1 h. To pellet the DNA, the mixture was centrifuged at at maximum speed (16060 × *g*) for 20 min at 4 ^{o}C. The pellet was rinsed with 70% ethanol and allowed to air dry. The pellet was resuspended in 10 µl DEPC-treated water to have a final concentration of linearized plasmid of about 1 µg/µl. For the synthesis of the digoxigenin (DIG)-labelled probe, the DIG RNA labeling kit (Boehringer no. 1175 025) was used following the manufacturer's instructions.

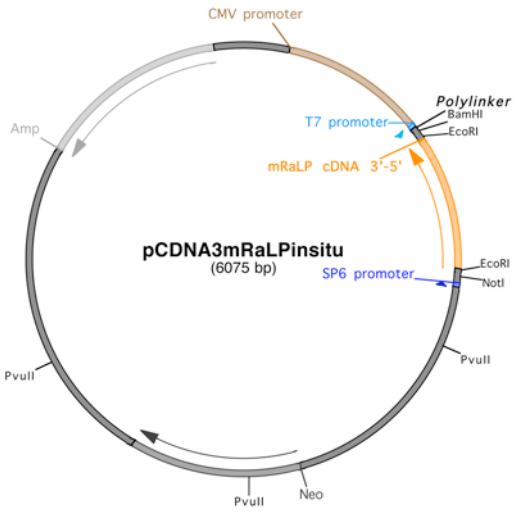

Figure 9. Map of the plasmid containing the RaLP cDNA used as template to synthesise the anti-sense probe for *in situ* hybridisation. The plasmid was linearised with NotI and the probe was *in vitro* transcribed by T7 RNA polymerase.

4.4.3. In situ hybridisation

Prior to hybridisation, embryos were rehydrated in reverse order in the methanol/PBT series. Embryos were rinsed twice in PBT for 5 min each. Embryos were then bleached by incubating for 1 h in fresh 6% hydrogen peroxide (H_2O_2) in PBT followed by three washes of 5 min each in PBT. Embryos were incubated in 10 µg/ml proteinase K in PBT for 5-10 min and washed for 5 min in 2mg/ml glycine in PBT, twice for 5 min each in PBT and fixed again in 4% PFA additioned with 0.2% glutaraldehyde for 20 min at RT. After another two washes in PBT, the embryos were washed for 10 min in a 1:1 mixture of PBT and hybridisation solution [50% formamide, 5× SSC, 0.1% Tween-20, 0.1% SDS, 50 µg/mL heparin, 50 µg/mL yeast tRNA and 60 mM citric acid (Sigma)]. Embryos were then incubated at 70 ºC in hybridisation solution for 2 h and then incubated with 50 to 100 ng of probe (2-4 µl/ml) in hybridisation solution and incubated overnight at 70ºC. The next day, embryos were washed in prehybridisation solution for 5 min at 70 ºC, followed by three 30 min washes in wash solution I (50% formamide, 5× SSC, 0.06 M citric acid, 1% SDS) at 70 ºC, then another three 30 min washes in wash solution II (50% formamide, 2× SSC, 0.024 M citric acid, 0.2% SDS, 0.1% Tween) at 65ºC. Then the embryos were

washed three times for 5 min each in MAB buffer (0.012 g/mL maleic acid, 0.17 M NaCl, 0.001% Tween-20; pH was adjusted to 7.5 by the addition of NaOH pellets) at RT. In order to prevent nonspecific binding, embryos were incubated for 1 h in MAB with 2% Boehringer blocking reagent (from DIG detection kit) containing 10% heat-inactivated sheep serum. Blocking solution was then removed and antibody was added and rocked overnight at 4 ^{o}C. The next day, embryos were washed five times for 1 h each in MAB and washed overnight in 2 mM levamisole (Sigma) in MAB at 4^{o}C in order to inhibit endogenous phosphatases. For colour development, the embryos were washed for 10 min three times in alkaline phosphatase buffer at RT then stained by incubation in development solution at RT until the desired level of staining developed. Then reaction was stopped by rinsing twice in 2 mM EDTA in PBT. Embryos were post-fixed in 4% PFA/0.1% glutaraldehyde in PBT for 1 h at RT or overnight at 4^{o}C and washed twice in PBT.

Results

1. Characterisation of RaLP expression in the mouse

In order to gain insight into the function of RaLP and to identify the ideal model system to characterise its role and dissect its signalling pathway, the expression pattern of this gene during development and in the adult mouse was first investigated.

1.1. Expression pattern of RaLP during embryogenesis

1.1.1. RaLP expression in preimplantation and early post-implantation embryos

Preliminary studies on RaLP expression conducted at the beginning of this PhD project using embryonic stem cells (ESCs) and the embryoid body differentiation protocol evidenced its expression at low levels in the ESCs and its upregulation during the early stages of ESC commitment (described in detail in results section 4). These results prompted us to investigate the expression of RaLP *in vivo* by qRT-PCR and whole mount *in situ* hybridisation (WISH) on the pre-implantation and early postimplantation embryos. The qRT-PCR analysis evidenced low RaLP expression in the morula at E2.5 and higher expression in the inner cell mass, isolated by immunosurgery, of the early blastocyst at E3.5 (Figure 10A). The first differentiation event that occurs in the embryo is during the formation of the blastocyst at E3.5 and at this stage, the cells are allocated to either the embryonic (inner cell mass) or extraembryonic lineages (trophoblast). In order to confirm RaLP expression specifically in the inner cell mass and not in the trophoblast, we decided to proceed with WISH of embryos at E3.5 (Figure 10B). We found that RaLP transcript was detected only in the inner cell mass.

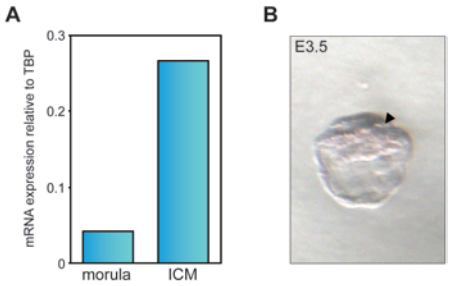

Figure 10. Analysis of RaLP expression in the morula and blastocyst by qRT-PCR and whole mount *in situ* hybridisation. (A) qRT-PCR for RaLP in the morula and inner cell mass (ICM) of wild-type embryos. The relative expression values were normalized to TBP. **(B)** WISH for RaLP in blastocyst at E3.5 shows the presence of the transcript in the ICM (indicated by black arrowhead).

The WISH on later stages of embryonic development revealed RaLP expression also in the epiblast of the embryo at E4.5 (Figure 11). Around the time of implantation at E4.5, the inner cell mass is further segregated into the epiblast and the surrounding primitive endoderm (hypoblast). However, from this WISH, the expression of RaLP in the primitive endoderm cannot be excluded. The expression of RaLP in the epiblast was transient as it could no longer be detected at E5.5 and throughout the stages of E6.5 and E7.5.

These results suggest a specific function of RaLP in a narrow developmental window during which the epiblast of the pre-implantation embryo transforms into the epiblast of the post-implantation embryo.

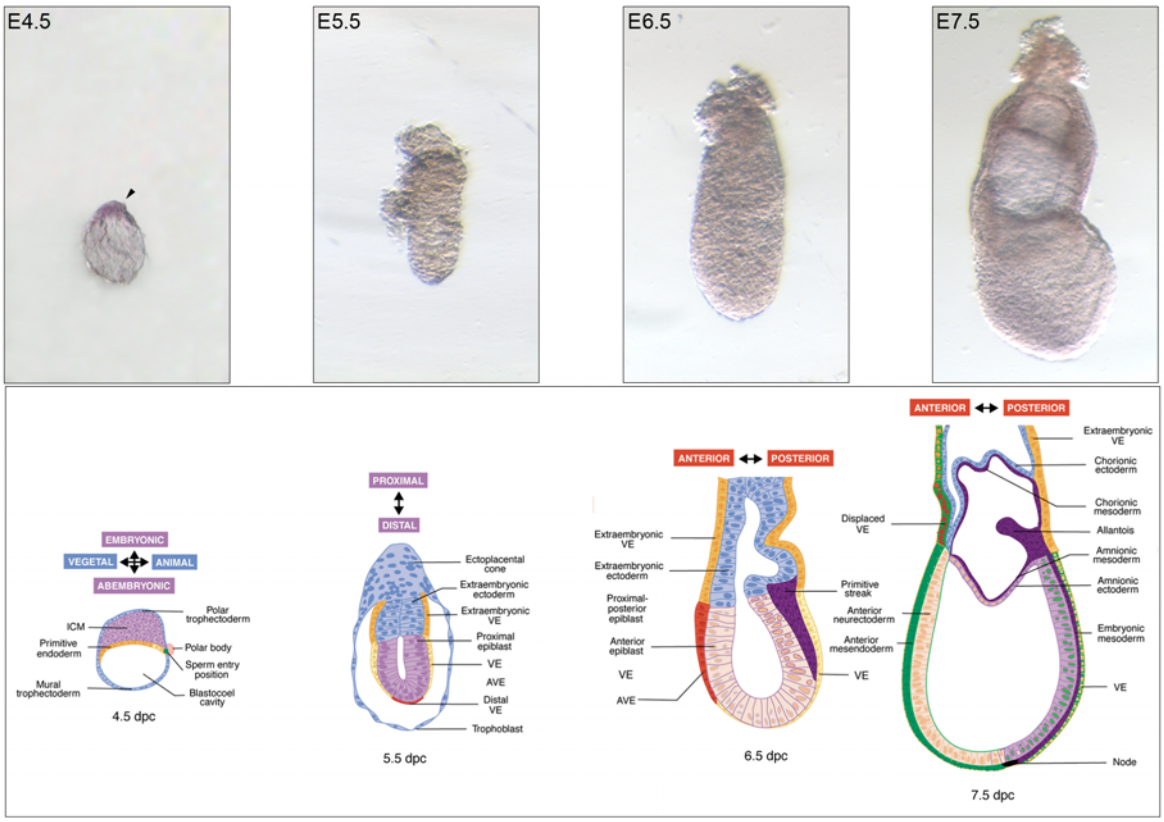

Figure 11. Whole mount *in situ* hybridisation of RaLP in early post-implantation embryos. Embryos at E4.5 (peri-implantation), E5.5, E6.5 and E7.5 were probed for the presence of RaLP transcript (upper panel). RaLP was detected at E4.5 in the inner cell mass/epiblast (black arrow). The illustration in the lower panel describes the formtation of the compartments of the embryo at the same timepoints (adapted from Lu C. et al., Curr Opin Genet and Dev 2001 [88]). Abbreviations: anterior visceral endoderm (AVE), days post coitum (dpc), inner cell mass (ICM), visceral endoderm (VE).

To investigate whether RaLP expression is then induced after gastrulation stages, embryos at E8.5 were analysed (Figure 12). RaLP expression appears in the developing neural tube, suggesting that when neural specification begins, RaLP is *de novo* upregulated.

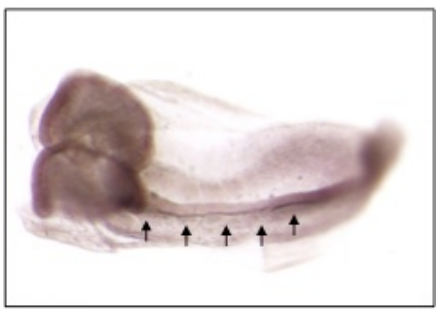

Figure 12. Whole mount *in situ* hybridisation of RaLP in E8.5 embryo. Signals of the RaLP transcript were detected along the neural tube (black arrows).

1.1.2. Radioactive in situ hybridisation in embryos from E10.5 to E16

For the determination of the temporal-spatial expression pattern of RaLP during later stages of development, with particular attention as to whether RaLP is expressed in the nervous system, RaLP transcripts were detected using radioactively labelled probes on sagittal and transversal sections of embryos of day E10.5, E12.5 and E16 (Figure 13). At E10.5 RaLP expression was evident in the cephalic ganglions V, VII, VIII, IX, subregion of the optic vesicle (ov), dorsal root ganglia (drg), basal region of the forebrain corresponding to the septum (se), cortex (cx) and the anterior hypothalamus (ahy). Notably, these are all regions that derive from neural crest cells. Signal was also detected in the dorsal aorta (da), a region rich in haematopoietic percursors, that is however often a source of aspecific signal.

Slightly later at E12.5, the general expression pattern remained constant, with evident expression also in the cephalic ganglion V (V), the pineal gland (pi), the internal ear (ie) at the level of the primordial cochlea (co) and the olfactory epithelium (oe). Furthermore, RaLP transcripts were observed ubiquitously in the developing central nervous system (CNS) and in particular, the subventricular region of the telencephalon (te), diencephalon (di), mesencephalon (ms) and the precursor area of the cerebellum (cbp).

At E16, RaLP expression was maintained in the CNS and signal could be detected also at the level of the basal ganglia (ba), in the pons (po) as well as the rostral migratory steam (rms) extending to the olfactory bulb (ob). At this developmental stage, it seemed that low RaLP levels were present also throughout other organs such as the intestines (gu), kidney (ki), liver (li), lungs (lu), thymus (ty), tongue (to) and mandible (ma).

These results show that RaLP is expressed in areas of the developing brain, suggesting a neural function of this gene during later stages of embryogenesis.

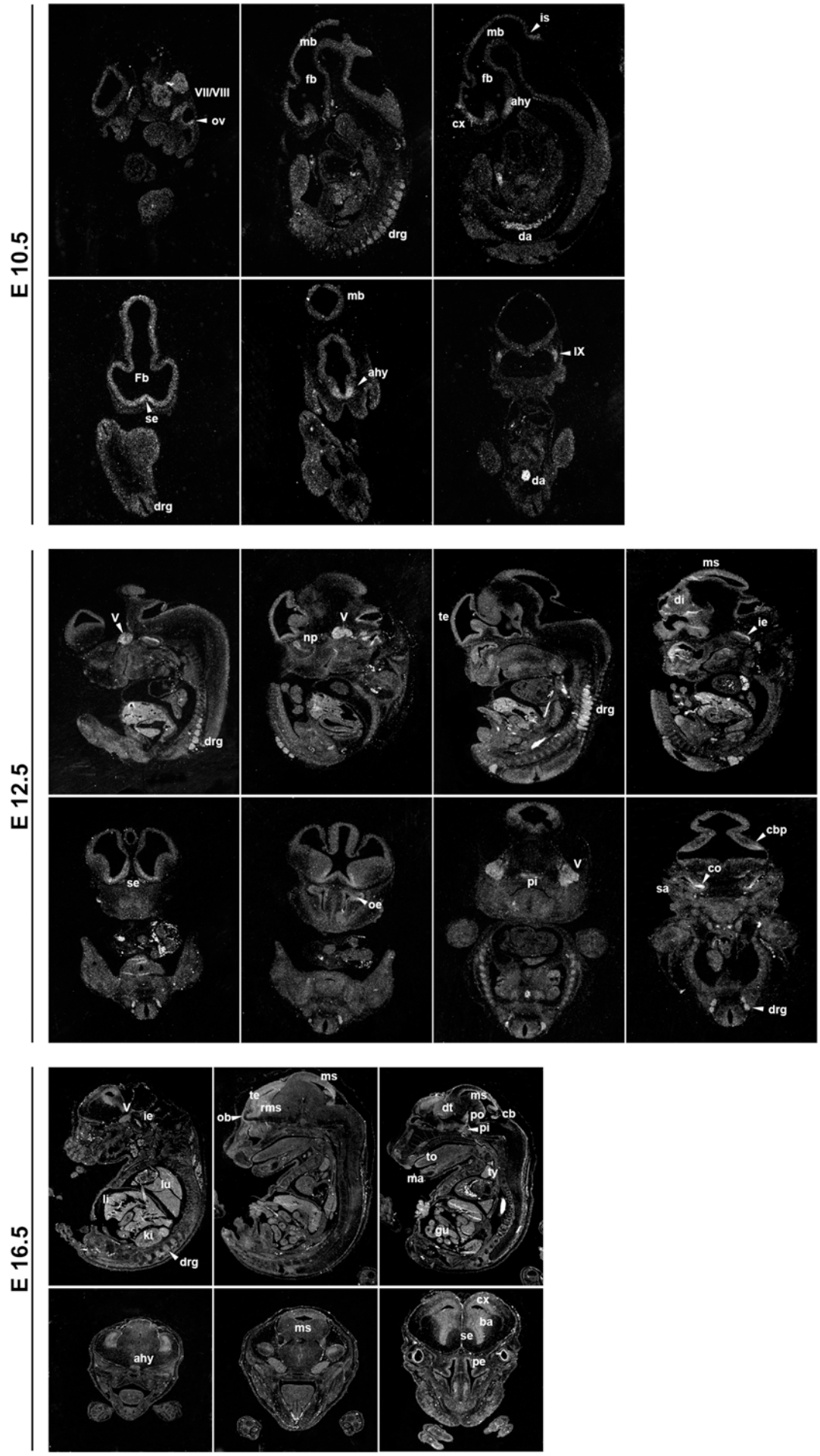
E 10.5
VII/VIII
ov
mb
fb
drg
is
mb
fb
ahy
cx
da
Fb
se
drg
mb
ahy
IX
da
E 12.5
V
drg
V
np
te
drg
ms
di
ie
se
oe
V
pi
cbp
co
sa
drg
E 16.5
V
ie
lu
li
ki
drg
ms
te
rms
ob
ms
dt
po
cb
pi
to
ma
ty
gu
ahy
ms
cx
ba
se
pe

Figure 13. Radioactive *in situ* hybridisation for RaLP in E10.5, E12.5 and E16.5 mouse embryos. For each embryonic stage, the panel consists of two rows: the upper row shows sagittal sections and the lower row shows transverse sections of the embryos, at different heights. Regions of signal are indicated by abbreviations and/or white arrowhead. In summary, RaLP transcripts were evidenced in the dorsal root ganglia, cranial ganglia and regions of the developing brain. Abbreviations: anterior hypothalamus (ahy), basal ganglia (ba), cephalic ganglion V (V), cephalic ganglion IX (IX), cerebellum (cb), cerebellar precursors (cbp), cortex (cx), primordial cochlea (co), dorsal aorta (da), diencephalon (di), dorsal root ganglia (drg), dorsal thalamus (dt), forebrain (fb), intestines (gu), internal ear (ie), kidney (ki), liver (li), lungs (lu), mandible (ma), midbrain (mb), mesencephalon (ms), olfactory bulb (ob), olfactory epithelium (oe), optic vesicle (ov), pineal gland (pi), pons (po), rostral migratory stream (rms), septum of forebrain (se), telencephalon (te), tongue (to).

1.2. Expression pattern of RaLP in the adult mouse

Following the specific expression of RaLP in the developing nervous system of the embryo during later stages of development, its expression in adult tissues was examined by quantitative real-time polymerase chain reaction (qRT-PCR) to determine whether this pattern of expression was maintained and whether it could be an interesting area to focus our studies on. The results showed that RaLP was expressed in all the different brain regions, the olfactory bulb, cerebral hemispheres and cerebellum, at high levels compared to the other tissues (Figure 14). The cerebellum expressed the highest levels of RaLP. All other tissues had low or undetectable levels of RaLP transcripts. This data is in agreement with results published by Jones and colleagues [22], at the protein level.

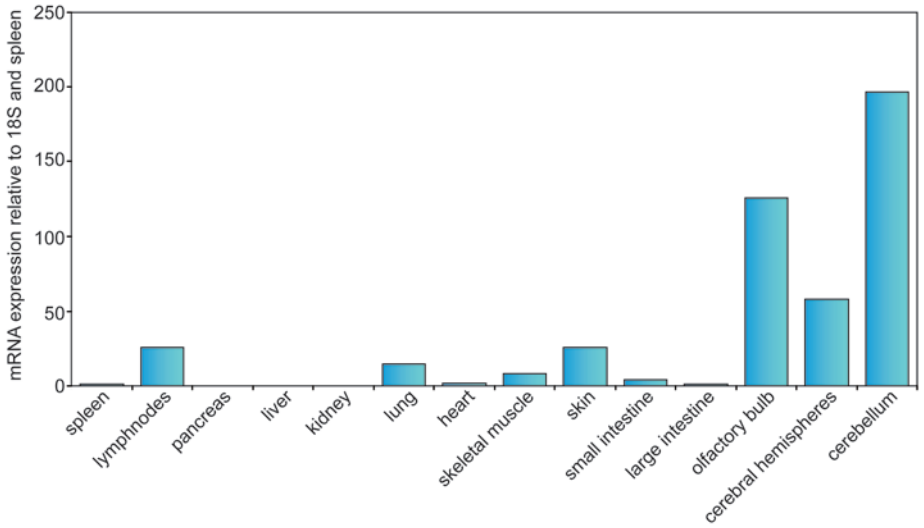

Figure 14. RaLP expression in adult mouse tissues. QRT-PCR analysis of RaLP in different organs. The RNA was pooled from three mice. Relative expression level of RaLP was determined by normalisation to the expression level of 18S and calibrating to RaLP levels in spleen.

Our analysis of RaLP expression in the mouse during embryogenesis and in the adult showed that it was expressed in two time frames. Firstly, during the early stage of embryogenesis in the pluripotent epiblast and secondly, during the later stages of development in regions of the developing nervous system. Then its expression persists in the mature central nervous system in the adult. This data suggests that RaLP could have distinct functions in the two different windows of time during development. We decided to pursue the studies of RaLP in both these contexts and therefore, the PhD project has been subdivided into these two broad lines of research:

- The role of RaLP during early embryonic development
- The role of RaLP during neurogenesis

2. The generation of the RaLP knockout mouse model

One of the most powerful tools for investigating and understanding the function of a gene *in vivo,* is the generation of a mouse mutant for the gene of interest. There are several strategies to obtain mutations in mice, one of the most widely used methods is to introduce a mutation by gene targeting in embryonic stem cells (ESCs) and to then introduce it into the animal through the germ-line transmission.

We decided to investigate the role of RaLP by generating a RaLP knockout (KO) mouse model in collaboration with Genoway. Although I was not directly involved in the work, the strategy, experimental procedures and results will be briefly explained in this section as it is pertinent to the following thesis work.

2.1. Mapping of the murine RaLP gene

With the murine C57Bl/6 BAC sequence (BAC AC104549) containing the RaLP gene, we identitified the corresponding murine RaLP locus in the C57Bl/6 Ensembl database. The

analysis of these two sequences allowed the rearrangement of the BAC sequence that was non-linear and to fill in the gaps in the Ensembl sequence. The murine RaLP gene is located on chromosome two and extends over more than 96 kb. The gene consists of 12 exons and 11 introns. The translation intitiation site is located in exon one and the coding region extends to exon 12.

2.2. Strategy for the genetic deletion of mRaLP gene

As the mRaLP gene extends over more than 96 kb and the deletion of the whole gene is technically difficult. For this reason, the null mutation has to be generated by targeting a specific domain of the mRaLP gene. The mRaLP protein contains, like the other Shc family proteins, two functional domains that mediate protein to protein interaction: from the amino-terminal end, the phospho-tyrosine binding domain (PTB) and the Src homology domain (SH2). These two domains are preceded by a region called the collagen homology domain two (CH2) and bridged by the collagen homology domain one (CH1).

There were two main aspects that were taken into consideration for selecting the region of the gene to target. Firstly, the homology of the regions and domains across the family members was investigated. Generally, the domains are well conserved among the Shc proteins, whereas the regions show lower similarity. In fact, RaLP had the lowest similarity in the CH2 region compared to the other family members [22], suggesting that this region may sustain an important specificity for the RaLP protein. Secondly, we considered the expression pattern of RaLP. The tissue specific and temporally regulated expression suggests the existence of regulatory elements upstream of the gene at the level of the promoter. Therefore, the region to disrupt was decided to be the mRaLP exon one, as this exon encodes for the whole CH2 region, together with the removal of a 2 kb region containing 1.5 kb of the promoter region and the first exon which contains the translation intiation site, ATG. Furthermore, at the level of exon five, there is another gene Eid1 that

is transcribed in the reverse direction, so targeting exon one, the expression of this gene may not be perturbed. The general scheme of the targeting strategy is illustrated below in Figure 15.

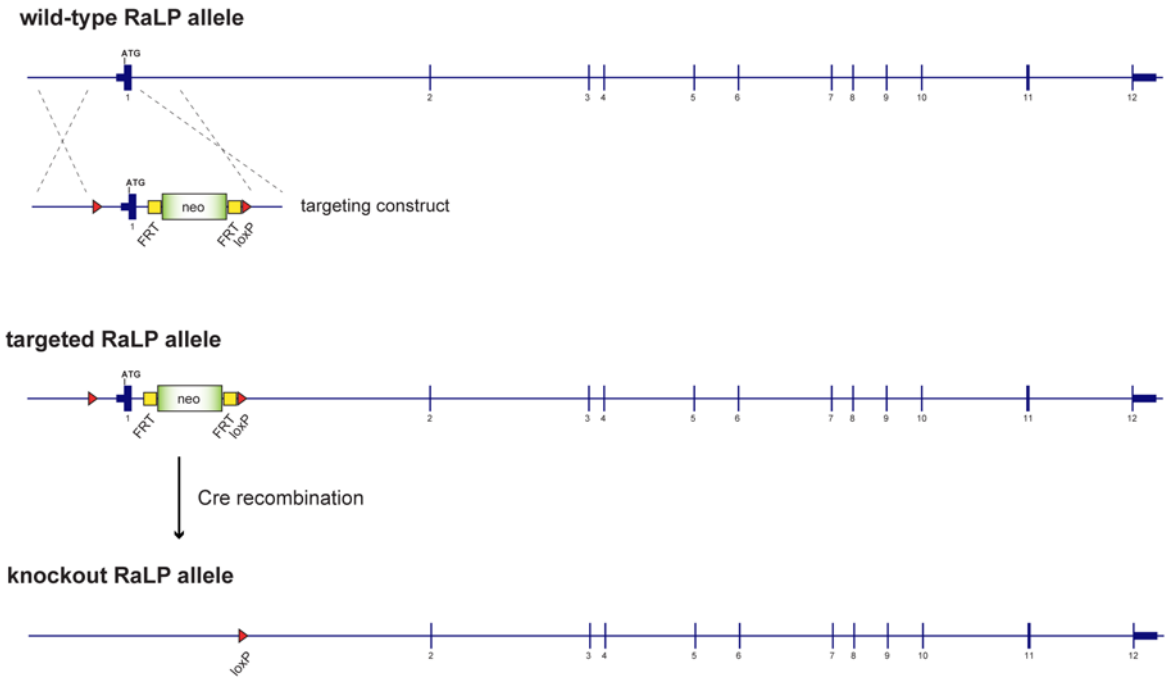

Figure 15. The targeting strategy for the generation of the knockout RaLP allele. Part of the promoter region and exon one containing the transcription intiation site was targeted by homologous recombination. The targeted allele can then be excised upon Cre treatment.

This strategy also allows the development of a conditional KO model from the same targeted embryonic stem cell (ESC) clone or chimera, as the mice carrying the targeted allele could be bred to specific mice expressing Cre in a tissue specific manner, to remove RaLP expression only in those tissues.

2.3. Cloning of the mRaLP targeting construct

The targeting vector was generated by first amplifying the two homology arms (the long 5' homology arm and the short 3' homology arm) by PCR from the BAC sequence containg the murine RaLP gene (BAC AC104549). These homology arms were subcloned into a pCR4-TOPO vector and the sequence was verified. The selection cassette FRT-NEO-FRT-

loxP was inserted at the 5' end of the short homology arm. In the long homology arm, the second lox-P site was introduced, and these arms were then joined together.

The final targeting vector (LAF1-HR) has the following features:

- two homology arms
- total homology with the targeting allele for 8 kb
- asymetrical repartion of the homology on the selection cassette sides (short and long homology arms)
- FRT sites allowing the Flp-mediated excision of the positive Neo selection cassette
- LoxP sites allowing the CRE-mediated deletion of exon one together with part of its promoter region of the RaLP gene
- DTA negative selection cassette

2.4. Targeting of ESCs by homologous recombination

For the introduction of the targeting vector in ESCs, the vector was first linearised by digestion with KpnI restriction enzyme and the resulting 16.5 kb fragment was purified by phenol/chloroform extraction followed by ethanol precipitation. Then 100 μg of linearised plasmid was then electroporated into 100 million 129Sv ESCs (from GenOway) at 800 Volt, 300 μF. Positive selection for clones that have internalised the plasmid was started 48 h after electroporation by the addition of 200 μg/mL of G418.

175 geneticin resistant clones were harvested and amplified in 96-well plates. These ESC clones were then screened by PCR for the detection of the homologous recombination event.

2.5. *In vitro* excision of the targeted region and ESC blastocyst injection of clones

The successfully targeted clones #2A6 and #3A5 that were verified by southern blot analysis for the integration were employed for the Cre-mediated excision of the target

region. The clones were electroporated with 40 µg of supercoiled Cre-expressing plasmid. The transfected cells were then plated at low density and allowed to form colonies. No selection was applied at this stage. Clones with the best morphology were then isolated and amplified in 96-well plates. The clones were then used for the PCR identification of the right CRE-mediated excision event.

ESCs that have successfully undergone Cre-mediated excision, #2A6-5 and #2A6-10, were injected into C57BL/6 blastocysts and were transferred into CD1 pseudo-pregnant females. The results are summarized below in Table 6.

Table 6. Summary of Cre-mediated excised clones blastocysts injections.

Clone number	Injected blastocysts	Foster mothers	Pregnant foster mothers	Total number of pups	Death	Male Chimera	Female chimera
2A6-5	60	4	1	5	0	-	1
2A6-10	60	4	2	14	10	-	-
2A6-5	30	2	1	2	0	-	-
2A6-10	30	2	0	0	-	-	-

The injections performed gave rise to 21 pups among which one female with 90% chimerism. As female chimeras have low probability of germ line transmission, this female was not selected for further breeding. As no male chimeras were obtained even at such large number of injections, we decided to pursue an alternative approach to accelerate the time of generation of the KO model.

2.6. *In vivo* excision of the targeted region and generation of floxed mRaLP mouse

The alternative approach taken for the generation of the KO model was to mediate Cre-excision *in vivo* by breeding the targeted mRaLP mice to ubiquitously Cre-expressing mouse line. To this end, the three floxed ESC clones #3A5, #2A6 and #2A12 were injected

into C57BL/6 blastocysts and were transferred into CD1 pseudopregnant females. The results are summarized below in Table 7.

Table 7. Summary of mRaLP floxed ESC clones blastocyst injections.

Clone number	Injected blastocysts	Foster mothers	Pregnant foster mothers	Total number of pups	Death	Male Chimera	Female chimera
2A12	44	3	1	7	0	1	-
2A6	13	1	0	-	-	-	-
3A5	30	2	1	1	0	-	-
2A6	15	1	1	6	0	1	-

The injections gave rise to 14 pups among which were two male chimeras, one at 95% generated from clone 2A12 and another at 65% of chimerism generated from clone 2A6.

These two males carrying the mRaLP floxed allele, were bred with 129Sv CMV/Cre-expressing female mice. From the breeding with chimera generated from ESC clone #2A12, 15 F1 mice were obtained, among which seven wild-type animals, two mRaLP floxed heterozygous animals and six mRaLP KO heterozygous animals. The resulting six animals in which the Cre-mediated deletion of the mRaLP promoter region, exon one and the slection cassette was observed, were further anlysed by Southern blot. The results further confirmed that these animals were true heterozygous mRaLP KO mice.

For the generation of the F2 animals, the heterozygous mRaLP KO male was then intercrossed with three heterozygous mRaLP KO females. This breeding resulted in the generation of 23 mice. Nineteen animals with the complete deletion of the targeted region, were obtained. These animals were then used for breeding to establish the RaLP KO colonies in our lab.

Up to date, the RaLP KO animals generated are viable and fertile. They show no gross morphological abnormalities at the levels of the organs, analysed by

immunohistochemistry. Detailed analysis of the KO animal will be described later in results section 5.3.

3. The derivation and characterisation of RaLP heterozygote and knockout ESCs

For *in vitro* studies to understand the function of a gene during embryogenesis, the system of choice is ESCs. ESCs are isolated from the pre-implantation embryo and are pluripotent, as they can differentiate towards any lineage of the three germ layers and self-renewing, as they can propagate indefinitely *in vitro* [37,38]. ESCs allow the circumvention of the limitations of quantity and inaccessibility that one encounters when manipulating early stage embryos.

For investigating the role of RaLP in early development, RaLP heterozygote (HT) and knockout (KO) ESCs were derived. For the derivation strategy, we followed the protocol optimised by Stefano Casola (IFOM-IEO campus), which consists in transferring the blastocysts and passaging the cells onto inactivated mouse embryonic fibroblasts (MEFs) in the presence of a specific mitogen-activated protein kinase/extracellular signal-regulated kinase (MEK1) inhibitor PD98059, which has been shown to facilitate the derivation process by suppressing differentiation cues and enhancing the effect of LIF on self-renewal [83,84]. In the first ESC derivation experiment, three couples of RaLP HT female and RaLP KO male mice were set-up. We obtained only twelve morulae from one female. Eight blastocysts could be used for the derivation and we obtained one ESC line, which revealed to be a RaLP HT ESC line (for the genotyping strategy, see section 3.1). We immediately proceeded with a second derivation experiment in order to obtain RaLP KO ESCs and we increased the number of couples, by setting up matings between eight couples of RaLP HT female and RaLP KO male mice. Three females were plugged and 23

morulae were recuperated at dpc 2.5 and after 48 h of *in vitro* culture, and 15 blastocysts of adequate quality were obtained which were used for ESC derivation. From this first experiment, four ESC clones were successfully derived. To have independently established RaLP KO ESC lines, a third derivation experiment was done, this time intercrossing three RaLP KO female and males. Sixteen morulae were flushed from two females and 15 blastocysts were used for the derivation. From this experiment, nine ES clones were obtained.

Table 8. Summary of ESC derivation experiments.

Derivation experiment	Crossing	Number of blastocysts	Number of ESCs derived
1	HT♀ × KO♂	8	1
2	HT♀ × KO♂	15	4
3	KO♀ × KO♂	15	9

3.1. Genotyping of derived ESCs

The established cell lines were genotyped using the PCR strategy designed by Genoway. The strategy consists in using two primer pairs that use a different reverse primer in order to distinguish the KO allele from the wild-type allele. The first primer pair is the GTRaLPF which anneals upstream of exon one and the targeted region, and FGRaLPR1 which anneals flanking the downstream region of exon one, which is no longer present in the knockout allele as it is excised upon Cre treatment. With this primer pair it is possible to distinguish the WT and HT from the KO allele, as the KO will not have any amplified product. The second primer pair, the GTRaLPF and the GTRaLPR2, which anneals to the sequence after the targeted region, will yield two different products for the wild-type and KO allele. The wild-type alle will give rise to a longer product of 6 kb, whereas the KO allele which a part of this region has been excised, will give rise to a shorter fragment of 3.5 kb. The PCR reaction with this primer pair yields one product of 6 kb for the wild-type

allele, two products of 6 kb and 3.5 kb for the heterozygote and only the 3.5 kb for the KO allele. This reaction however, will favour the amplification of the shorter product and therefore it is difficult to distinguish both the bands in the HT, and so it will only discriminate between the WT and HT allele. The summary of the genotyping strategy and the PCR reactions for the derived ESCs that were used for this study can be seen in Figure 16.

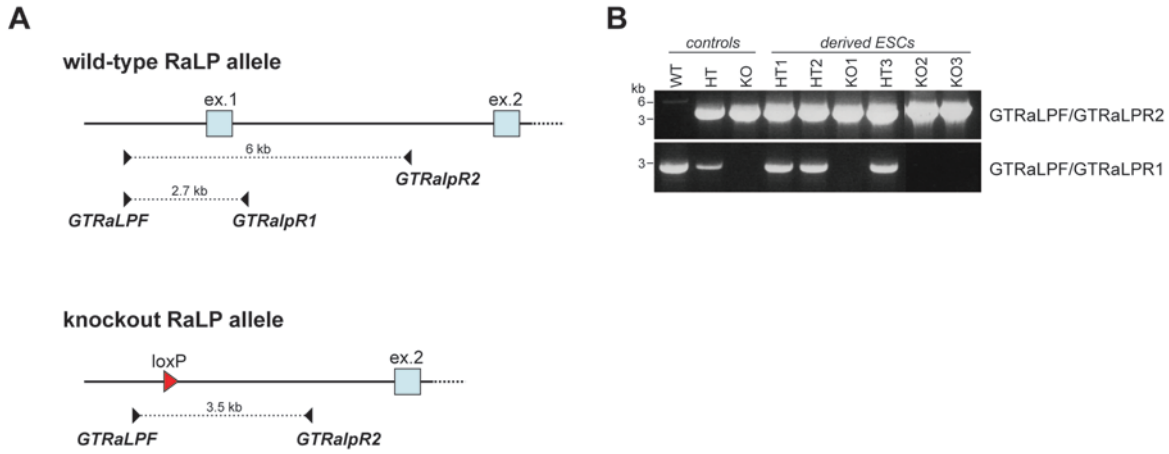

Figure 16. Genotyping strategy and RT-PCR for RaLP wildtype, heterozygote and knockout alleles. (A) The relative annealing positions of primer pairs GTRaLPF and GTRaLPR1, FGRaLPF and FGRaLPR2 are shown together with the amplified products that they will yield in the wild-type and KO allelels. **(B)** The RT-PCR with the primer pairs for the derived ESCs used for this study. The controls are gDNA from mice that have been previously genotyped.

3.2. Karyotyping of derived ESCs

As a next step in the characterisation of the derived ESCs, the karyotype analysis was done to exclude chromosomal abnormalities. ESCs are known to accumulate abnormalities and metacentric chromosomes are the most frequent chromosome abnormality observed throughout the period of culture. Aneuploidy in ESCs is the major cause of failure in obtaining contributions to all tissues of chimeras including the germ line [89], as well as a source of misinterpretation of data in *in vitro* experiments. Furthermore, ESCs with abnormal karyotype can still retain ESC markers such as Oct3/4 and SSEA-1 [90], therefore the control of chromosomal number in addition to the expression of ESC markers

is essential. Generally, ESCs with 70 to 80% normal karyotype are used for chimera production, therefore we decided to use as the requisite for ESC lines to use for our studies, a threshold of 80% and above of normal karyotype. Representative pictures of the karyotype of the ESC lines used for this study are in Figure 17. One heterozygote line (HT3) carried a metacentric chromosome and was excluded from the studies.

Studies have shown that also long-term culturing of ESCs favours the accumulation of chromosomal abnormalities even in lines that start off with a normal karyotype [90]. Therefore, for our studies, our derived ESCs were used for experiments at the maximum of 30 passages in culture.

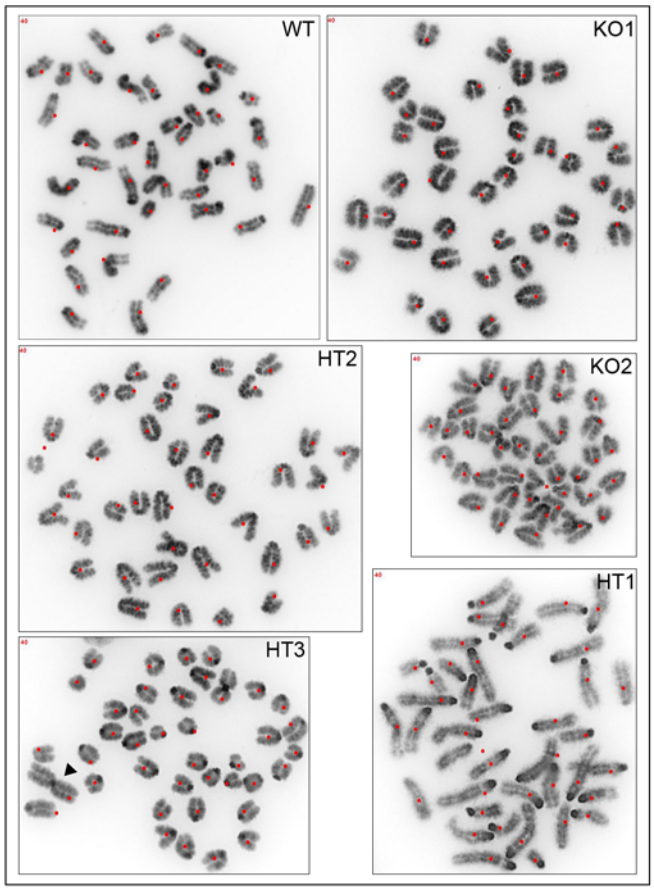

Figure 17. Karyotype of derived ESC lines used for this study. Reverted images of DAPI banded karyotypes of wild-type (WT) ESCs at passage 23, RaLP heterozygous (HT1, HT2 and HT3) and RaLP knockout (KO1 and KO2) ESC lines. The RaLP HT and KO ESCs have been karyotyped at early passages as soon as stable lines were established. Red dots indicate chromosomes and the total number of chromosomes (2n=40) is indicated in red at the top left corner of each image. An example of chromosomal abnormality observed in HT3, with the presence of a metacentric chromosome indicated by a black arrowhead.

3.3. Characterisation of derived ESCs for pluripotency markers

ESCs possess three defning properties: self-renewal, pluripotency and primary chimera formation. The property of pluripotency is governed by a triad of transcription factors: Oct4, Nanog and Sox2 [91,92]. The derived ESCs were analysed for the expression of the pluripotency markers Oct3/4 and Nanog by immunofluorescence and alkaline phosphatase activity (Figure 19). All ESC lines were positive for Oct3/4, Nanog and alkaline phosphatase activity. Several other markers are also expressed in ESCs, such as Klf4, Rex1, Sox2 and Fgf4. The expression of these markers was confirmed in all cell lines by qRT-PCR (Figure 18).

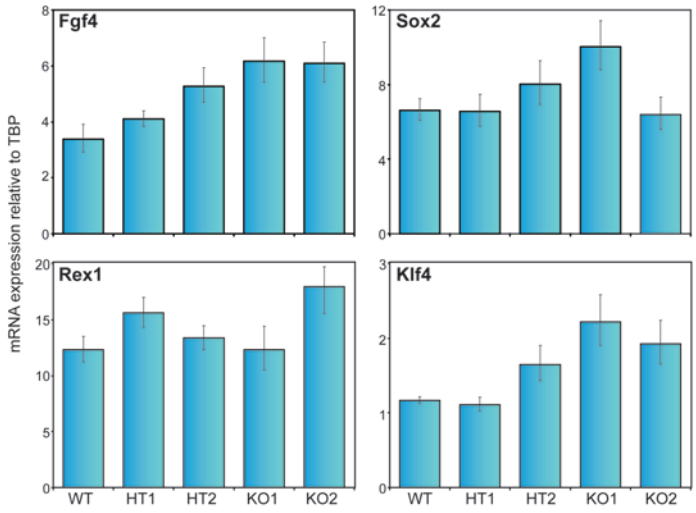

Figure 18. qRT-PCR for ESC markers Fgf4, Sox2, Rex1 and Klf4 in WT, derived HT (HT1 and HT2) and KO (KO1 and KO2) ESC lines. All ESCs express the pluripotency markers. Bars represent the means ± S.D. of triplicates.

The commonly used E14Tg2a WT ESCs and the two derived RaLP HT ESCs (HT1 and HT2) were used as independent control populations for all experiments. ESCs are mutable in culture and can display different behaviour among cell lines, therefore it is important to validate any observed phenotype on more than one cell line. Unless otherwise specified, all the experiments presented in this thesis have been performed with at least two independently derived RaLP KO ESCs (KO1 and KO2).

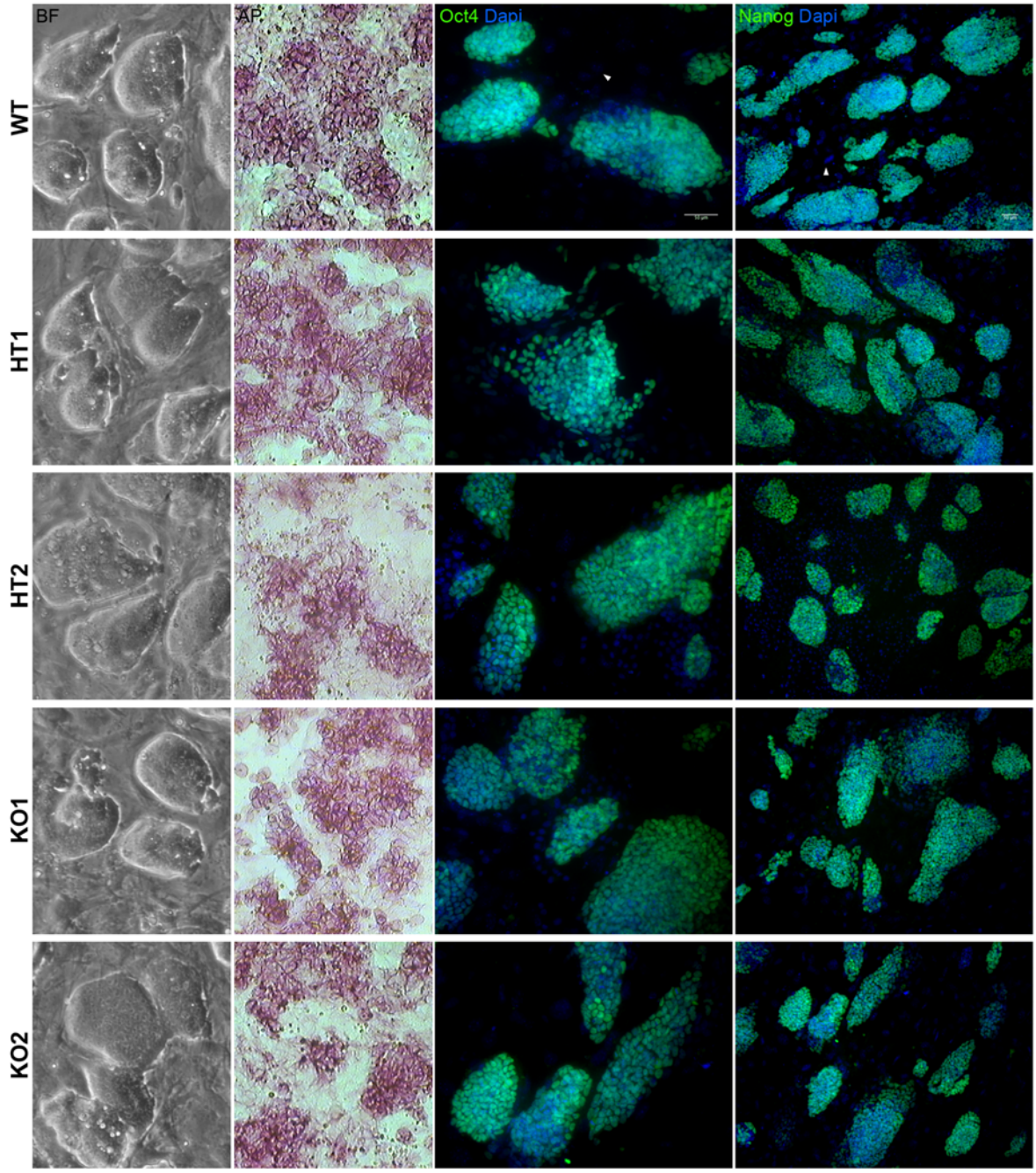

Figure 19. Characterisation of derived ESCs. WT ESCs and derived ESCs RaLP heterozygote (HT1 and HT2) and knockout (KO1 and KO2) lines were characterised for ESC markers. Panels from left to right: first panel shows a bright field picture of ESCs grown on inactivated feeder cells. The second panel is alkaline phosphatase staining of ESCs grown on gelatin. Third panel is immunofluorescenct images of Oct3/4 and merged with DAPI. Fourth panel is immunofluorescent images of Nanog merged with DAPI. Scale bar represents 50 μm. White arrowheads in the immunofluorescence images of ES WT indicate nuclei of MEFs as an example, they are present in also all the other images.

3.4. Genotyping of derived ESCs for Y-chromosome linked gene SRY

The ESCs were also genotyped for the Y-linked gene Sry, by RT-PCR. ESC lines used for experiments are shown below in Figure 20. The WT, KO1, KO2 and HT1 ESC lines

resulted positive for the Sry gene, therefore are male whereas the HT2 line resulted negative and therefore, female.

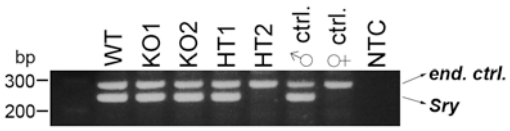

Figure 20. RT-PCR for Sry in ESC lines used for this study. The derived ESCs were genotyped for their sex by RT-PCR for the Y-linked gene, Sry.

3.5. Summary

It is possible to derive, in the absence of RaLP, self-renewing ESCs. Under self-renewal culture conditions in the presence of LIF and serum, RaLP KO ESCs showed no overt difference in morphology, expression of ESC and differentiation markers, compared to WT or RaLP HT ESCs. We conclude that the absence of RaLP does not impair the derivation and the establishment of *bona fide* ESCs.

4. *In vitro* functional characterisation of RaLP during development

4.1. Analysis of RaLP expression during embryonic stem cell differentiation

4.1.1. Embryoid body differentiation of ESCs and the regulation of RaLP *expression*

Firstly, we examined whether RaLP expression was regulated in a similar manner as *in vivo*, by inducing ESC differentiation that comprises the change of culture conditions from a two-dimensional monolayer to a three-dimensional suspension culture and subtracting a cytochine that promotes the self-renewal of ESCs, the Leukemia Inhibitory Factor (LIF), from the medium. Under these conditions, ESCs form spheroid aggregates and these structures were first termed embryoid bodies (EBs) because of their resemblance to mouse blastocysts [40]. EBs are used as a model system for investigating events in embryogenesis *in vitro* as they recapitulate many aspects of early mammalian development in a

progressive manner. They first generate the visceral/primitive endoderm and subsequently, the three embryonic germ layers endoderm, ectoderm and mesoderm are formed. The germ layers then develop into more differentiated lineages such as neural progenitors [93], haematopoeitic cells [94], cardiomyocytes [95] and hepatocytes [96]. Although EBs are able to form a wide variety of cell types and follow events occurring during embryogenesis, it was thought that it takes place in a rather disorganised manner. However, a recent study revealed that EBs display an unexpected degree of self-organization, seen by the establishment of anteroposterior polarity and the formation of a primitive streak-like region that is dependent on the local activation of the Wnt pathway [45]. This strongly supports the use of EBs as a good model system to address developmental questions.

There are several protocols for the production of EBs, the most used are suspension culture in bacterial-grade dishes [44], methylcellulose culture [97] and hanging drop culture [94]. Each method has its advantages and disadvantages, and one of the important issues to consider is the formation of a homogenous population of EBs. The size and shape of EBs influences their differentiation bias and speed and therefore, heterogeneously sized EBs will rapidly lose synchrony and grow at different rates while generating different lineages in varying proportions. This will be an issue for interpreting results within a single experiment as well as the reproducibility between experiments. For these reasons, we decided to use the hanging drop protocol for the derivation of EBs (Figure 21A), as it provides a system to control the number of ESCs aggregating in a single EB. First, we optimised the protocol in our hands. WT and RaLP HT ESCs were allowed to aggregate to form EBs and the differentiation was monitored by verifying the gene expression pattern during the process by qRT-PCR on day zero (ESCs), day two, day three, day four, day six and day nine of differentiation (Figure 21B). It is known that the first three days of differentiation correspond to the pre-implantation to peri-implantation stage of

embryogenesis. In fact, also in our system the pattern of gene expression was in agreement. Rex1, a stringent marker of the inner cell mass or ESC, decreased rapidly after day one of differentiation (Figure 21C). ESC and epiblast markers Oct3/4, Fgf4 and Nanog were gradually downregulated between day zero to day three, and then their expression became negligible. Day two, which marks the formation of the epiblast as seen by the upregulation of its marker Fgf5, was accompanied by the upregulation of the endoderm marker Gata 4 and postimplantation epiblast and mesoderm marker, Brachyury, were also upregulated at the beginning of the differentiation. After the first phase (first three days of differentiation) during which the three primary germ layers have been generated, a central cavity starts to form in the EB and they resemble the embryo in the egg cylinder stage and gastrulation at this stage. This is reflected by the upregulation of markers of more differentiated cell types, such as Sox1 for the neuroectoderm and nestin for neural precursors. Both WT and HT ESCs gene expression profiles were similar. Overall, the gene expression profile were in agreement with previous studies that have characterised the EB differentiation process [47,50], confirming that the protocol is efficient and is reproducible in our hands.

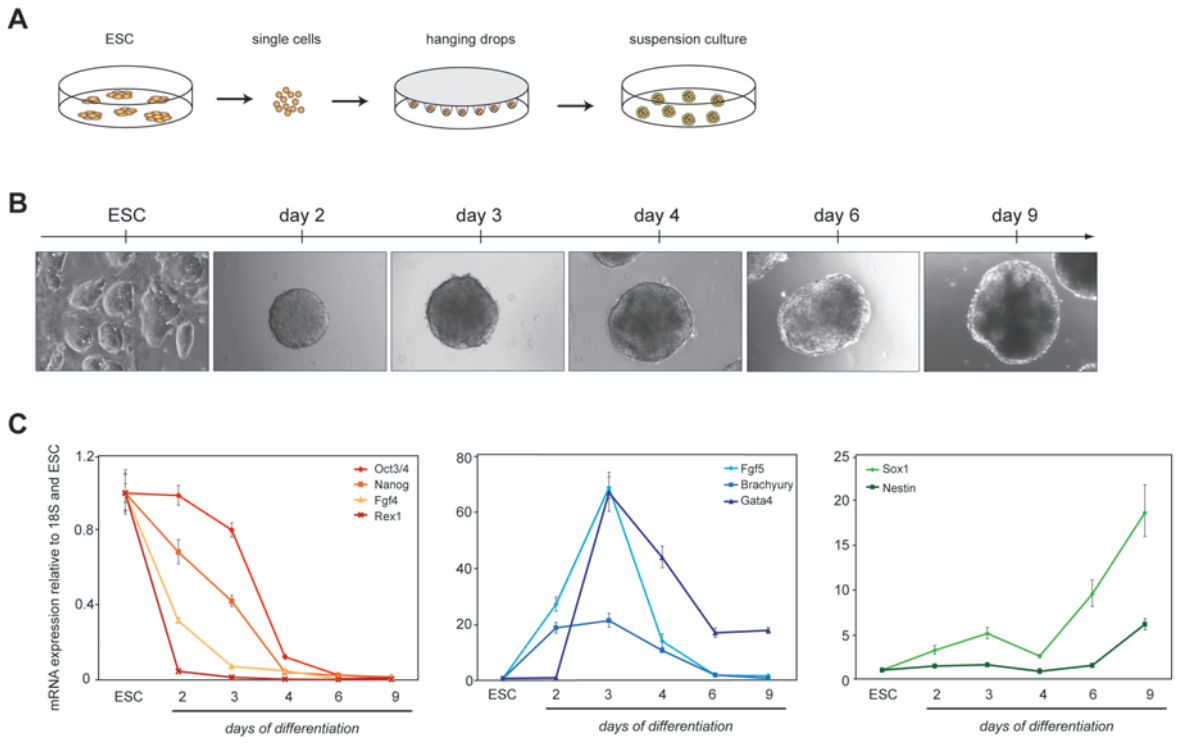

Figure 21. Embryoid body differentiation of ESCs. (A) Scheme of the method used for ESC differentiation to embryoid bodies. Single ESCs were allowed to aggregate by hanging drops and after two days, the EBs were transferred to bacterial dishes for suspension culture. (**B)** The morphology of EBs at the stage of differentiation corresponding to the experimental points in which EBs were collected for analysis. Day two and day three EBs are known as simple EBs and from day four onwards are termed cystic EBs as they start to cavitate. **(C)** The qRT-PCR analysis of marker gene expression patterns during EB differentiation. Three groups of marker genes were analysed: ICM and epiblast markers Oct3/4, Nanog, Fgf4 and Rex1; the germ layer markers Fgf5 (epiblast/primitive ectoderm), Brachyury (epiblast/mesoderm) and Gata4 (endoderm); and neuroectoderm markers Sox1 and Nestin. Bars represent the means ± S.D. of triplicates.

We then studied the kinetics of RaLP expression during EB formation by qRT-PCR analysis. Results evidenced its low levels of expression in ESCs and its tight upregulation during a narrow time-window spanning day two and day three of differentiation (Figure 22). Previous studies [47,98] and our gene expression profiles during the EB differentiation have shown that this time-window corresponds to the formation of the primitive ectoderm or post-implantation epiblast. Notably, after day three after the formation of the three germ layers, RaLP transcript levels were rapidly downregulated and remained at low levels of expression. These results evidenced that: 1) ESC differentiation to EB mimics closely the events *in vivo,* 2) RaLP expression is correlated to the emergence of the epiblast and is downregulated once the epiblast differentiates further and 3) RaLP regulation *in vitro* using the EB system, is similar to *in vivo*.

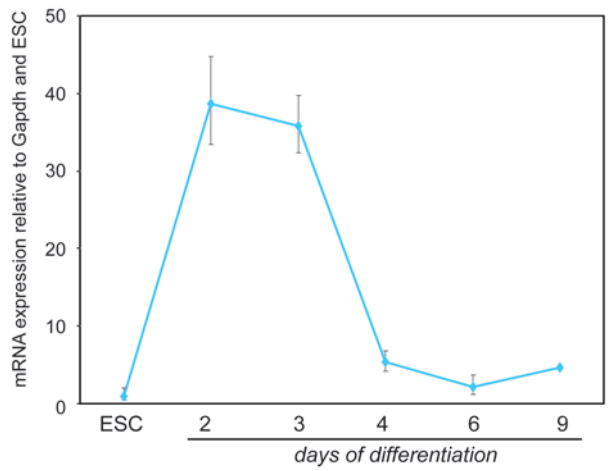

Figure 22. The kinetics of RaLP expression during EB differentiation of ESCs. (A) RaLP expression was analysed by qRT-PCR at different timepoint of EB differentiation of WT ESCs. RaLP was upregulated sharply during day two and three of differentiation. RaLP expression levels were normalised to Gapdh and ESCs. Bars represent the means ± S.D. of triplicates.

Next, we examined the response of RaLP KO ESCs to EB differentiation. Overall, the differences in gene expression of some of the markers could be seen in the time window during which RaLP is expressed, day two and three (Figure 23). The pluripotent marker Oct4 gradually downregulated in the HT while in the KO on day two it remains at the same levels and followed by a sudden drop in expression. Rex1, another pluripotent marker behaved in the same way between HT and KO. Interestingly, all the early germ layer markers, Fgf5, Gata4 and Brachyury were upregulated in anticipation in the KO. It was very difficult to give an interpretation to these results as the population consists of several cell types. Perhaps in the absence of RaLP, ESCs respond to differentiation more quickly, although this cannot account for delay in Oct4 downregulation on day two. A more specific differentiation protocol is necessary to dissect the effects more precisely.

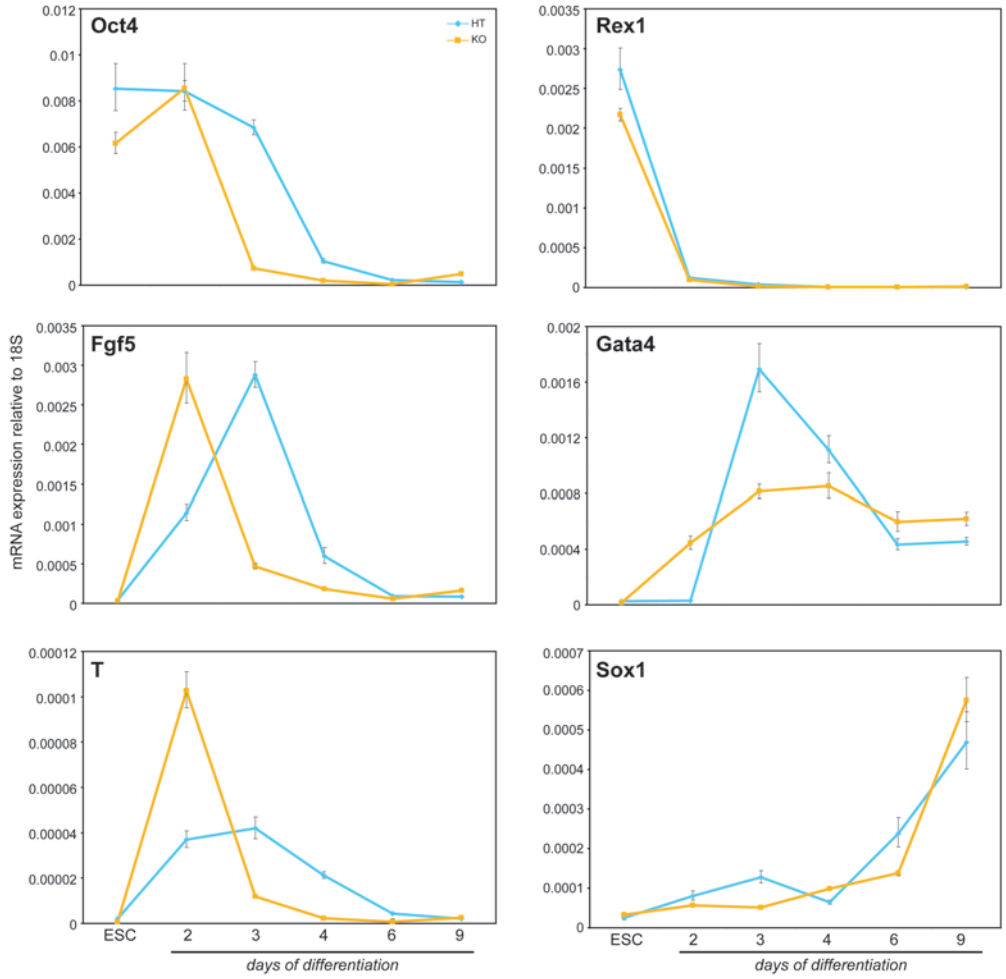

Figure 23. Comparison of gene expression profiles during embryoid body differentiation of RaLP HT and KO ESCs. Analysis of Oct4, Rex1, Fgf5, Gata4, Brachyury (T) and Sox1 during the EB differentiation by qRT-PCR. Bars represent the means ± S.D. of triplicates. Shown are representative results from five independent experiments.

4.1.2. Neural differentiation of ESCs

To confirm that the transient RaLP expression is due to the formation of epiblast during *in vitro* differentiation and not due to the phenomenon of the aggregation of ESCs, we transferred ESCs into a differentiation induction system comprising an adherent monolayer culture in the absence of exogenous growth factors and feeder-free conditions [48]. These conditions are permissive for neural commitment and are driven by autocrine signalling. It is the best characterised system for derivation of neural lineages from ESCs. Studies have shown that this differentiation *in vitro* appears to accurately mirror what occurs *in vivo* both in terms of the order of events and the signalling pathways [50,51].

In order to be able to monitor the differentiation process and to ascertain that it is undergoing optimally in our hands, we first used a reporter cell line, the 46C ESCs (Austin Smith, Cambridge) that harbours a knock-in of GFP to one allele of the neural specification marker gene Sox1 [85]. Sox1 is the earliest neural specific marker of neural precursors in the mouse embryo [99] and during the monolayer differentiation, its expression gradually increases during the first few days as the ESCs commit to neural fate and this can be followed by FACS analysis for GFP positive cells. At day four in our differentiation, the population of cells consisted of 50% GFP positive cells as was reported [85] and furthermore, the qRT-PCR analysis of gene expression markers showed the expected pattern of downregulation of pluripotency markers Oct4 and Rex1, transient upregulation of epiblast marker Fgf5 and gradual upregulation of neuroectodermal marker Sox1, confirming that the protocol is optimal also in our hands (Figure 24).

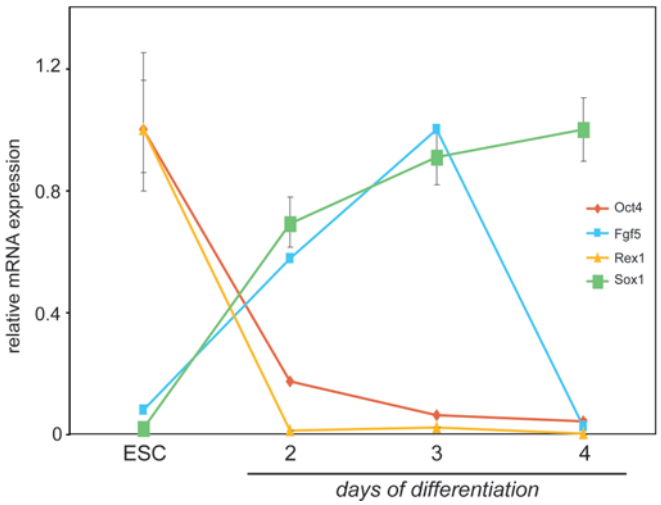

Figure 24. Expression profile of pluripotent and differentiation markers during the first days of neural differentiation of ESCs. Analysis of Oct4, Rex1, Fgf5 and Sox1 during the first days of differentiation by qRT-PCR. Bars represent the means ± S.D. of triplicates.

During the first few days of neural induction, ESCs acquire the epiblast identity prior to undergoing neural commitment [50]. This was also observed during our differentiation with the upregulation of epiblast marker Fgf5 and downregulation of inner cell mass marker Rex1, by qRT-PCR. To assess whether the upregulation of RaLP during epiblast formation is a general event *in vitro* and not only confined to the EB system, we subjected the 46C ESCs and RaLP WT ESCs to neural commitment conditions and monitored the kinetics of RaLP expression in the differentiating cells at several stages: day zero (ESCs), day two, day four, day six and day eight by qRT-PCR (Figure 25A) and Western blotting (Figure 25B). RaLP expression showed a similar pattern to the one observed in EB differentiation. It was regulated in a narrow-time-window, being upregulated on day two of differentiation and then rapidly downregulated by day four, both at the RNA and protein level in WT ESCs. Also the RaLP HT ESCs showed the same RaLP expression pattern as the WT ESCS (data not shown). The 46C ESCs showed similar pattern although there RaLP protein persisted for a longer time, as a weaker band was present at day four. The peak of RaLP expression at day two was consistent. The slower downregulation of RaLP in the 46C is probably due to an instrinsic characteristic of the cell line.

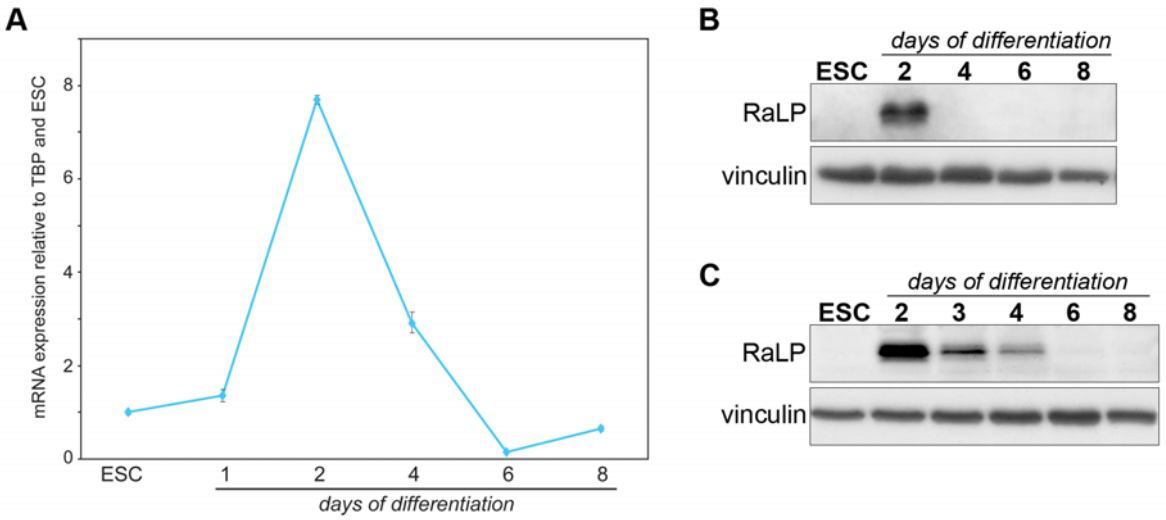

Figure 25. RaLP expression profile during the neural differentiation of ESCs. (A) RaLP expression by qRT-PCR shows a timed upregulation on day two of differentiation in WT ESCs. Expression level was normalised to TBP as housekeeper gene and ESC as calibrator. Bars represent the means ± S.D. of triplicates. **(B)** Western blotting of RaLP on WT ESCs show the same kinetics as RNA regulation, with a peak of expression on day two. (**C)** RaLP expression in a commonly used ESC line 46C show a slightly different kinetics with longer window of RaLP expression, but with the same peak on day two.

Shc family proteins are known to mediate the stress response of cells [13]. In order to discriminate whether RaLP upregulation in this differentiation protocol is not due to stress caused by change in culture conditions (for example by the removal of serum), we examined separately the components that were removed for the differentiation in relation to the increase in RaLP transcript levels, by qRT-PCR after 48 h (Figure 26). Results showed that RaLP is not upregulated by the removal of serum; therefore it is not caused by a stress response of the cells to change in culture conditions. In contrast, RaLP was upregulated only in the conditions that allowed differentiation, i.e. when the self-renewal factor LIF was removed, suggesting that RaLP upregulation is strictly correlated to the differentiation process of ESCs.

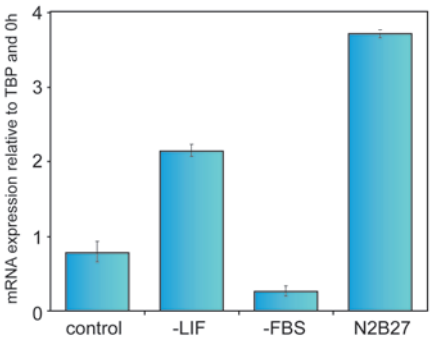

Figure 26. RaLP expression under several culture conditions. WT ESCs were cultured under several culture conditions for 48 h: normal ESC conditions (control), ESC medium without LIF (-LIF), ESC medium without FBS (-FBS) and neural differentiation medium (N2B27). RaLP expression was analysed by qRT-PCR. RaLP was not upregualted due to the removal of FBS and was upregulated only under conditions that allow the exit from self-renewal (i.e. –LIF and N2B27). Bars represent the means ± S.D. of triplicates.

The expression pattern during ESC to NSC differentiation of the other Shc family members was analysed by qRT-PCR (Figure 27). p66ShcA is the only member that is expressed in ESCs and its levels gradually decrease during neural differentiation. Interestingly, ShcB/Sli and ShcC/Rai had a complementary pattern to p66ShcA, starting with low levels in ESCs and increasing during the differentiation, with the highest levels when the ESCs are fully committed to neural fate. This *in vitro* data is in agreement with *in vivo* studies that have shown that ShcA proteins are expressed in non-neuronal tissues while ShcB and ShcC are expressed in nervous tissue [100]. Furthermore, it has been shown that there is a switch from ShcA to ShcC when the neural progenitor cells differentiate and mature into neurons [101]. RaLP showed a distinct pattern from the rest of the members of the family, with a sharp peak on day two of differentiation. Each Shc family member displayed their own specific expression pattern that did not overlap with that of RaLP, suggesting a unique role of this member in this the process of ESC exit from self-renewal and commitment to the epiblast identity.

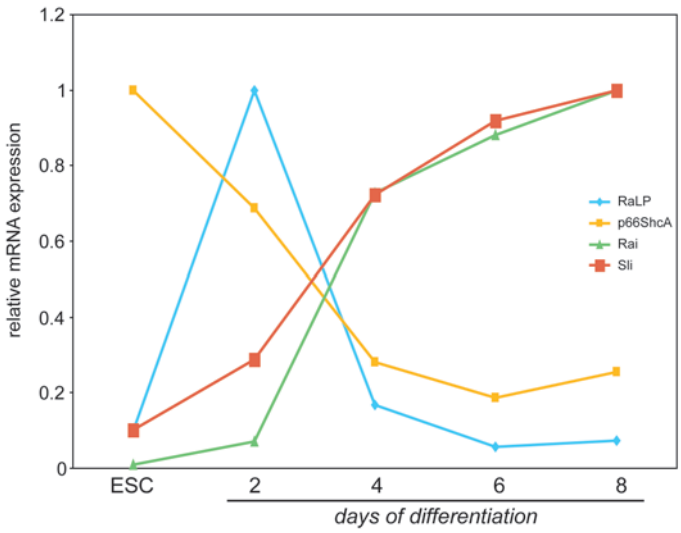

Figure 27. Expression profiles of Shc family members during the neural differentiation of ESCs. The kinetics of expression of the Shc family members (RaLP, p66ShcA, Rai and Sli) were analysed by qRT-PCR. The relative expression values were normalised to TBP. Bars represent the means ± S.D. of triplicates.

These data, together with the *in vivo* data, confirm the epiblast -specific expression of RaLP, suggesting a specific role/s of this protein in this cell type. Furthermore, the similar regulation of RaLP expression in this *in vitro* system compared to the *in vivo* counterpart, sustains the use of ESCs for our purpose of characterising the function of RaLP.

4.2. RaLP is specifically expressed in Epiblast stem cells

The transient pattern of RaLP expression during the EB and NSC derivation protocols provides only a two-day time-window in the context of a population that comprises several cell types, to study the role of RaLP. This represented an important challenge for our studies and in fact, initial experiments using these differentiation protocols (see previous section 4.1.1) did not give clear-cut results and were difficult to interpret. To facilitate our studies of dissecting the function of RaLP, we decided to use an alternative ESC differentiation protocol, based on our *in vivo* and *in vitro* data that suggests that RaLP expression is epiblast-specific. Epiblast stem cells (EpiSCs) have been isolated from the egg cylinder of the early post-implantation mouse embryo [59,60]. These cells are self-renewing and pluripotent as they can be maintained in culture indefinitely and can form

derivatives of the three germ layers *in vitro* and generate teratomas. On the basis of their global gene expression and epigenetic patterns, these cells are considered most similar to the pluripotent cells of the post-implantation epiblast [59,60,78]. We decided to investigate whether RaLP expression is truly specific to the epiblast by qRT-PCR in two independently established post-implantation embryo derived EpiSC lines, OE6 and OE7 (renamed for our studies, EpiSC1 and EpiSC2, respectively), compared to OES ESCs (from Austin Smith, Cambridge [78]). These ESC and EpiSC lines have been derived from mice carrying the Oct4GiP transgene [102], in which the GFP and puromycin resistance genes are under the control of the pluripotent cell-specific Oct4 promoter. This allows the monitoring of the cell population and to select only for cells that express Oct4 either by GFP or by puromycin resistance, allowing therefore, in both ESCs and EpiSCs to have a homogenous pluripotent population of cells in culture. The qRT-PCR analysis for RaLP expression showed that it was indeed expressed at very high levels in the two EpiSC lines (Figure 28) and its fold induction relative to its levels in ESCs was between 80 to 100-fold. This was significantly higher compared to the induction of RaLP observed during the EB and NSC differentiation protocol, as previously described. This was probably due to the fact that these differentiation protocols generate a mixed population and do not consist of a pure epiblast population. This data confirms that RaLP expression is specific to the epiblast *in vivo* and *in vitro*.

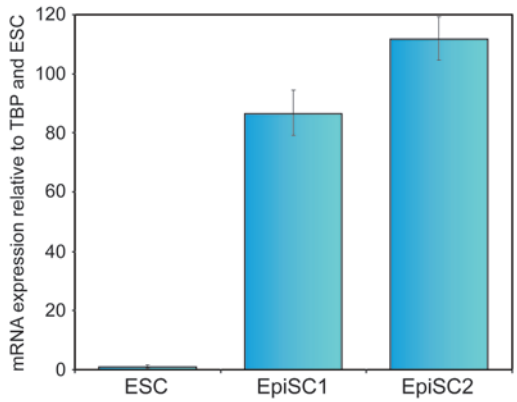

Figure 28. RaLP expression in ESC and EpiSC lines. qRT-PCR for RaLP in ESCs, EpiSC lines EpiSC1 and EpiSC2 derived from Oct4-GFP mice. MRNA levels of RaLP were determined by normalising to TBP and ESC. Bars represent the means ± S.D. of triplicates.

It is possible to study the formation of the epiblast by a protocol recently established by Guo and colleagues [78]. It consists in plating ESCs on fibronectin and culturing them in the presence of factors important for the self-renewal of EpiSCs; basic Fibroblast growth factor (bFGF) and activin A (Figure 29A). These cells can be propagated for many passages in culture and can also be cryopreserved. The protocol was first optimised in our hands. We saw that the optimal initial seeding density was low at 100,000 cells per 6-well. After 24 h the medium was switched from ESC medium to N2B27 medium containing bFGF and activin A. ESCs grew as flattened colonies consisting of morphologically homogenous small cells growing in close contact to one another (Figure 29B). After the first passage of these cells, the differentiation is accompanied by a notable amount of cell death, probably due to a selection of those cells that are not able to undergo the program of differentiation towards the epiblast. We observed that the key to an optimal differentiation is to maintain the cell density high during passaging. After several passages, usually between passage four and five, it was possible to obtain a relatively homogenous population of ESC derived EpiSCs (ES-EpiSCs). It must be mentioned however, that a certain degree of differentiation is always present in the culture, as reported also by others [103]. The cells generated at these passages grow as tight, flattened colonies that are morphologically indistinguishable from EpiSCs derived from the post-implantation embryos (Figure 29C). Alkaline phosphatase activity is a hallmark of ESCs [104] and primordial germ cells (PGCs) [105] Therefore the lack of alkaline phosphatase activity of the ES-EpiSCs distinguishes them from ESCs, PGCs and embryonic germ cells (EGCs) (Figure 29D). QRT-PCR analysis for ESC and EpiSC markers on cultures at passage five, showed the characteristic gene expression profile of EpiSCs (Figure 29E): maintenance of the expression of Oct4, which is a marker for both cell types and the downregulation of

inner cell mass and ESC markers Rex1, Klf4 and Tbx3 [59,60] was observed. Stella is an ESC marker as well as a germ cell marker and it was also downregulated [106,107]. Nanog was slightly downregulated but still expressed in EpiSCs, although its expression was slightly lower when not cultured on feeders [103]. In contrast to ESCs, EpiSCs express early lineage specification markers, underlining their more "primed" state to differentiate. Markers of the primitive ectoderm, Fgf5 and Orthodenticle homeobox 2 (Otx2) and of the early mesoderm Brachyury were all expressed in our ES-EpiSCs. Postimplantation epiblast associated genes such as Cerberus 1 (Cer1) and Forkhead transcription factor 2 (Foxa2) were also highly upregulated. Furthermore, as an assay to test the pluripotency of the ES derived EpiSCs, we differentiated them towards EBs, as they should retain the ability to differentiate into the three germ layers. And indeed, they could form EBs that when then transferred to adherent conditions, could differentiate as they attached and expanded with many cell types outgrowing from the EBs (Figure 29F). After ten days of differentiation of the EBs they expressed many markers of derivatives of all three germ layers, ectoderm, mesoderm and endoderm at high levels, evidencing their advanced differentiation status. They also expressed the trophoectoderm markers Cdx2 and Hand1, which has also been previously reported in postimplantation derived EpiSCs [60]. To our knowledge, this is the first time that ES-EpiSCs have been shown to have the capacity to form EBs. In summary, this protocol effienciently derives EpiSCs that possess the markers and ability of the postimplantation embryo derived EpiSCs and is an ideal system to study the commitment of the ESCs towards EpiSC fate.

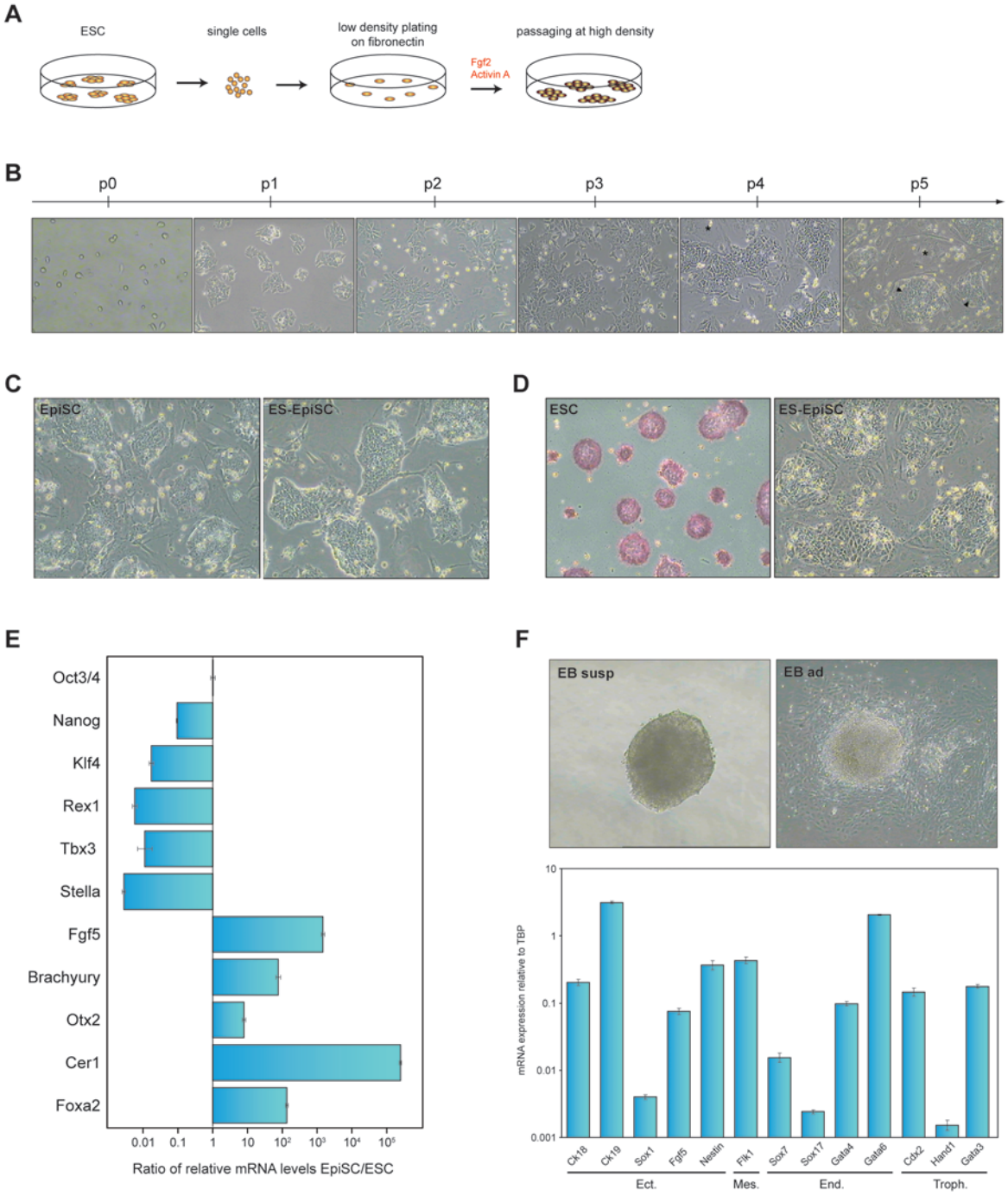

Figure 29. Characterisation of the derivation of EpiSCs from ESCs. (A) Scheme of the protocol for the derivation of EpiSCs from ESCs. ESCs were plated at low density on fibronectin in ES medium. After 24 h the medium was changed to N2B27 containing Activin A and Fgf2 and the cells are passaged at high density. **(B)** The morphology of cells at each passage of differentiation corresponding to the experimental points in which cells were collected for analysis. Black arrowheads indicate EpiSC colonies and asterisks indicate differentiated non-EpiSC cells **(C)** Comparison of morphology of postimplantation derived EpiSCs (left) with ESC derived EpiSCs (right) grown on MEFs. ES-EpiSCs show typical flattened colonies indistinguishable from the postimplantation derived EpiSCs. **(D)** Alkaline phosphatase (AP) staining of ESCs before the differentiation and EpiSCs after differentiation. EpiSCs are negative for AP. **(E)** Gene expression profile of EpiSCs at passage five of differentiation; The relative expression of each gene is compared to its expression level before differentiation. Bars represent the means ± S.D. of triplicates. **(F)** Embryoid body differentiation of postimplantation derived EpiSCs and ESC derived EpiSCs. EB susp is an EB in suspension, EB ad is EB allowed to attach and differentiate further in a culture dish for seven days. Shown below is the gene expression profile of EpiSCs derived EBs after ten days of differentiation, The expression of each gene is relative to the housekeeper TBP. Bars represent the means ± S.D. of triplicates. Abbreviations: ectoderm (Ect), mesoderm (Mes), endoderm (End) and trophectoderm (Troph).

After optimising the protocol in our hands and critically assessing its validity, we looked at the kinetics of RaLP expression during this differentiation. Interestingly, it was upregulated starting from passage two and its levels remained more or less constant even up to many days in culture (passage ten, which corresponds to about one month in culture) as long as the cells were of EpiSC identity (Figure 30A). At the protein level, RaLP expression could be detected already at passage one although at much lower levels than at passage two. The weaker bands at passage four and five could be due to lower amounts of protein loaded on the gel, compared to the previous passages. However, the differences in loading are not so large to completely account for the lower levels of RaLP protein at these passages. It cannot be excluded that there could be possible post-translational regulation of RaLP, for example through microRNAs. This aspect would be definitely worth investigating further. In summary, this protocol allowed us to have a system with a longer timeframe and specific cell population to study the role of RaLP. Furthermore, its upregulation during this differentiation strongly suggests its possible role in epiblast formation.

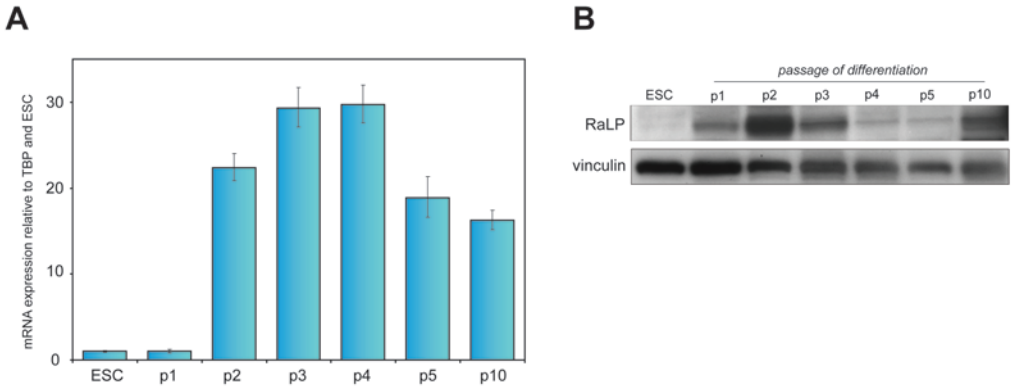

Figure 30. RaLP expression pattern during ESC to EpiSC differentiation. (A) QRT-PCR analysis of RaLP expression at sequential passages during the differentiation. Relative levels of RaLP transcript were normalised to TBP and calibrated to ESCs. Bars represent the means ± S.D. of triplicates.

4.3. Derivation of EpiSCs from RaLP HT and KO ESCs

To assess a potential contribution of RaLP to the formation and/or maintenance of epiblast identity, RaLP HT and KO ESCs were subjected to EpiSC differentiation.

4.3.1. Morphology and cell growth of RaLP HT and KO cells

After plating of RaLP HT and KO ESCs and during this first passage of differentiation, no significant morphological differences nor starting number of cells, could be observed. Depending on the progression of the differentiation replicate, morphological and cell growth differences between the RaLP HT and KO ESCs could be seen at the earliest at passage two (Figure 31). A fraction of RaLP KO cells started to acquire a more flattened and enlarged morphology compared to the HT, as well as the WT. The striking differences in morphology was consistently observed at passage three and four, when RaLP KO cells consisted of very few colonies and most of the cells were large and flattened and no longer growing in close contact to one another.

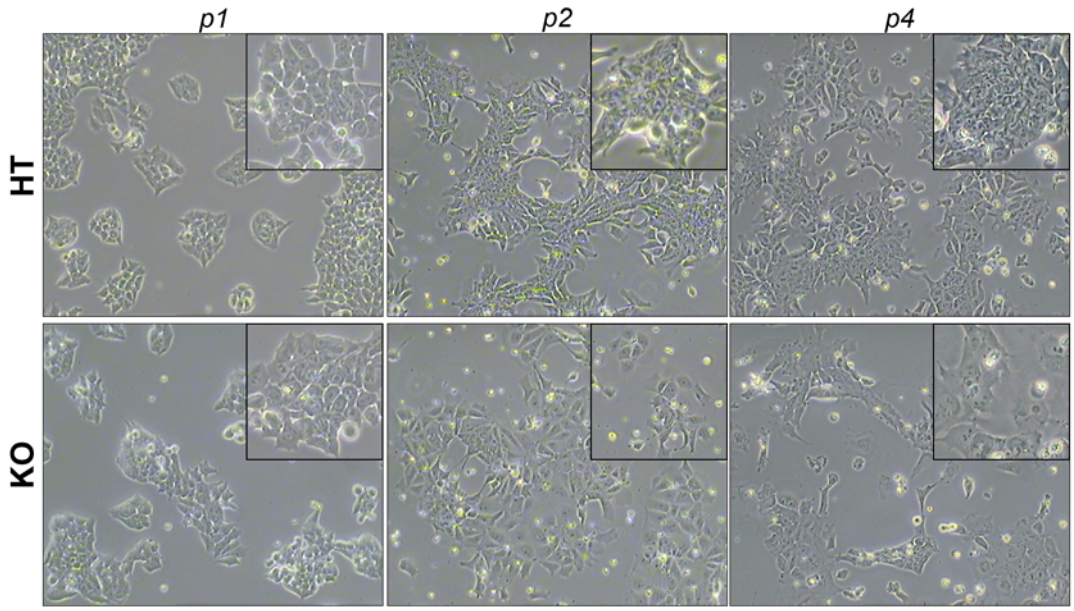

Figure 31. Morphology of RaLP HT and KO cells during ESC differentiation to EpiSCs. Bright field images of RaLP HT and KO cells at passage one (p1), passage two (p2) and passage four (p4) of differentiation. Large images are taken at magnification x 10 while the smaller boxed images at top right corner are images taken at a magnification of x 20.

During the differentiation, the number of cells in KO cultures gradually decreased from passage three and was significantly lower in RaLP KO cultures compared to the HT (Figure 32) in which the cells grew at a steady rate.

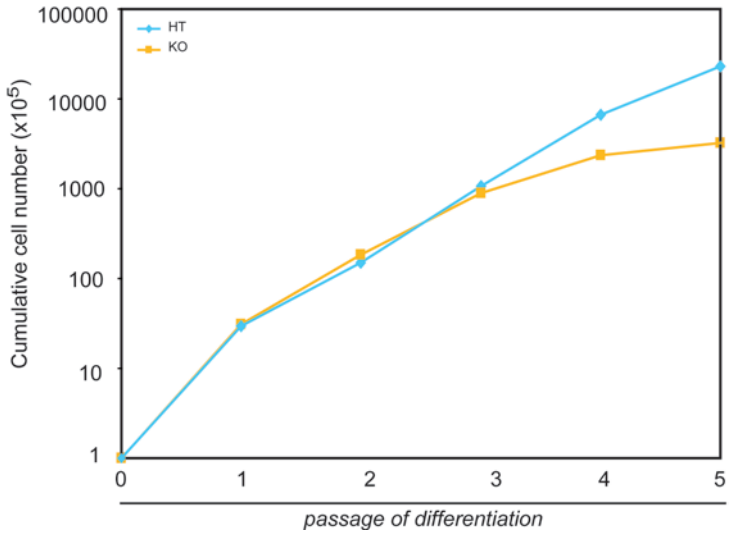

Figure 32. Cumulative growth curve of RaLP HT and KO cells undergoing EpiSC differentiation. RaLP HT and KO ESCs are plated at a starting number of 100,000 cells for the differentiation and cumulative cell numbers were plotted at each passage of differentiation. For the first few passages cells grow at similar rates to HT. At passage three there was already a slight drop in growth rate of KO cells and the lower proliferative capacity persists into later passages.

4.3.2. Analysis of ESC to EpiSC differentiation by multiparameter FACS

In order to distinguish whether the lower number of cells in RaLP KO culture is due to a higher amount of cell death by apoptosis, a lower proliferation rate or the result of both the conditions and taking into account the possible heterogeneity of the cells composing the entire population, it was necessary to use several markers simultaneously to analyse the population. We decided to analyse the cultures by a multicolour fluorescence activated cell sorting (FACS) strategy using several markers: cleaved Caspase-3, Oct4, 5-ethynyl-2'deoxyuridine (EdU) and propidium iodide (PI). This analysis provides us with several advantages when having to study differentiation *in vitro*, as firstly, it allows the analysis of a higher number of cells compared to the immunofluorescence method in a statistically significant manner. Secondly, the cleaved Caspase-3 staining allows the discrimination

between the apoptotic population and viable population, thereby not only obtaining information on the apoptotic index but also to analyse the viable population separately from apoptotic cells as the latter may downregulate markers because of their state. Thirdly, Oct4, which is a marker of both ESCs and EpiSCs, would allow us to follow the pluripotent population in relation to proliferation and apoptosis, during the differentiation. Fourthly, EdU in combination with DNA content measurement by PI allows us to analyse the distribution of the population during the different phases of the cell cycle and to investigate the proliferative capacity of the Oct4 expressing and not expressing cells. EdU is a thymidine analogue and is used as a substitute to BrdU to measure cell proliferation, as it can be given to live cells for a specific amount of time and only proliferating cells will incorporate EdU and in contrast to BrdU, it allows simultaneous detection of other antigens as it is not necessary to denaturate the DNA to detect it. Analysing the proliferation of the cells is important to discriminate whether the RaLP KO cells are cycling slower overall (therefore the completion of one cell cycle takes longer, i.e. the doubling time) or are persisting in a certain phase of the cell cycle for a longer period of time (for example, they are stuck in G1 for a longer time). For the analysis, HT and KO cells were collected at several timepoints during the differentiation: the starting population of ESCs, passage two, three and four.

Setting up the protocol for flow cytometry using four fluorochromes was not so straightforward, as several parameters must be taken into consideration and tested. Not only the combination of fluorochromes must be considered but also the intensity relative to the abundance of the antigen that must be measured, fixation and permealisation methods that allow efficient detection of intracellular antigens as well as DNA in order to obtain a clean read-out. Many conditions as well as combinations of fluorochromes were tested and after several trials, we found that the most efficient combination resulted in the detection of cleaved caspase-3 in FITC, Oct4 in Cy5, EdU in pacific blue and DNA with PI.

As could be seen by observing the cultures during the differentiation, this protocol was accompanied by a substantial amount of cell death and this was also confirmed by the FACS analysis (Figure 33). The subG1 population seen by PI staining (columns one and three from the left) show a gradual increase of cell death during the passages and it is by programmed cell death, as cells stained positive for cleaved Caspase-3 (columns two and four from the left). Both in the HT and KO ESCs, the starting amount of apoptotic cells in the population are the same and constitute a minority of the population, as expected. Starting from passage two, there is an overall increase in apoptotic cells in both populations. Overall, KO cells showed similar amount of cell death as the HT. In particular, at passage three, there were slightly lower amounts of Caspase-3 positive cells. This cannot account for the significantly less number of cells observed during the differentiation in KO compared to the HT, indicating that there must be other processes that could provide the explanation, for example, differences in the rate of proliferation of the cells.

We then decided to analyse the proportion of the pluripotent cells at each passage by using the region defined on the basis of cleaved Caspase-3 negativity (Figure 33, lower region) to analyse Oct4 expression only in the viable population (shown as green dots in lower region).

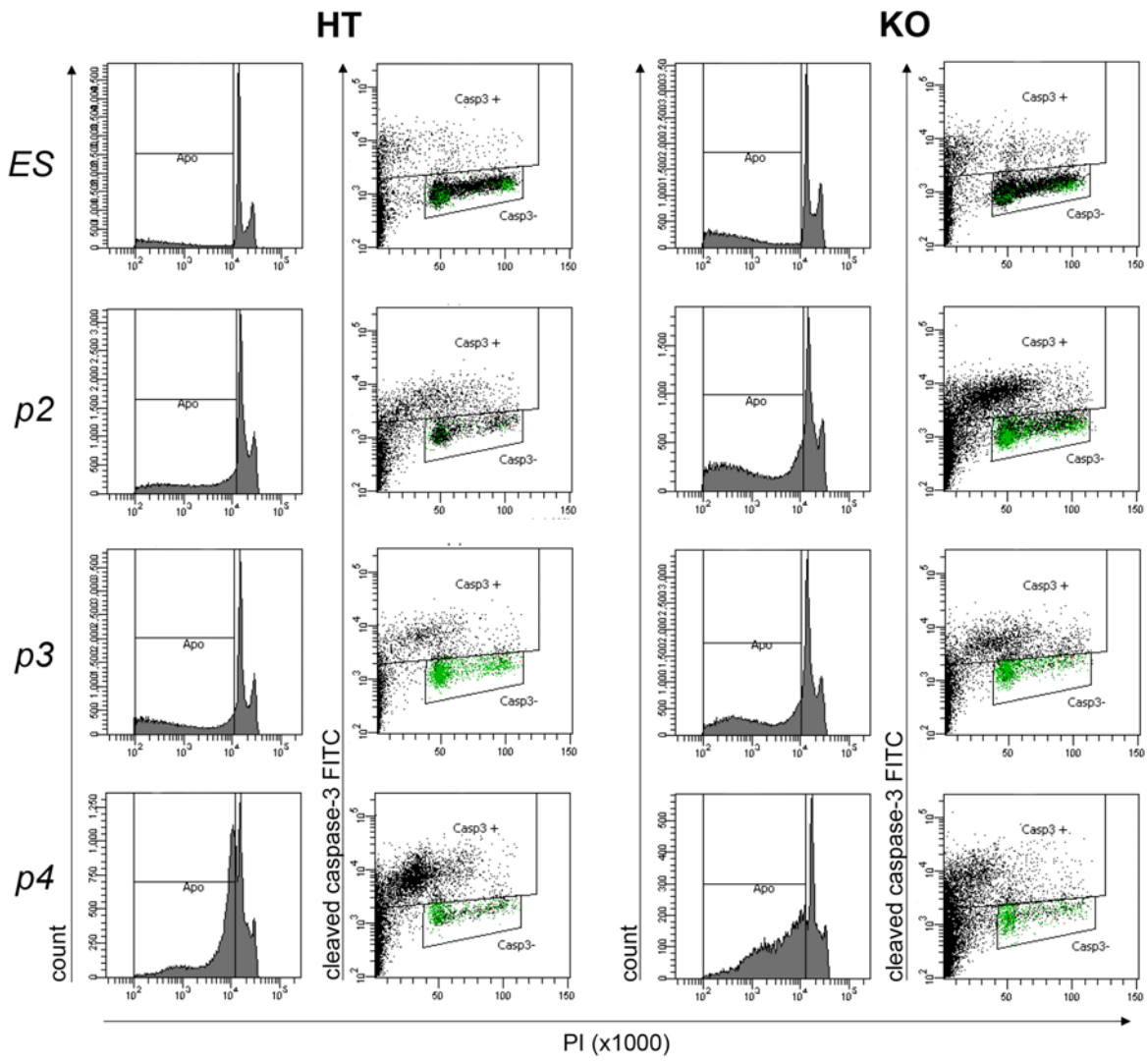

Figure 33. Analysis for the overall cell death and rate of apoptosis during the derivation of EpiSCs from ESCs by FACS staining for cleaved Caspase-3. RaLP HT (columns one and two from the left) and KO (columns three and four from the left) cells were analysed for cleaved Caspase-3 at passage zero (ESCs), two (p2), three (p3) and four (p4) of differentiation. The analysis is shown in a dot plot with PI intensities on the x-axis and FITC intensities on the y-axis. The cleaved Caspase-3 negative population is the region below and the Caspase-3 positive in region above. Shown as green dots are cells expressing Oct4 within the cleaved Caspase-3 negative region.

An interesting general trend of Oct4 regulation could be observed during the transition of ESCs to EpiSCs (Figure 34). In the ESC population, there is a small fraction of cells (between 2 to 4%) that are negative for Oct4.which are probably differentiated cell types co-existing in culture with the ESCs. This is expected, as a certain degree of differentiation in culture is always present in ESC cultures. Upon differentiation initiation by the withdrawl of LIF and addition of FGF2 and activin A, there is a general downregulation of Oct4 which is the most striking at passage three when the majority of the population

becomes negative, leaving a 4 to 10% of cells expressing Oct4 in the HT and KO respectively. Then Oct4 expression is restored gradually so that by passage four in the HT, approximately half of the cells of the population are positive for Oct4 and this probably corresponds to the timewindow when EpiSCs are established, as can be seen already by the gene expression profile of the cultures.

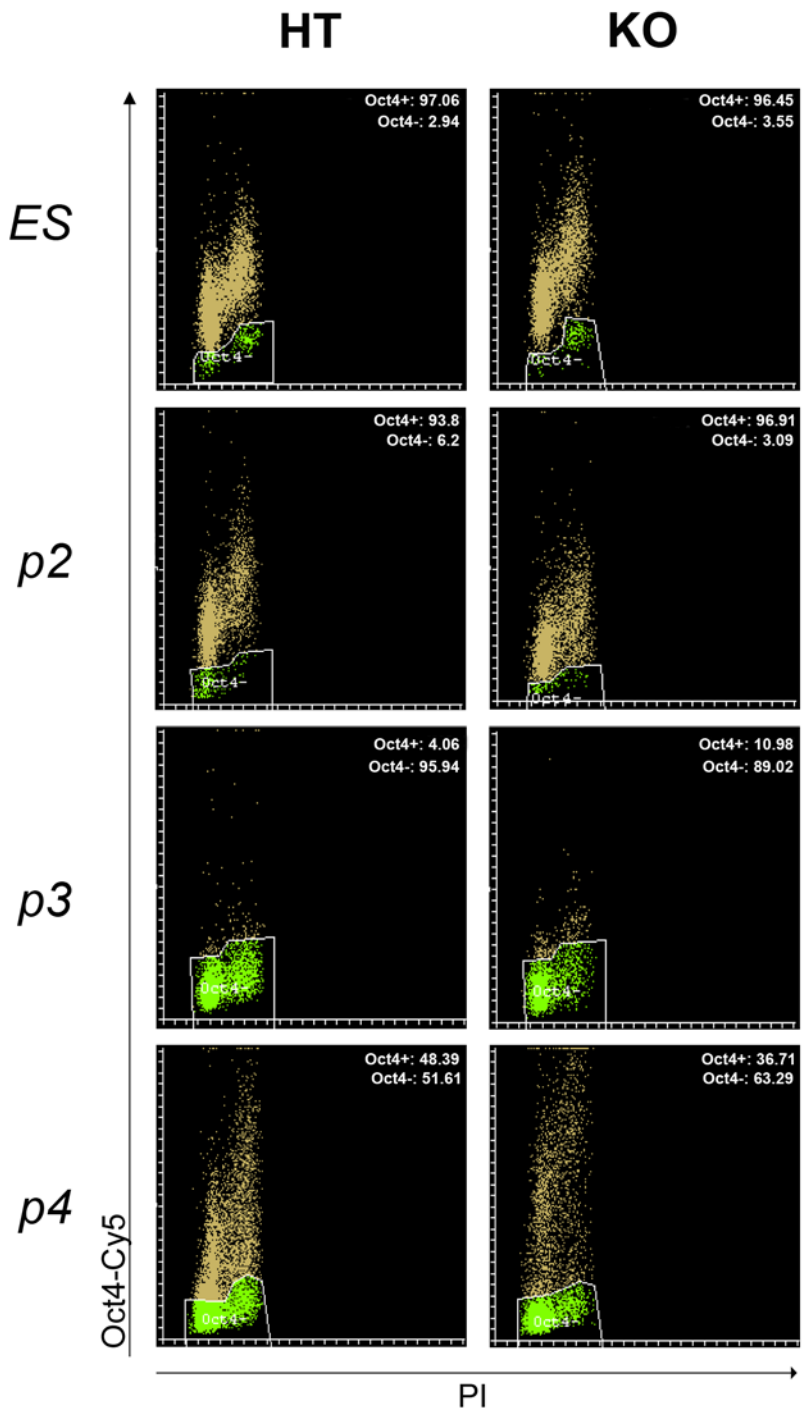

Figure 34. FACS analysis of Oct4 expression in HT and KO cells during ESC to EpiSC differentiation. Oct4 expressing (Oct4+, in yellow) and Oct4 non-expressing (Oct4-, in green) populations for the RaLP HT

(left column) and KO (right column) were analysed at passage zero (ESCs), two (p2), three (p3) and four (p4) of differentation. Shown are dot plots with Cy5 intensities on the y-axis and PI on the x-axis. For each sample, percentages of Oct4 positive cells are indicated.

The comparision of the profiles between HT and KO evidenced an overall similar pattern of Oct4 regulation. However, the restoration of the Oct4 positive population at passage four is retarded in the KO, as the portion of cells expressing it remains lower in the KO compared to the HT, 42.09% and 36.71%, respectively. This observation could be due to the fact that the Oct4 expressing cells cannot differentiate efficiently and/or have proliferative defects in the absence of RaLP.

In order to investigate further whether these differences could be explained by different proliferation capacities, we analysed separately on the Oct4 positive and negative population (both from the cleaved Caspase-3 negative population), the EdU incorporation in the HT (Figure 35) and KO cells (Figure 36). EdU together with DNA content by PI allows us to distinguish the cell cycle phases into S phase (EdU positive), G0/G1 (EdU negative, DNA content 2n) and G2/M (EdU negative, DNA content 4n).

Generally we observed that in the ESC population, as it has been described in numerous studies, a significant portion of the cells expressing Oct4 are cycling cells (from 35 to 50%) seen from the high number of cells that have incorporated EdU. On the other hand, the majority of the Oct4 negative cells were EdU negative and in the G0/G1 or G2/M phases, indicating that they were either cycling at a slower rate or not cycling at all. This could also be seen clearly from the different profiles of the DNA content by PI (first and third columns from the left in both Figures), where there are two high peaks corresponding to the cells in G0/G1 and G2/M phase of the cell cycle in the Oct4 negative populations.

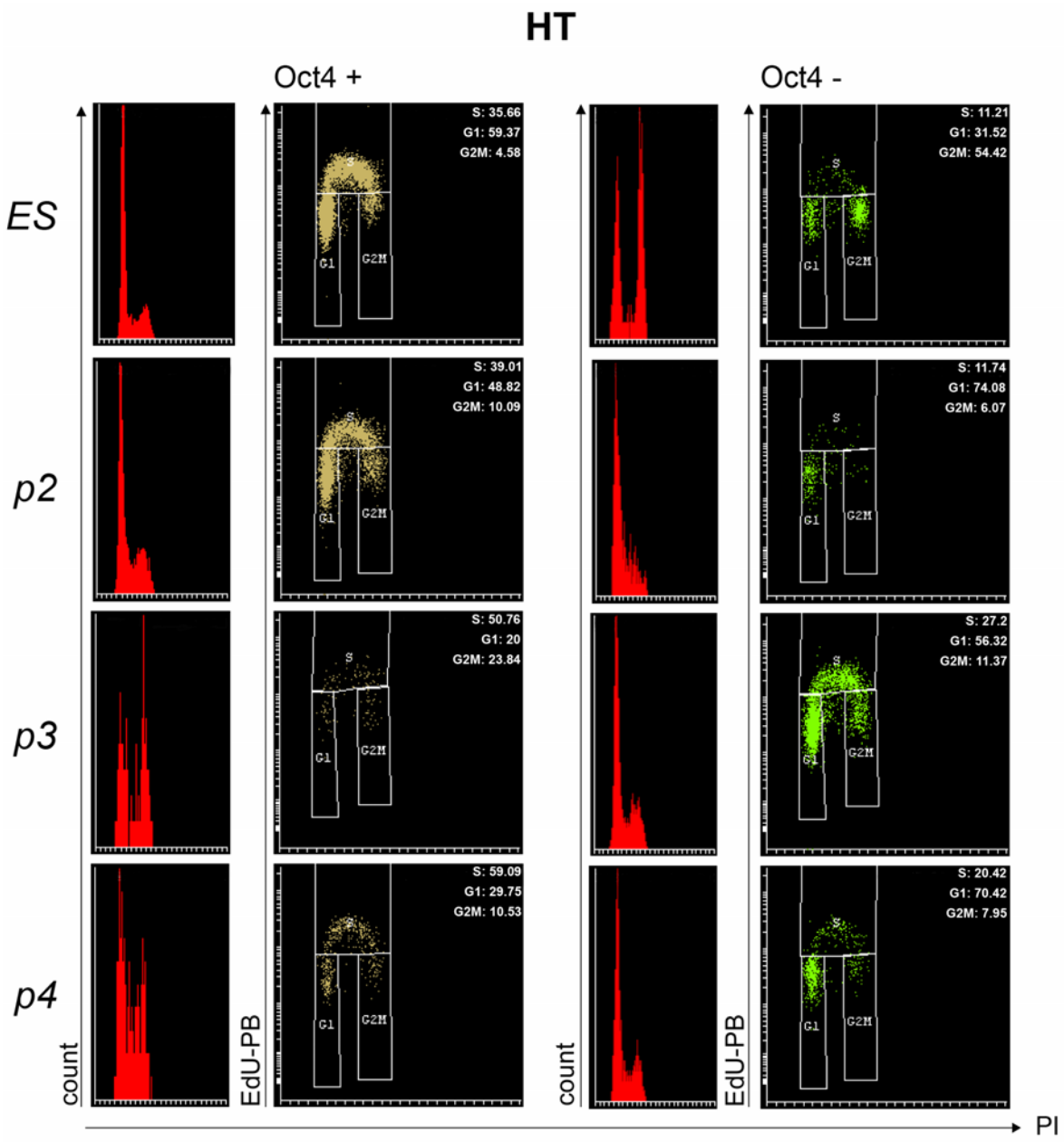

Figure 35. FACS analysis of cell proliferation by EdU incorporation, classified according to Oct4 expression in HT cells during ESC to EpiSC differentiation. Oct4 positive RaLP HT cells (columns one and two from the left) and Oct4 negative RaLP HT cells (columns three and four from the left) analysed for EdU at passage zero (ESCs), two (p2), three (p3) and four (p4) of differentiation. Columns one and three show the cell cycle of viable cells (Caspase-3 negative). Columns two and four are dot plots with Pacific Blue intensities on the y-axis and PI on the x-axis. The cell cycle phases were gated according to their EdU positivity and negativity, and DNA content based on their PI intensity. For each, the percentages of cells in S phase, G1 phase and G2/M phase are indicated.

Interestingly, as ESCs are subjected to these differentiation conditions both the Oct4 positive and negative populations contain cycling cells. The Oct4 negative cells now have an increase in their proliferation ability as a substantial portion of the cells have incorporated EdU. The proliferation capacities were particularly evident, at passage three

at which the majority of the Oct4 positive and negative populations in the HT are cycling cells (50.76% and 27.2%, respectively) whereas, in the KO there was a lower proportion of cells that have incoporated EdU in both the Oct4 positive (21.88%) and positive populations (8.73%). These differences from the HT were still evident at passage four, indicating that the absence of RaLP results in a defect in proliferative capacity.

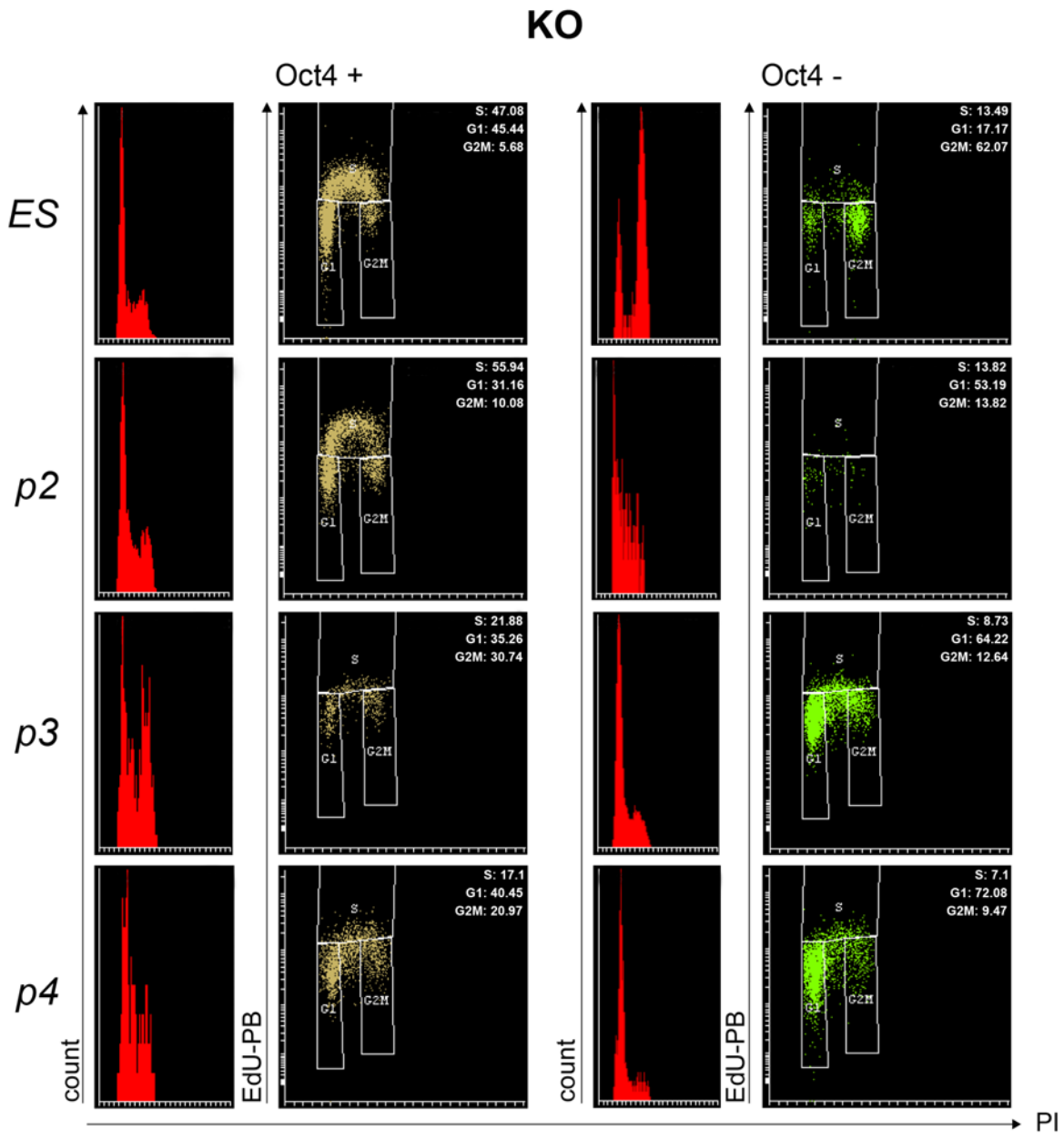

Figure 36. FACS analysis of cell proliferation by EdU incorporation, classified according to Oct4 expression in KO cells during ESC to EpiSC differentiation. Oct4 positive RaLP KO cells (columns one and two from the left) and Oct4 negative RaLP KO cells (columns three and four from the left) analysed for EdU at passage zero (ESCs), two (p2), three (p3) and four (p4) of differentiation. Columns one and three show the cell cycle of viable cells (Caspase-3 negative). Columns two and four are dot plots with Pacific Blue intensities on the y-axis and PI on the x-axis. The cell cycle phases were gated according to their EdU

positivity and negativity, and DNA content based on their PI intensity. For each, the percentages of cells in S phase, G1 phase and G2/M phase are indicated.

Taken together, this FACS experiment (which has been confirmed by an independent experiment and an additional control biological control with WT ESCs, data not shown) has shown interesting dynamics of the behavior of the Oct4 expressing cells during the differentiation of ESCs to EpiSCs. Furthermore, the absence of RaLP results in a defective ability of the cells to undergo proliferation and to maintain the Oct4 positive cells in their population.

We next analysed the RaLP HT and KO EpiSCs cultures by immunofluorescence to assess whether the proliferative defect is overcome by long-term passaging (passage 10, which corresponds to about one month in culture; Figure 37). Firstly, the Oct4 staining clearly evidenced the two subpopulations observed in the FACS analysis: Oct4 expressing cells growing in colonies surrounded by Oct4 negative cells, suggesting that EpiSC cultures are heterogenous even at later passages. The HT cultures consisted of large colonies with the majority of the cells that were Oct4 positive. The RaLP KO cultures consisted of smaller Oct4 positive colonies surrounded by a majority of Oct4 negative cells, suggesting that there were still growth defects that affected particularly the Oct4 expressing compartment, suggesting that the phenotype caused by the absence of RaLP is not a transient phenomenon in this *in vitro* system.

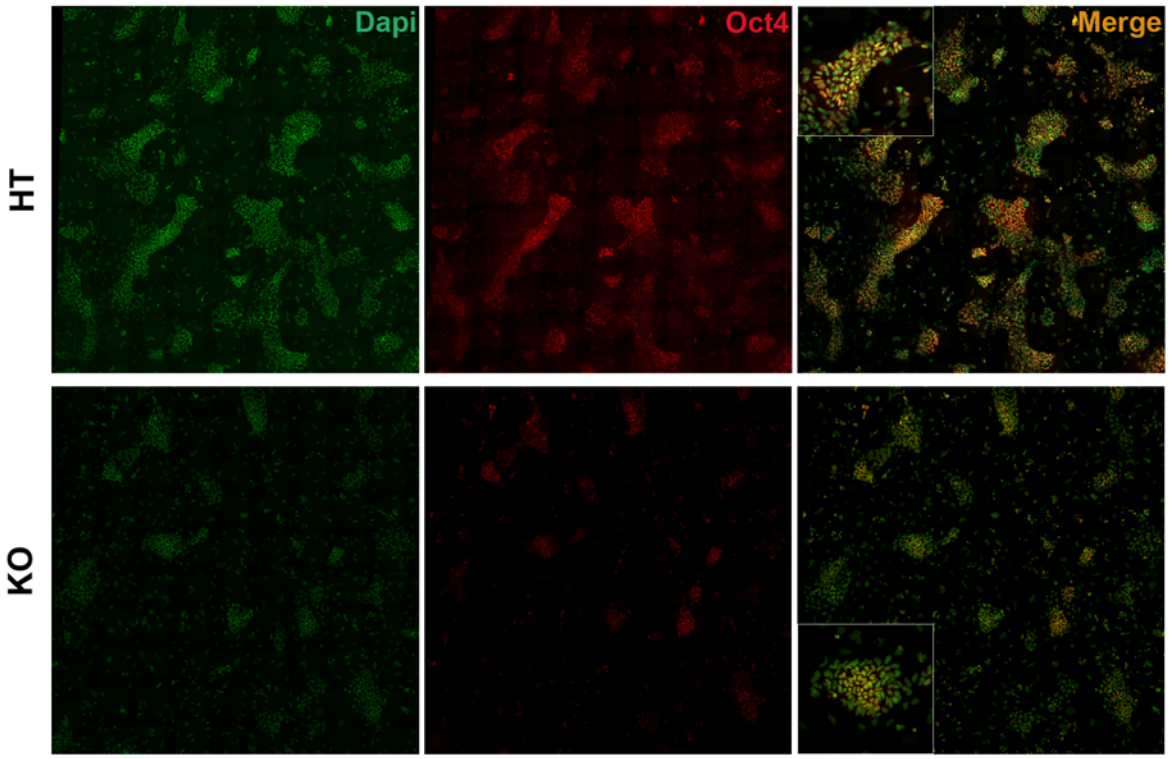

Figure 37. Immunofluorescence for Oct4 on RaLP HT and KO EpiSC cultures at passage 10. Images were taken at x40 and assembled with mosaic approach to view a wider field. Boxed images in the merged panel are zoom-in of EpiSC colonies.

4.3.3. Investigating the heterogeneity of the EpiSC cultures

The FACS data indicated the lower number of Oct4 positive cells in the RaLP KO cultures during the formation of the epiblast population and observing the cells during culturing, striking morphological differences could be seen. To visualise whether the Oct4 positive and negative population possessed different morphological characteristics, we stained the cells at the same timepoints taken for FACS, with Oct4 and actin (Figure 38).

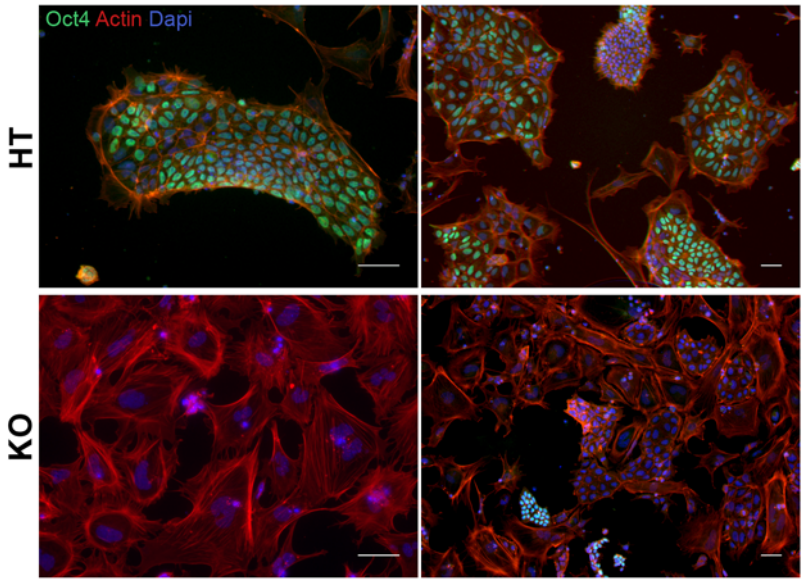

Figure 38. Immunofluorescence for Oct4 and actin on HT and KO cells at passage four of EpiSC differentiation. At passage four, the majority of RaLP KO cultures consisted of Oct4 negative cells that were large and flattened and grew in isolation. Scale bar represents 50 μm.

The immunofluorescence also confirmed lower levels of Oct4 overall seen by the FACS analysis, in the RaLP KO population. In particular, at passage four almost all cells in culture consisted of large, flattened, polinucleated cells that were Oct4 negative. Notably, the presence of these enlarged, flattened cells during the differentiation was not a phenomenon restricted to the KO cultures, as they were also present in the controls, the RaLP HT ESCs (Figure 39) and WT ESCs (data not shown). These large flattened cells typically arise on the borders of the colonies and they grew in isolation.

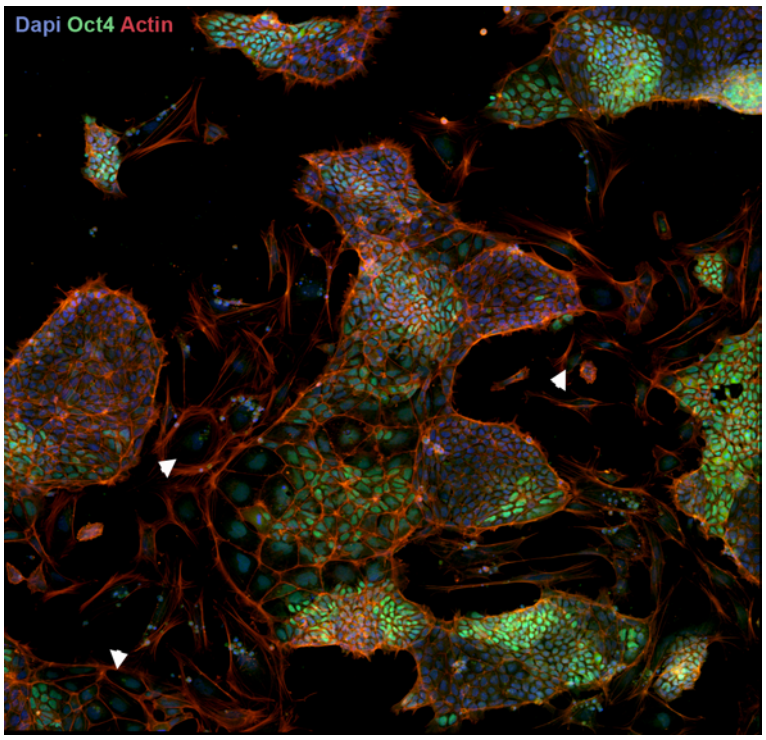

Figure 39. Immunofluorescence for Oct4 and actin of HT cultures at passage four of EpiSC differentiation. Images were taken at x40 and assembled with mosaic approach to view a wider field. The white arrowheads indicate the enlarged, flattened cells that are Oct4 negative typically located around the colonies and grow in isolation.

The lower proliferation rate could be a result of the cells unable to undergo proper differentiation and therefore become senescent or the generation of a cell type that divide slower. The large, polinucleated morphology of the cells seemed reminiscent of a senescent phenotype, which could be caused by DNA damage. The RaLP KO and HT cells from passage zero to passage four were stained for DNA damage and senescent markers by immunofluorescence to examine this aspect (data not shown). p53 and phospho-histone2AX signals were present but there were no differences between the RaLP HT and KO. There are studies that suggest that these markers might have a physiological role in ESC and in their differentiation process, in particular, p53 [108] and pH2AX (Andrew Xiao, personal communication). This would be an interesting aspect to examine, however, they are not informative markers in the contest of these studies and furthermore, we did not see any differences that could suggest that the KO are more senescent or have undergone more DNA damage than the HT. So we decided to shift our attention to understanding the

identity of the KO cells, in other words, whether the cells generated in the KO cultures are of another embryonic lineage, caused by a perturbed signalling pathway in the absence of RaLP, To this end, we screened for several markers of all lineages types by qRT-PCR on RaLP HT and KO cells from ESCs to passage five of differentiation (Figure 40).

Oct4, which is a marker of ESC and EpiSCs, show fluctuating expression levels during the differentitiation but it is always expressed during the process. There did not seem to be striking differences of Oct4 between the HT and the KO. Nanog and Klf4 are downregulated more dramatically than Oct4, and their levels did not show any differences between the genotypes. Marker of EpiSC, FGF5 seemed slightly higher at passage two and three in the HT, however the general trend and upregulation was also observed in the KO. Endoderm (Gata6), postimplantation epiblast and mesoderm (Brachyury) markers showed overall a similar pattern of regulation between the HT and the KO, although they seem to be expressed at slightly lower levels in the KO at later passages. Overall, these markers did not show behave in very different manner, in the absence of RaLP.

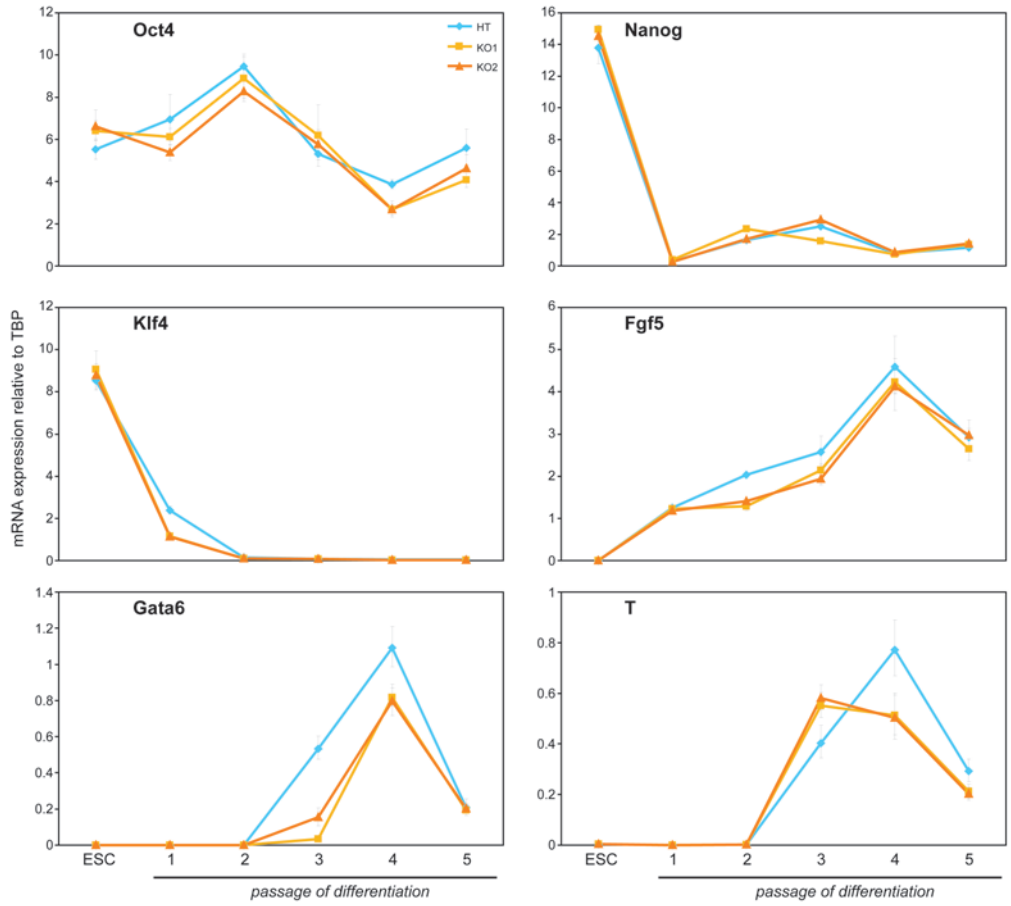

Figure 40. qRT-PCR profiles of pluripotency and early lineage genes on RaLP HT and KO ESCs during EpiSC differentiation. Analysis of Oct4, Nanog, Klf4, Fgf5, Gata6 and Brachyury (T) during the EpiSC differentiation by qRT-PCR. Bars represent the means ± S.D. of triplicates. Shown are representative results from three independent experiments.

However, when cells were analysed for extraembryonic trophoblast markers, the transcription factors caudal-type homeobox protein 2 (Cdx2) and the basic helix-loop-helix gene Hand1, the KO cells consistently showed an upregulation starting from passage two with a much higher expression fold by passage four (Figure 41.A). The formation of the trophectoderm and the inner cell mass marks the first differentiation event that occurs during embryogeneisis. The morula gives rise to the blastocyst with an outer epithelial layer which is the trophoblast, surrounding a compact mass which is the inner cell mass, in the cavity, the blastocoel at E3.5. The trophectoderm is fundamental for the implantation of the embryo and generates the specialised population of trophoblast cells that will form the placenta. Cdx2 is among the first transcription factors that are expressed to determine the trophoblast lineage and is required for trophoblast survival and maturation [109]. The

qRT-PCR data was confirmed at the protein level by immunofluorescence for Cdx2 on cells at passage four (Figure 41.C). Almost all cells in the KO cultures showed clear nuclear staining for Cdx2, whereas the majority of the HT cells showed weak cytoplasmic staining. This seems to suggest that in the absence of RaLP under EpiSC generating conditions, the majority of the cells in culture are trophoblast-like. Furthermore, several other important trophoblast specification genes such as Gata3 [110] and TEAD4 [111] were also expressed and at higher levels in the KO (Figure 41.B). The platelet derived growth factor receptor α (PDGFR) is expressed in a more differentiated type of trophoblast cells, the labyrinthine trophoblasts [112] and it was also expressed suggesting that in these cultures besides the presence of undifferentiated trophoblast-like cells, there was also differentiated subtypes.

Notably, these Cdx2 positive cells were present also in the HT and WT. This is an interesting aspect, as murine ESCs contribute poorly to extraembryonic lineages of the trophoectoderm and endoderm when reintroduced into early embryos [42]. In fact, also *in vitro*, murine ESCs do not readily differentiate into cells of extraembryonic origin. These limitations could only be overcome by the genetic manipulation of key transcription factors that govern trophoblast development such as, Oct4 [113] and Cdx2 [114], or as shown recently by specifically manipulating cell culture conditions by modulating Wnt signalling [115] and the extracellular matrix [116].

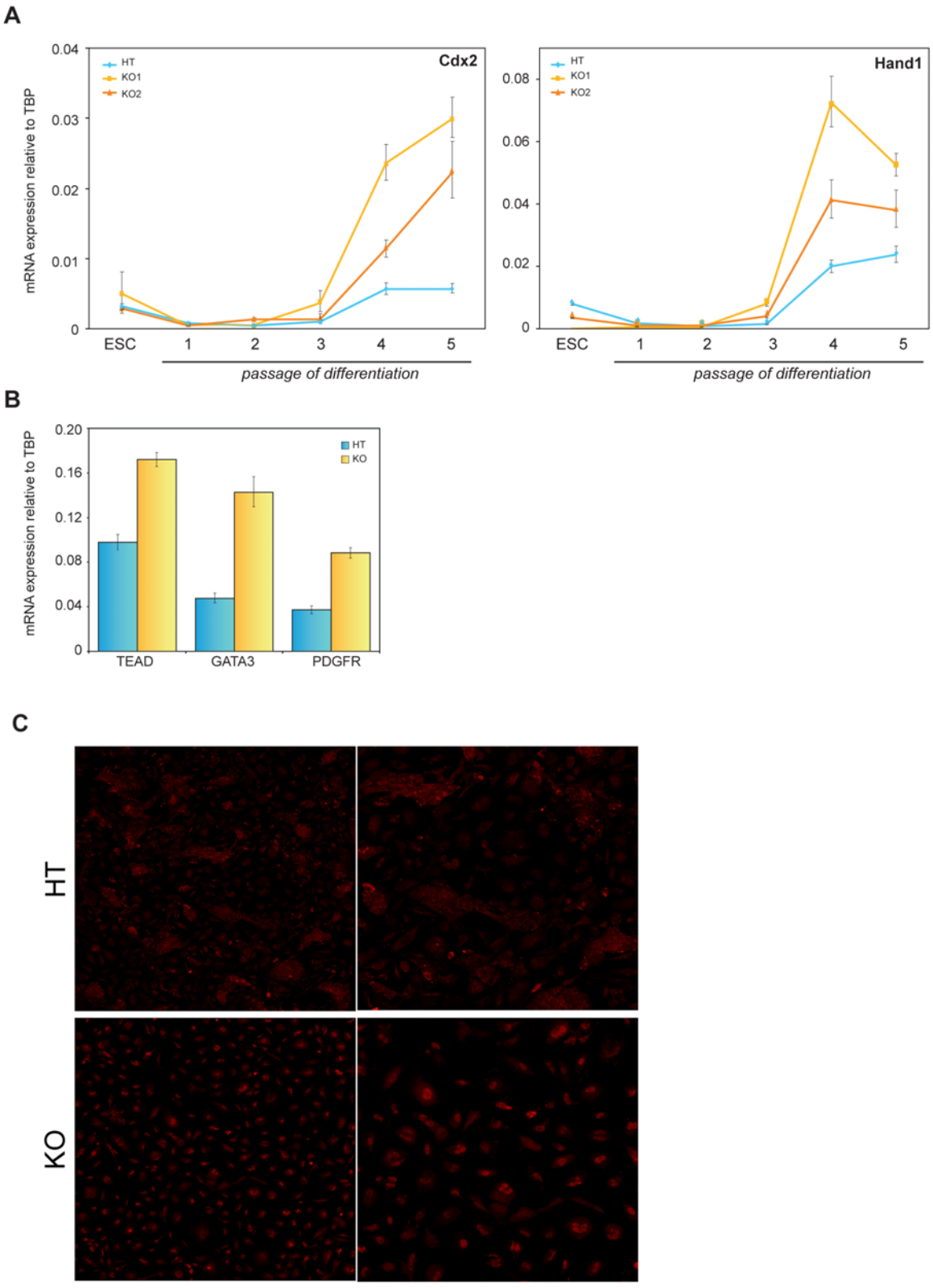

Figure 41. Trophectoderm markers are highly upregulated during EpiSC derivation in RaLP KO cells. (A) QRT-PCR for Cdx2 and Hand1 in RaLP HT and KO cells during differentiation at sequential passages. The relative expression levels for these markers have been normalised to TBP. Bars represent the means ± S.D. of triplicates. **(B)** QRT-PCR for TEAD4, Gata3 and PDGFR in RaLP HT and KO cells at passage four of differentiation. The relative expression levels for these markers have been normalised to TBP. Bars represent the means ± S.D. of triplicates. **(C)** Immunofluorescence for Cdx2 in RaLP HT and KO cells at passage four. Images were taken at x40 and assembled with the mosaic approach. Right panel are zoom-in images.

4.3.4. Dissection of the signalling pathway of RaLP

ESCs and EpiSCs rely on different signalling pathways for their self-renewal *in vitro*. ESCs depend on the LIF-STAT3 and bone morphogenetic protein (BMP4) signalling, whereas EpiSCs are dependent on FGF-Erk1/2 and Nodal/Activin A-Smad2/3 signalling. It is very interesting that FGF-Erk1/2 signalling have opposite effects in these two cell states, as its activation is a differentiation cue in ESCs and in contrast, they are a self-renewal factor in EpiSCs. In order to gain insight in the role of RaLP and to understand how the absence of RaLP causes a defect in EpiSC formation *in vitro*, it is necessary to collocate this adaptor protein in a signalling pathway. We decided to start examining these two pathways that are important for the establishment and maintenance of EpiSCs, by Western blot analysis. Smad2/3 levels did not differ in a significant manner between the HT and KO during differentiation (Figure 42). However, Erk1/2 levels were consistently higher in the KO compared to the HT from passage two.

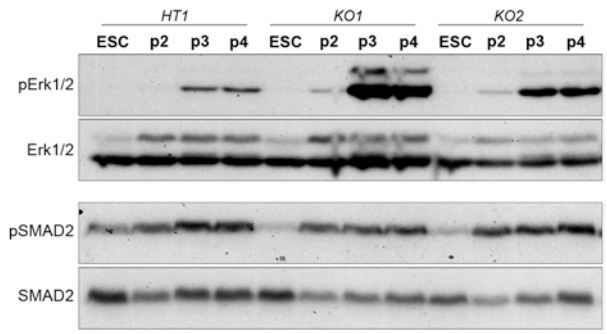

Figure 42. Activation of Smad2 and Erk1/2 during EpiSC differentiation of RaLP HT and KO ESCs. The levels of phospho-Erk1/2 and phospho-SMAD2 were analysed at passage zero (ESCs), two, three and four of differentiation by Western blotting.

There are several genetic manipulations that can be done to induce trophoblastic differentiation of ESCs: the knockdown of Oct4 [113], overexpression of Cdx2 [114], knockout of DNA methylase Dnmt1 [117] and overexpression of constitutively activated form of Ras [118]. Studies have shown that the Ras-MAPK signalling pathway during embryonic development can determine different lineage outcomes according to the levels

of its activation - higher levels determines differentiation towards extraembryonic lineages and moderate levels leads to the segregation to embryonic lineages. Although Erk activation is higher in the RaLP KO population, this effect might simply be a consequence of the perturbation of another pathway that is crosstalking with the Ras-MAPK pathway. In fact, the kinetics of Erk activation followed closely that of the Cdx2 expression during the differentiation of the KO cells, which could suggest that higher Erk1/2 levels are due to the higher number of trophoblast-like cells in the population. We investigated this further by immunofluorescence for phospho-Erk1/2 (Figure 43) on passage three of differentiation when the biggest differences was seen between the HT and KO by Western blotting. Generally, pErk1/2 is present within the population of both HT and KO, indicating that indeed during differentiation, this pathway is activated. Interestingly, different localisation of pErk1/2 was observed within the cell types within the population: cells growing in colonies had cytoplasmic pErk1/2 while isolated cells or cells located on the periphery of the colonies had nuclear pErk1/2. Furthermore, more cells with nuclear phospho-Erk1/2 were observed in the KO population compared to HT. This data is in agreement with the hypothesis that the cells that are growing isolated are the differentiated cells and those that upregulate Cdx2, which is downstream of MAPK/Erk signalling.

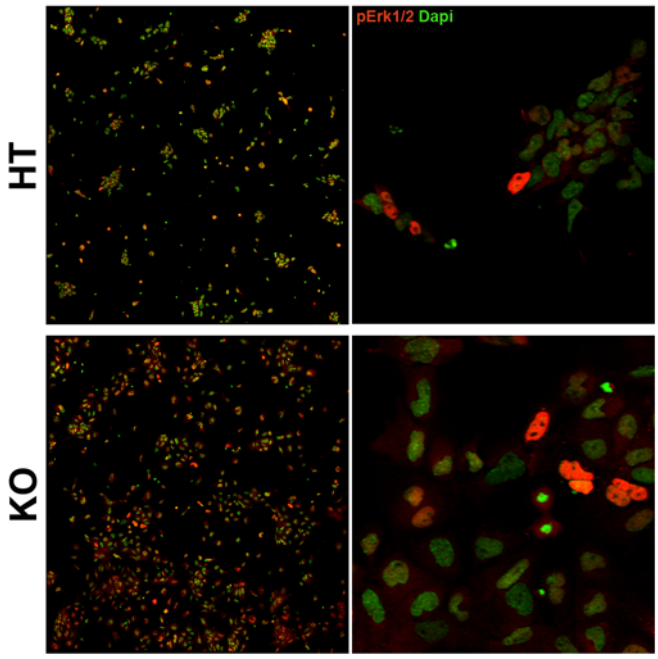

Figure 43. Phospho-Erk1/2 by immunofluorescence at passage three of ESC to EpiSC differentiation of RaLP HT and KO cells. HT cultures (top panel) are mostly constituted of small cells growing as colonies and occasional isolated cells while the majority of the cells in the KO cultures (bottom panel) are growing as isolated, large cells. Images were taken at x40 and assembled with mosaic approach to view a wider field. The zoom-in (right column) of the mosaic images (left column) shows the different localisation of pErk1/2 within the population.

Firstly, in order to understand whether also in this context, the higher levels of Erk activation provides an instructive signal for the differentiation to Cdx2 positive trophoblast cells, we decided to inhibit its activation during the differentiation, starting from the timepoint when RaLP is upregulated (passage two) and to monitor its effects on Cdx2 expression. A specific inhibitor of the upstream effector of Erk, MEK, the PD0325901 was added to the cultures at different concentrations, in order to have a partial inhibition of Erk, as abolishing its activity completely would have negative effects on the differentiation process itself (Figure 44A) [74].

The results show that firstly, high levels of Erk inhibition with the addition of 1 μM of PD caused overall cell death and it was not possible to obtain samples for analysis. Therefore we analysed only concentrations of 0.1 μM and 0.5 μM. The addition of the inhibitor did not counteract the morphological difference of the KO compared to the WT (Figure 44B). There are several possible explanations: one is that the inhibitor itself is not enough to

block the differentiation as other pathways are involved in the process or the addition of the inhibitor at passage two was too late, so once the cells are committed to this differentiation, the addition of the inhibitor does not disrupt them, as can be seen from the majority of flattened cells that survive even at high doses of PD0325901 both in the HT and in the KO. This could suggest that once the cells have committed to trophoblast fate, phospho-Erk1/2 provides only a sustaining signal. The interesting observation was that HT and KO populations showed a different sensitivity to the presence of the inhibitor. Most HT cells died and the only ones that survived and continued to grow were the flattened cells. In the KO, the majority of the population survived and there was less cell death overall than in the HT.

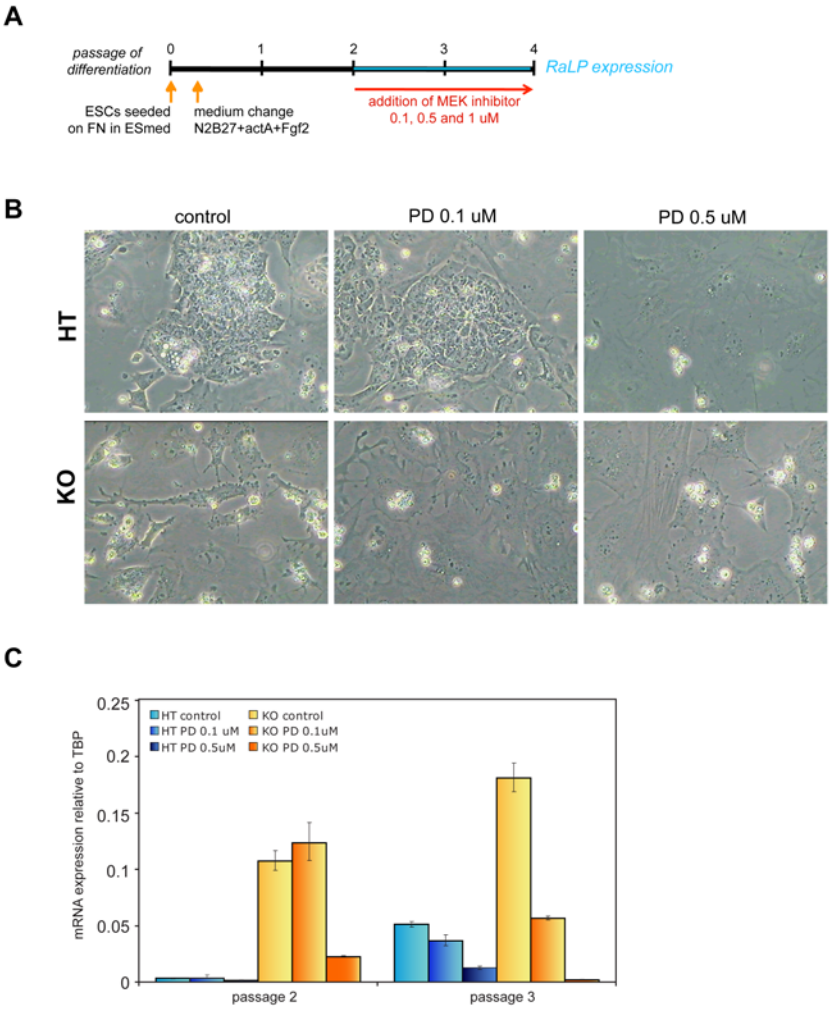

Figure 44. Inhibition of phospho-Erk by MEK inhibitor PD0325901 during ESC to EpiSC cell differentiation passage two and three of RaLP HT and KO cells. (A) Scheme of the experimental set-up.

Different concentrations of PD0325901 was added starting from passage two when RaLP is upregulated. **(B)** The morphology of the cells with and without the PD0325901. **(C)** QRT-PCR analysis for Cdx2 expression in RaLP HT and KO cells at different concentrations of the inhibitor at passage two and three of differentiation. The relative expression levelsof Cdx2 were normalised to TBP. Bars represent the means ± S.D. of triplicates.

This reflects the different composition of the population of the HT and KO. EpiSCs cannot survive under ESC conditions of 2i/LIF and probably most cells that have died are because they are of EpiSC identity.

We then analysed whether the partial attenuation of Erk1/2 activation has a consequence on overall Cdx2 levels in the RaLP HT and KO cultures, by qRT-PCR. At passages two and three, as has been observed previously, Cdx2 transcripts levels were higher in the KO compared to the HT. In the KO cultures at passage two, the addition of the PD0325901 at 0.5 μM resulted in a lower level of Cdx2 compared to the control KO culture. At passage three, the decrease of Cdx2 expression was also observed in the presence of the PD0325901 at a lower concentration of 0.1 μM, in both RaLP HT and KO cultures. This data indicate that in this *in vitro* system, higher levels of phospho-Erk1/2 are correlated to higher levels of Cdx2.

This experiment does not provide, however, a direct connection of RaLP with MAPK signalling. Previously in our lab, RaLP was proven to mediate MAPK signalling in the context of metastatic melanoma cells by its association to Grb2 upon IGF stimulation [12]. Further experiments are necessary to investigate how RaLP is involved in the regulation of MAPK signalling in this *in vitro* system and this will be described in the future plans in the discussion.

4.4. Teratoma assay of RaLP HT and KO ESCs

As an alternative assay to assess the effect of the absence of RaLP in ESC differentiation *in vivo*, we performed a teratoma assay using RaLP HT and KO ESCs. One million cells were injected subcutaneously into the hind flank of immunocompromised mice, the

interleukin 2 (IL2) gamma chain KO mice. The teratoma were measured and recuperated at three, four and five weeks after innoculation. The tumors were photographed and measured along the two major axes before and after the careful removal of the surrounding skin. At week four and five, the KO teratomas were reduced in size compared to the HT. All tumours at the three timepoints showed no presence of adherences with no extensions to the underlying fascia. Grossly, all the tumors were firm and homogenous, fleshy on the cut surface. No haemorrhage and necrosis were apparent. Internals organs were also grossly examined to exclude the presence of macroscopic metastatic deposits.

Immunohistochemical analysis by hematoxylin and eosin staining of teratomas at three and four weeks evidenced the presence of derivatives of all the three germ layers in HT and KO (Figure 45A). This analysis also allowed distinguishing the nondifferentiated, proliferative portion of the tumour from the highly differentiated areas. The KO teratomas showed reduced areas of proliferative areas compared to the HT on several sections (data not shown).

Immunohistochemical analysis of the teratomas was done using specific markers to further confirm the presence of differentiated tissues. Glial fibrillary acidic protein (GFAP; ectoderm), myogenin (mesoderm) and cytokeratin (endoderm) were all present in the HT and KO teratomas (Figure 45B), implicating that the differentiative ability in the absence of RaLP is not perturbed.

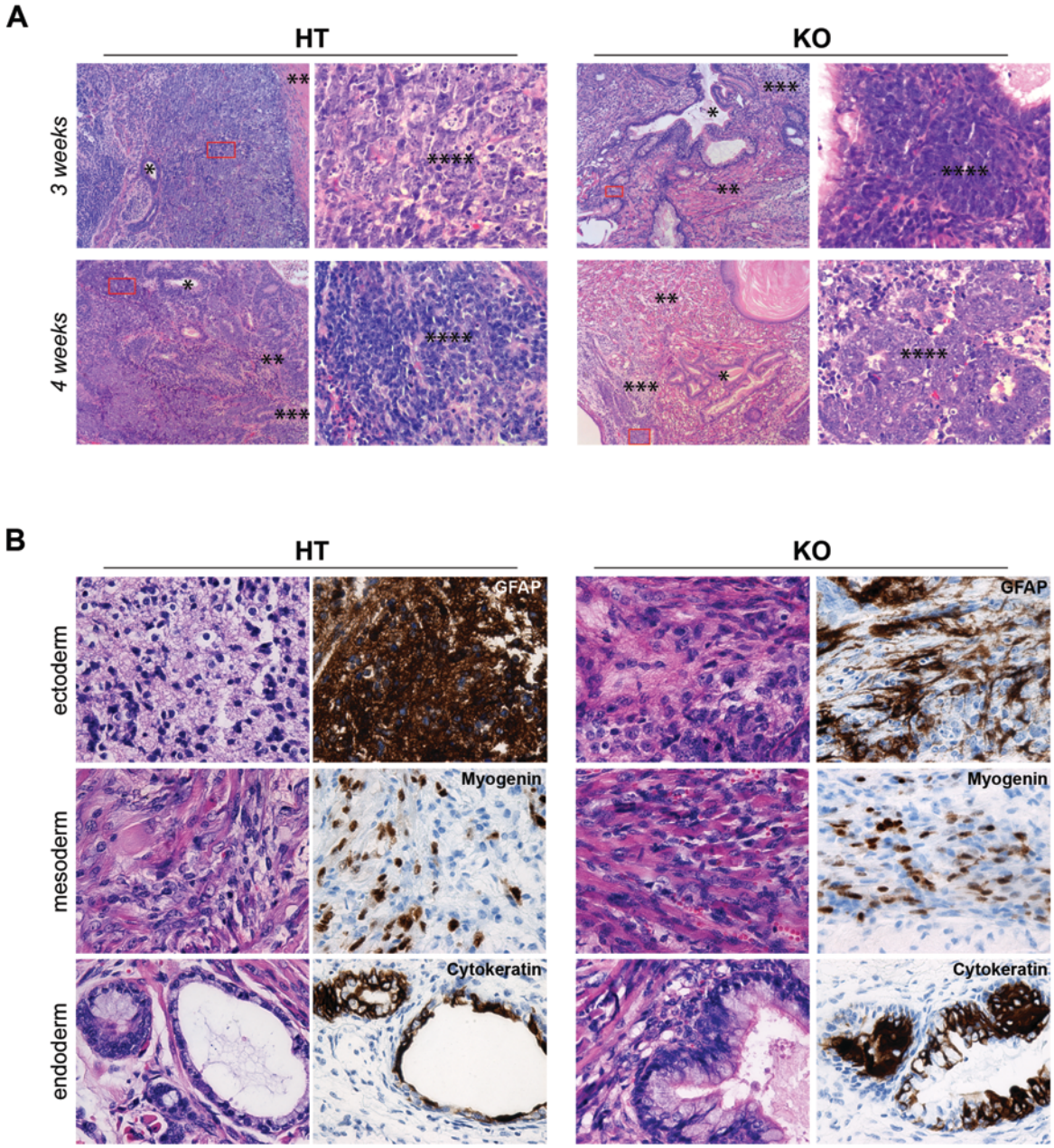

Figure 45. Analysis of RaLP HT and KO teratomas by immunohistochemistry.(A) Hematoxylin and eosin staining of RaLP HT and KO teratomas at 3 weeks (first row) and 4 weeks (second row). Derivatives of all three germ layers were present in both genotypes, first column of each genotype is at a magnification of X10. * glandular tissue (endoderm), ** muscular tissue (mesoderm) *** nervous tissue (ectoderm). **** Proliferative non differentiated areas of the teratoma (boxed in red) are shown in the second column at a higher magnification of X40, for each genotype. **(B)** Immunohistochemical analysis of the germ layer derivatives by staining with specific markers (for each genotype, right column) together with the corresponding hematoxylin and eosin staining (for each genotype, left column), magnification of X40. Glial fibrillary acidic protein (GFAP) for ectoderm, myogenin for mesoderm and cytokeratin for endoderm.

5. Functional characterisation of RaLP in neurogenesis

5.1. Derivation and characterisation of RaLP HT and KO NSCs from ESCs

The RaLP expression data during embryogenesis and in the adult, suggests a strong correlation with brain development and a brain specific function in the adult. In order to investigate which role RaLP plays in this context, we decided to derive neural stem cells (NSCs) from ESCs, using the monolayer differentiation protocol under defined conditions [48] which was already introduced in section 4.1.2 of results. As mentioned earlier, as ESCs commit to neural fate, they undergo distinct transitory states, which correspond to specific phases during development.

We decided to use this protocol to investigate the role of RaLP but this time, allowing the cells to continue further through the process instead of stopping at day eight. On this day, the population of cells that have been primed to commit to neural fate are selected further for the neural stem cell population by culturing them in a medium containing factors important for proliferation and survival of NSCs, FGF2 and epidermal growth factor (EGF) (Figure 46A). Cells undergo profound morphological changes under these differentiation conditions (Figure 46B). The round colonies of the ESCs after two days flatten and enlarge and by day eight, the colonies have expanded with numerous cells branching out from them, forming the typical neural rosettes. At this point the cells are harvested and grown in the presence of FGF2 and EGF. Under these conditions there is a selection for the cells that have committed to NSC fate and in fact, after a few days these cells form neurospheres, which is a hallmark of their identity. The neurospheres are allowed to proliferate further and then gently disaggregated and allowed to outgrow. The cells at this stage now consist of a homogenous population of self-renewing NSCs that grow as adherent cells that can be indefinitely propagated and undergo multi-lineage differentiation to the three populations of oligodendrocytes, astrocytes and neurons [49].

We confirmed the NSC identity of our cells by immunfluorescence for the neural progenitor marker, nestin (Figure 46C). The cells were almost completely negative for the markers of differented cell types, GFAP and beta III tubulin. Characterisation by RT-PCR for ESC and NSC markers showed that ESC markers Oct4 and Nanog were no longer expressed in these cells, while they maintained Sox2 expression and they upregulated neural specification markers such as Otx2 and Musashi (Figure 46D). Taken together, the ESC monolayer differentiation protocol worked optimally in our hands and the NSCs that we obtained are of true neural progenitor identity.

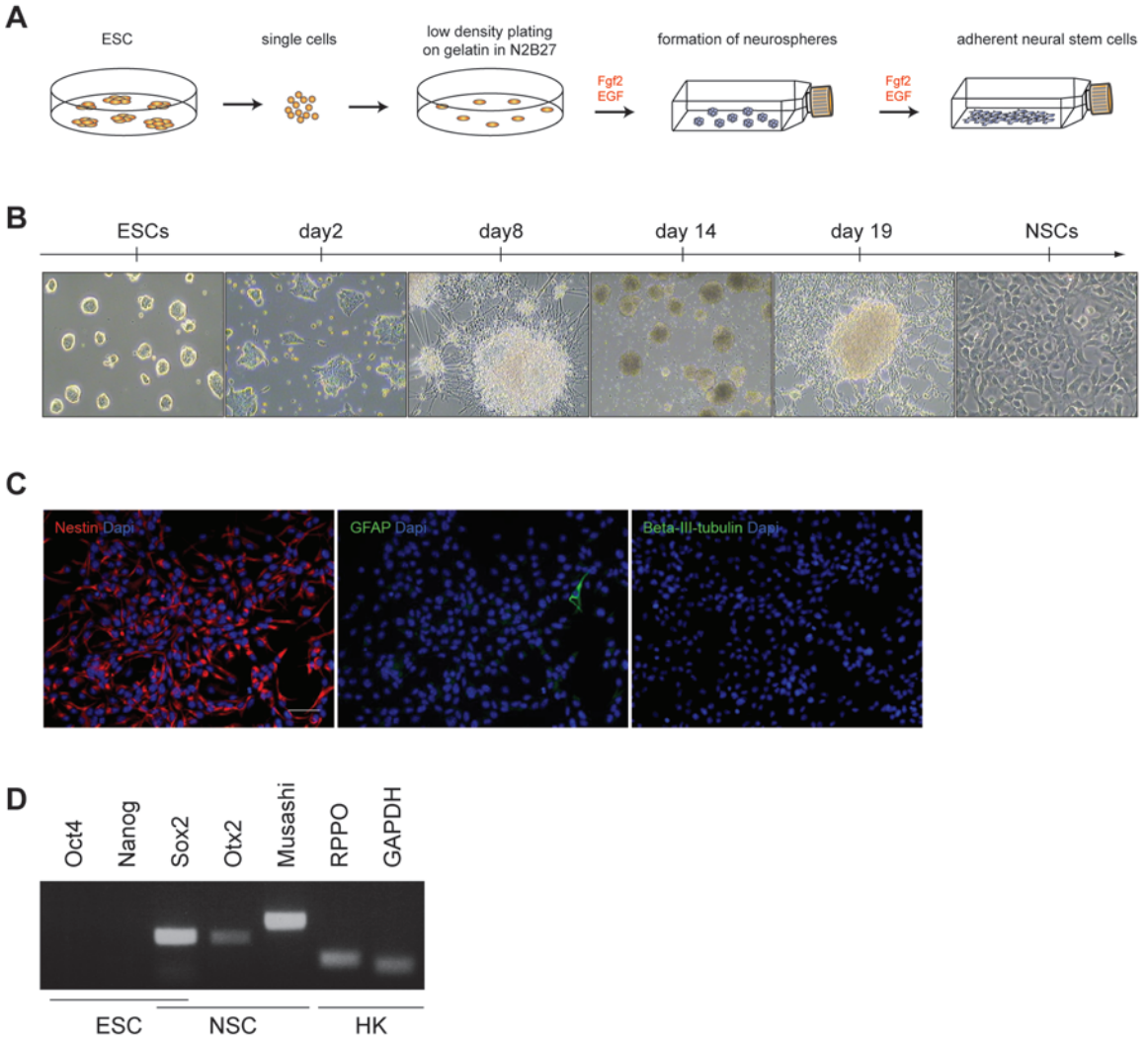

Figure 46. Characterisation of the neural differentiation of WT ESCs. (A) Schematic representation of the different phases of monolayer differentiation protocol. **(B)** Characteristic morphology of the differentiating cells during the protocol. During the first phase (day zero to day eight), ESCs commit to neural fate. In the second phase, neural progenitors are selected and amplified. During this phase, the neural progenitors first proliferate as neurospheres (day 14) and then they adhere (day19) and neural progenitors

grow out from the spheres and can then be expanded as adherent population of NSCs. **(C)** Immunofluorescence for neural marker Nestin and markers for differentiated lineages GFAP for astrocytes and beta-III-tubulin for neurons. **(D)** RT-PCR for ESC markers Oct4 and Nanog, neural markers Otx2 and Musashi, and Sox2 which is expressed in both cell types. RPPO and GAPDH are housekeeper genes.

During the neural specification of ESCs, several pro-neural genes are upregulated during this process, as can be seen from the qRT-PCR profiles for Sox1, Pax6 and nestin. RaLP expression was also investigated during the entire length of the differentiation protocol by qRT-PCR (Figure 47). As was seen previously, RaLP is upregulated on day two of differentiation when the epiblast is forming and then is downregulated. Interestingly, as the population contains neural progenitors and more differentiated progeny, RaLP was upregulated and steadily increased during the process and remained expressed in the homogenous population of NSCs at the end of the protocol (day 23). This suggests that RaLP has a dual function, firstly as an epiblast stem cell lineage gene then as a neural specific gene.

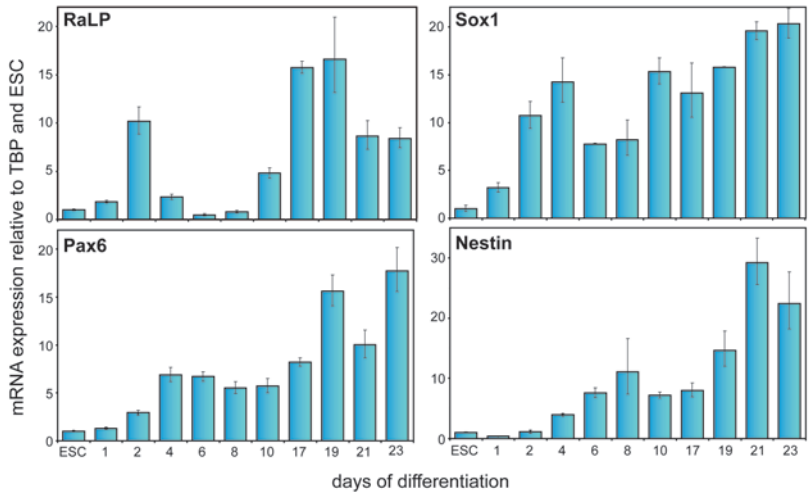

Figure 47. Neural specification markers and RaLP expression by qRT-PCR during the neural differentiation of ESCs. Bars represent the means ± S.D. of triplicates.

When RaLP WT and KO ESCs were subjected to the differentiation process, during the first few days RaLP KO cells seem to differentiate even faster than HT cells. This could be seen already by day two when the cultures contained larger flattened colonies compared to

the RaLP WT cultures. As the differentiation progressed, on day eight, the KO culture dish was completely covered with characteristic neural rosettes that were Nestin and Sox1 positive whereas the WT cultures contained smaller neural rosettes (Figure 48). Although these differences were consistently observed, it was difficult to quantify and to characterise, as the population at these timepoints were heterogenous, consisting of committing neural progenitors, ESCs and as well as a small percentage of non-neural cells [85].

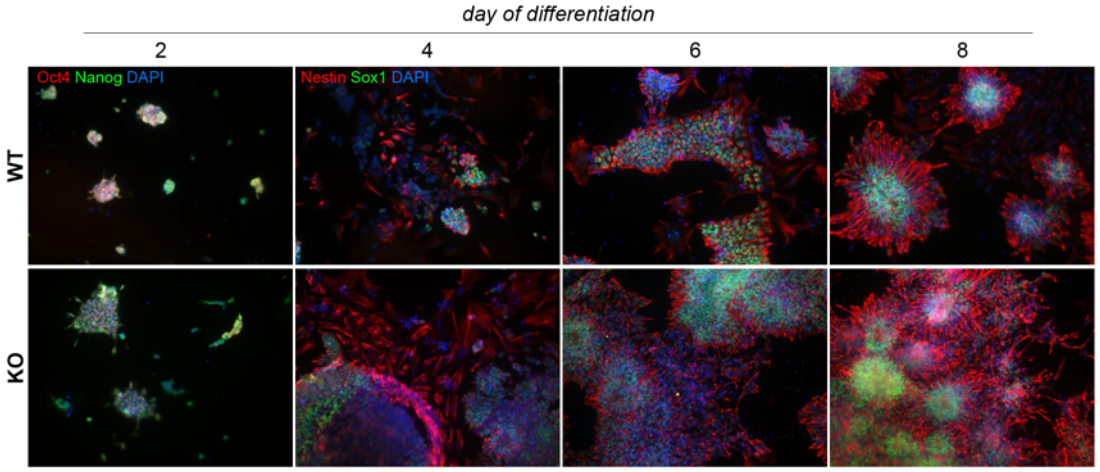

Figure 48. Immunofluorescence for pluripotent and neural differentiation markers of RaLP HT and KO ESCs during the first phase neural commitment. Cells have been stained for Oct4 and Nanog on day two. On days four, six and eight, cells were stained for Nestin and Sox1. As the cells progress through the differentiation, the formation of neural rosettes was observed.

There are two possible explanations to this phenomenon of premature differentiation. The first is, a possible compensatory mechanism by another family member, which results in a sudden spurt of differentiation. There is evidence that the upregulation of p66ShcA is involved in this process [119] and in this study, the overexpression of p66ShcA resulted in an accelerated differentiation of these ESCs towards neural fate. It is possible that the absence of RaLP results in a "physiological" overexpression of p66ShcA, therefore resulting in the faster differentiation of the RaLP KO ESCs. The second explanation is based on our data that suggests that RaLP is involved in the process of ESC to EpiSC

transition. Perhaps the absence of RaLP causes an inefficient transition to EpiSC stage and directly goes through to the successive differentiation stages.

The RaLP KO cells were nevertheless able to differentiate to NSCs as efficiently as the wild-type cells. The RaLP KO NSCs had similar morphology to the WT NSCs (Figure 49A) and uniformly stained positive for nestin (Figure 49B). They showed very low presence of differentiated cell types such as astrocytes and neurons. Furthermore, the RaLP KO NSCs showed the exact same profile of markers as the WT NSCs, as they were no longer positive for ESC markers Oct4 and Nanog while they retained Sox2 expression and upregulated the neural markers Otx2 and Musashi (Figure 49C).

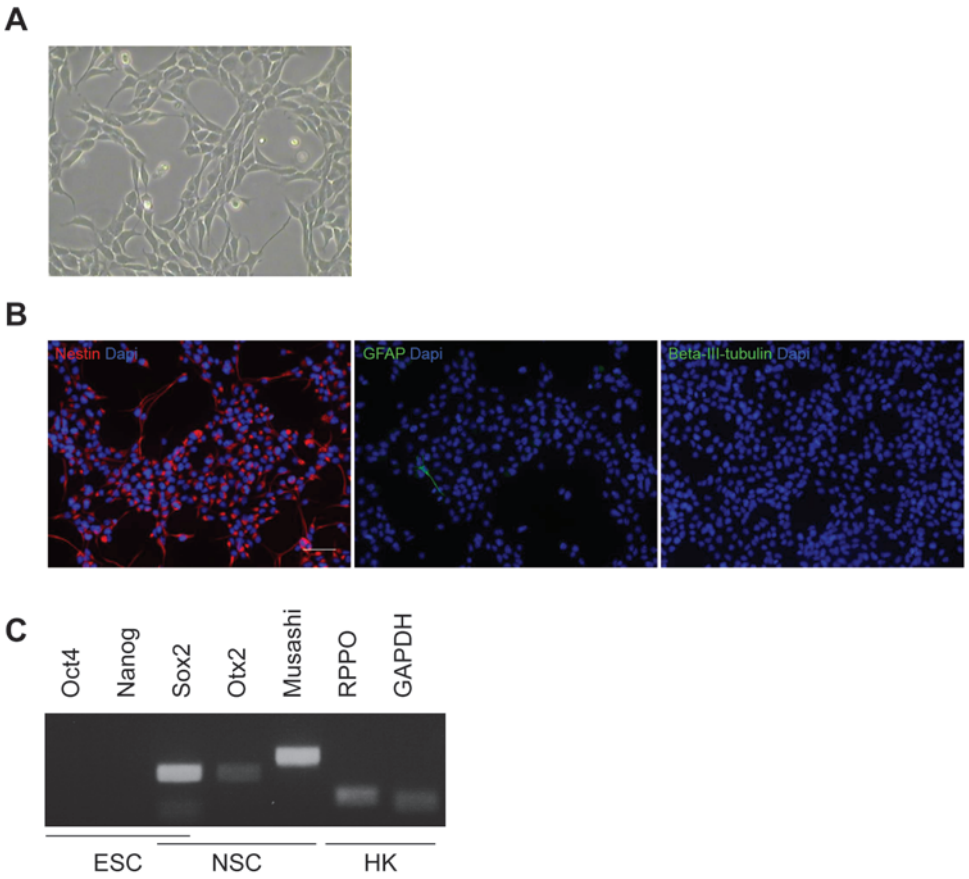

Figure 49. Characterisation of ESC derived RaLP KO NSCs. (A) Bright field image of cells at the end of the differentiation protocol. The cells are homogenous and possess the characteristic bipolar shape of NSCs. **(B)** Immunofluorescence for neural marker Nestin and markers for differentiated lineages GFAP for astrocytes and beta-III-tubulin for neurons. **(C)** RT-PCR for ESC markers Oct4 and Nanog, neural markers Otx2 and Musashi, and Sox2 which is expressed in both cell types. RPPO and GAPDH are housekeeper genes.

According to this differentiation protocol, the absence of RaLP does not prevent the determination of ESCs to NSCs. As RaLP expression is brain specific, we investigated further whether the absence of RaLP could have effects on the capacity of these cells to differentiation to more specified lineages, the astrocytes and neurons.

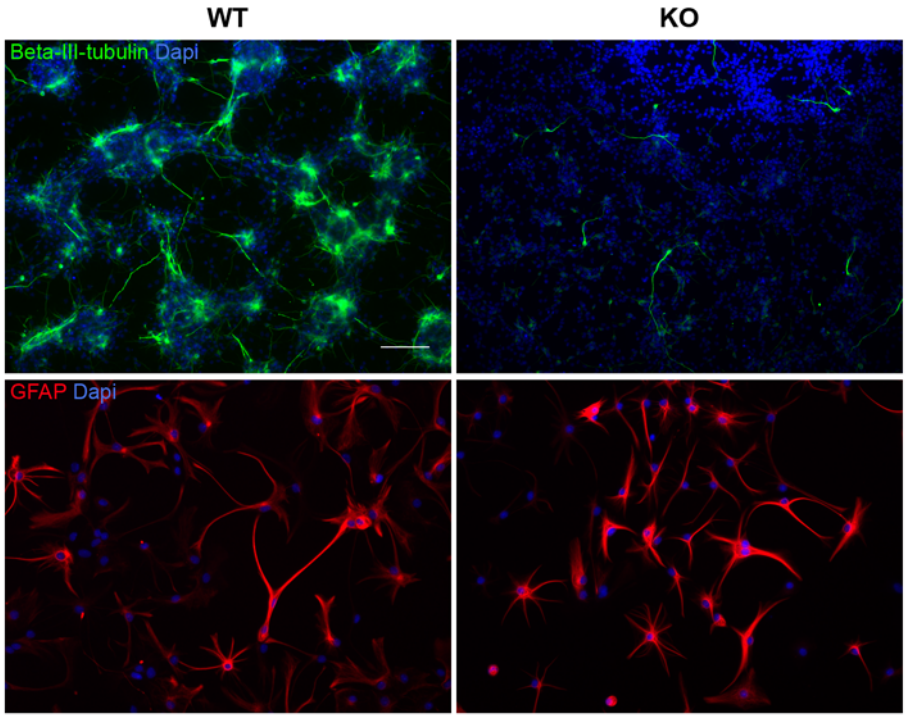

Figure 50. Astrocytic and neuronal differentiation of RaLP KO NSCs. Immunofluorescence for beta-III-butulin to visualise the neurons and GFAP for the astrocytes. RaLP KO NSCs showed a defect in neuronal differentiation whereas they did not show an impairment in the differentiation towards astrocytes.

The differentiation of RaLP WT, HT and KO cells towards neuronal fate showed that in the absence of RaLP there is a strong defect, as the number of neurons present in culture were dramatically lower in the KO (Figure 50). The KO neurons also showed less branching and as can be seen from the nuclear staining by DAPI, the cells have not organised into networks typically seen in neuronal cultures, that is evident in the WT: Interestingly, the capacity to undergo astrocytic differentiation did not seem perturbed in the RaLP KO culture, suggesting that RaLP might be involved specifically in the neuronal differentiation of NSCs.

5.2. Characterisation of RaLP WT and KO adult neural stem cells

The effects of defective neurogenesis in the absence of RaLP could be due to a result of altered NSCs that have formed due to a non-upregulation of RaLP in the first time window of differentiation. In order to distinguish whether this could have affected the final capacity of the derived NSCs, we decided to use an alternative system to see whether we could also observe a defect in neuronal differentiation. This system consists in the direct the isolation of NSCs from the subventricular zone of the adult brain. It was possible to derive KO neurospheres as efficiently as the WT, confirming the result of ESC differentiation to NSCs. The derived neurospheres were then characterised for growth *in vitro* and differentiation abilities.

When WT and KO neurospheres were plated and subjected to differentiation, the same neuronal defects were observed during the differentiation of RaLP KO NSCs. This protocol differs from the neuronal differentiation protocol used for ES derived NSCs, as both astrocytes and neurons are generated. The number of GFAP and beta-III-tubulin expressing cells were quantified by immunofluorescence. The number of astrocytes in the population did not differ between WT and KO (data not shown), whereas the percentage of neurons were significantly less in the KO (Figure 51).

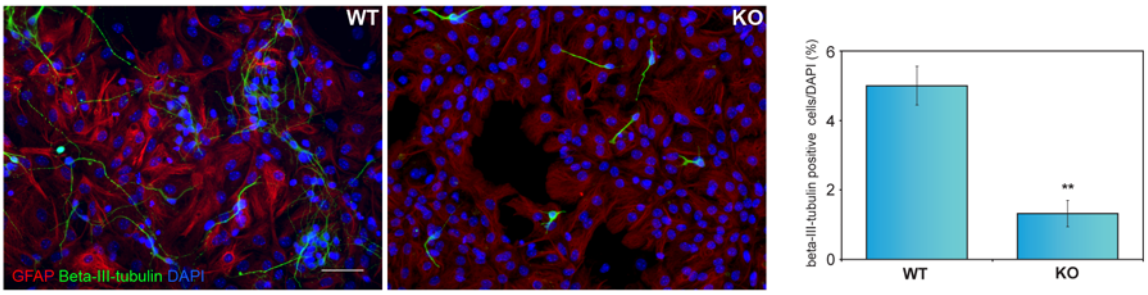

Figure 51. The differentiation of WT and KO adult NSCs isolated from the SVZ. The differentiation ability was analysed by immunofluorescence for neuronal marker beta-III-tubulin and astrocytic marker GFAP after 10 days of differentiation. The percentage of neurons in the cultures were calculated by counting the cells staining positive for beta-III-tubulin over the total number of cells by DAPI. Scale bar represents 50 μm. ** $p < 0.01$.

Neurons undergo migration during their differentiation process, and we asked whether there is a defect in migratory abilities in the absence of RaLP in this context, as previous studies in our laboratory have shown that the intereference of RaLP expression in metastatic melanoma cells abrogates this ability [12]. We employed two different techniques to measure migration: the Boyden chamber and wound healing assay, in the presence and absence of serum, EGF and FGF2. We did not observe any differences in the migratory abilities between the WT and KO (data not shown), therefore excluding this possibility as an explanation to the neuronal differentiation defects.

5.3. Characterisation of RaLP in the brain

The *in vitro* data seems to suggest a specific neuronal defect in the absence of RaLP. We examined how RaLP expression varies during postnatal development, as in mice the development of the brain is very intense during these stages with synaptogenesis. RaLP expression gradually increases during this processs suggesting that it also has a function during postnatal development of the brain.

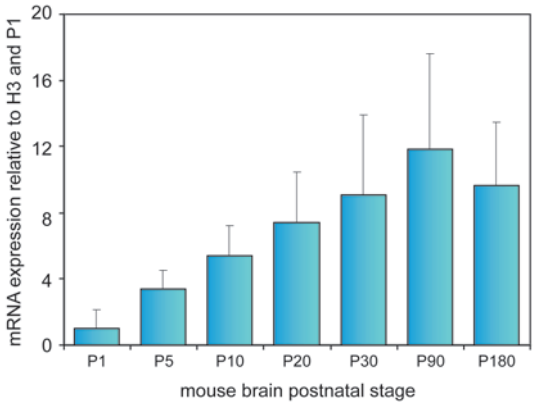

Figure 52. RaLP expression during postnatal synaptogenesis. QRT-PCR analysis for RaLP expression on postnatal mice brains at different stages P1, P5, P10, P20, P30, P90 and P180. Expression levels of RaLP are relative to histone H3 used as housekeeper gene and calibrated to P1 stage. Bars represent the means ± S.D. of triplicates.

Next, we decided to investigate whether this neuronal defect could also be seen *in vivo*. Adult brains were sectioned and stained for glial specific marker, GFAP and pan-neuronal marker, NeuN to analyse the proportions of these populations in the brain, however, there were no significant differences (data not shown) suggesting that RaLP probably enacts during the first stages of neuronal commitment from the neural stem cells/progenitors. Further characterisations of the brains are needed and are currently ongoing.

Discussion

This study revealed novel aspects on the role of ShcD/RaLP, a new member of the Shc family of adaptor proteins, in the context of development and the formation of early lineages. The physiological role of this member was unknown previously to this study and our results support its role in the determination of epiblast fate and in the proliferation of epiblast stem cells (EpiSCs). We showed that RaLP is expressed *in vivo*, in the epiblast of the preimplantation and peri-implantation embryo and *in vitro*, during epiblast formation in the embryoid body, neural differentiation and EpiSC derivation of embryonic stem cells (ESCs). This expression pattern was unique for this family member, underlining its specific role in this developmental context.

EpiSCs have been isolated from the early postimplantion embryo for the first time in 2007 and represent a new tool in the research field of pluripotency [59,60]. These cells are a functionally distinct type of pluripotent stem cell from mouse ESCs and are a developmentally relevant system to directly study the mechanisms involved in specification events that occur during gastrulation, that cannot be done with ESCs [120]. EpiSCs express the core pluripotency factors Oct4, Sox2 and Nanog, however they are not able to contribute to blastocyst chimeras. Interestingly, these cells are morphologically and molecularly more similar to human ESCs and yet, they are derived from the postimplantation embryo while human ESCs are derived from the preimplantation blastocyst [43], raising many questions regarding the true identity and *in vivo* counterpart of these pluripotent stem cell populations. There are still many questions that have yet to be answered on how pluripotency is determined and maintained in these cells through the specific signalling pathways.

The transition of the preimplantation epiblast to the postimplantation epiblast is very difficult to study *in vivo* due to their limited accessibility, quantity and low temporal

precision in this short window of time. The protocol recently published in 2009 by Guo and colleagues that allows the commitment of ESCs to EpiSC fate [78], provides a useful tool to dissect the mechanisms involved in this process. Furthermore, as described in the paper, these ES derived EpiSCs are comparable to the postimplantation derived EpiSCs, as their gene expression profiles and epigenetic markers are superimposible. We have shown in addition to this characterisation, that these cells can differentiate to embryoid bodies, providing a functional proof of their pluripotency. Through our studies on RaLP using this model system, we have analysed in detail the commitment of ESCs to epiblast fate and to our knowledge, we have described for the first time, a characteristic regulation of the pluripotency marker Oct4 and trophectoderm marker Cdx2 expression together with proliferation and apoptosis occurring during the differentiation and provided some insight into this uncharacterised process.

Firstly, we observed an intriguing pattern of the regulation of Oct4 during EpiSC establishment. We found that Oct4 levels are downregulated generally in the whole population during the first passages of differentiation (most evident at passage three). The overall downregulation is dramatic and it involves the majority of the cells and to an extent that it is difficult to argue that the low levels is simply because of the selection process. In fact, such a dramatic downregulation is not accompanied by an equally high extent of apoptosis, suggesting that ESCs must first downregulate Oct4 to undergo commitment to EpiSC fate and then upregulate it again when it has become committed. Immunofluorescence for Oct4 on control cells also support the FACS data as there is an overall decrease in Oct4 intensity at these passages even in the cells growing in the EpiSC-like colonies. This speculation is in line with the sudden increase in Oct4 levels at the following passage of differentiation (after two days), which cannot be due only to the proliferation of the few cells that have maintained Oct4 expression. This observation could be partially explained by the fact that Oct4 expression is regulated under different enhancer

elements [121]. In particular, ESCs use the distal enhancer while the proximal enhancer is used in the mouse postimplantation epiblast *in vivo* and has been found also by EpiSCs *in vitro* [75]. It has been shown that there is an enhancer switch during implantation and perhaps during this switch in enhancer usage *in vitro*, Oct4 expression is transiently downregulated. After this characteristic drop in Oct4 expression, by the following passage (typically by passage four or five of differentiation), Oct4 levels are increased overall in the population, indicating that the majority of the cells are pluripotent and have now committed to EpiSC fate, as can be seen by their morphology and their gene expression profile.

Our approach with the multiparameter FACS analysis allowed us to dissect in detail not only Oct4 expression, but also its regulation in conjunction with apoptosis and proliferation occuring within the differentiating population, providing a useful method to simultaneously assess several events. In the absence of RaLP, we found that the commitment of ESCs to EpiSC fate is deregulated. The RaLP KO ESCs manifested a similar pattern of Oct4 regulation during the differentiation as the RaLP HT, however the reconstitution of the pluripotent population after the drop in Oct4 levels is not as efficient as in the controls, with Oct4 levels remaining lower. The analysis of proliferation and cell cycle phases of the Oct4 positive and negative population provided some insight to this observation. ESCs are able to undergo rapid symmetric cell division and this is accomplished by a shortened G1 phase and a constitutively active cyclin E (cdk2) that is independent of cell cycle phase that allows to bypass the restriction checkpoint R in the early G1 phase [122]. In fact, our analysis confirmed that within the ESC population, almost all Oct4 positive cells have incorporated EdU and therefore are in the S phase of the cell cycle. This was observed for both the RaLP HT and the KO ESCs. The Oct4 negative cells present in ESC cultures are cycling slower, as most of them are EdU negative and according to the DNA content, they are in G0/G1 or G2/M phase. As the cells are induced

to differentiate, also the Oct4 negative cells show an increase in EdU uptake as this population also acquires the ability to proliferate. During later passages, when the Oct4 population is reconstituted, both the Oct4 positive and negative compartment in the HT continue to be proliferative with a clear subpopulation in the S phase, whereas in the KO there is a depletion of the proportion of cells in S phase even at passage four, indicating that in the absence of RaLP the Oct4 positive population are less proliferative. In fact, from these passages onwards, the time necessary to passage the KO cultures are approximately double that of the controls (every five to six days compared to every two days), indicating that the population is proliferating at a slower rate. This lower rate of proliferation was also confirmed by the lower growth curve of the KO during these passages. Even at late passages (passage 10), the RaLP KO EpiSC colonies are smaller in size and the majority of the population consists of Oct4 negative cells, suggesting that in this *in vitro* context the phenotype is not transient.

The FACS analysis also revealed an interesting general pattern of Oct4 regulation during the cell cycle of ESCs and this relation has not been described to date. We observed that there is an increase in Oct4 expression with respect to the DNA content of the cell by PI. This increase is non-linear, meaning that it cannot be simply accounted for the fact that the cell is preparing for division. This kind of profile is characteristic of genes involved in proliferation, such as c-Myc. This aspect could be interesting for further studies.

"It is the population as a whole that is regulated rather than individual cells" [123]. The concept of cells within a population possessing functional heterogeneity was first suggested by Till and McCulloch using simple biological system to trace the fate of cells within the population. In fact, recent studies have provided insightful information on the heterogenic nature of both embryonic stem and adult stem cells, suggesting that this property might be an intrinsic characteristic of these cells. Using ESCs as a population system, it was possible to observe the intrinsic nature of these cells and how they were not

a homogenous but a heterogenous population of cells in different states, according to their transcriptional status. One of the first trancription factors that was found to be differentially expressed within the ESC population was Nanog. Under standard culture conditions, approximately 80% of cells express Nanog, while the remaining population do not [124,125]. The Nanog low population expresses Gata6, which is a transcription factor important for primitive endoderm formation. Interestingly, this heterogeneity is not a phenomenon of the presence of two distinct populations in culture, as the isolation of these two populations and culturing them separately restored this distribution, demonstrating that these populations interconvert. This heterogeneity is not an *in vitro* phenomenon, as it has also been seen *in vivo*. In the blastocyst stage, the inner cell mass expresses in a mutually exclusive manner, Nanog and Gata6 [126]. Furthermore, reinforcing the idea of the how these intrinsic transcriptional control is sensitive to extracellular signals, the expression of these factors in this way has been linked to the MAPK pathway signalling through the Grb2 adaptor protein, as the deletion of Grb2 results in the uniform expression of Nanog in the ICM at the expense of Gata6, resulting in the absence of primitive endoderm formation.

We found that EpiSCs cultures are heterogenous cultures, consisting of Oct4 positive and negative cells, even at their steady state when the cultures are established. During the establishment of EpiSCs, we observed that the viable (cleaved Caspase-3 negative) Oct4 negative cells within the population are cells expressing the extraembryonic marker of the trophoblast lineage, caudal-type homeobox protein (Cdx2). In contrast to the Oct4 expressing cells that grow in tight contact with one another as colonies, the Oct4 negative cells are flattened, large and growing in isolation and they arise at the border of the colonies. These cells are proliferative as could be seen from the FACS analysis for EdU incorporation of the Oct4 negative cells, albeit at lower rates, co-exisiting with the Oct4 expressing cells. The heterogeneity of EpiSC cultures has been studied with respect to the

presence of primordial germ cells (PGCs) and visceral endoderm cells that are generated spontaneously [127]. We have provided evidence that during the establishment of EpiSCs, Cdx2 positive cells also emerge. Interestingly, RaLP seems to play an important role in the formation and maintenance of the Oct4 positive population as in its absence, the population is made up by a majority of Cdx2 expressing cells, as was evidenced by immunofluorescence. These cells have been further characterised by markers and express several others of the trophoblast lineage, such as Hand1, Gata3 and TEAD4, and their levels were higher in the KO at passage four. An interesting question arises from this observation. From which cells do these Cdx2 positive cells originate from? There are three possible scenarios: (i) these cells are generated from ESCs together with the EpiSCs during the differentiation, (ii) the cells derive from an intermediate population that is generated during the differentiation or, (iii) the cells are continuously delineated from the EpiSCs once they are present in the culture. The first scenario is quite controversial, as numerous and important studies have already shown that mouse ESCs rarely generate extraembryonic lineages. In order to obtain trophoblast cells from ESCs, most studies required the genetic manipulation of key transcription factors of trophoblast development such as the knockdown of Oct4 [113], overexpression of Cdx2 [114], knockout of Sox2 [128], and the genetic deletion of DNA methyltransferase Dnmt1 [117]. Up to date, only two studies have also shown that it is possible to generate trophoblast cells by the specific manipulation of cell culture conditions [115,116]. There is an observation that has been made during this study that could account for the second scenario. As described previously, during the early passages of differentiation there is an overall drop in Oct4 levels. This “physiological” downregulation could create a window of time during which these metastable cells that have not yet committed to EpiSC fate, to either initiate the commitment definitively to EpiSC, to differentiate to another cell type that can survive under these culture conditions or undergo cell death. It could be possible that these

intermediate cells that are no longer ESCs nor EpiSCs yet (as can be seen from their gene expression profile) that do not apoptose and are unable to upregulate Oct4, (as was seen from the FACS analysis) then differentiate. It is known that Oct4 represses the expression of Cdx2, and Cdx2 is rapidly upregulated upon Oct4 downregulation in ESCs [114]. Perhaps this momentary downregulation of Oct4 during the differentiation allows these Cdx2 expressing cells to emerge. And for several passages, these cells persist in culture, as they do have proliferative ability but the majority are eventually eliminated with progressive passaging, as by late passages (around passage 10) their presence is a minority. This was also suggested by preliminary observations showing the presence of few Cdx2 positive cells in the postimplantation embryo derived EpiSCs (data not shown).

It has been reported that mouse EpiSCs can differentiate into extraembryonic tissues upon their stimulation by bone morphogenetic protein (BMP4) and the inhibition of the activin receptor [60] and we have also shown that trophoblast markers are upregulated upon the EB differentiation of ES derived EpiSCs. BMP4 also promotes the differentiation of human ESCs, which are considered to be similar to mouse EpiSCs, to trophoblast fate [70]. Furthermore, a persistent fraction of Oct4 negative cells with flattened morphology around the human ESC colonies has been observed [129]. These reports do support the notion that the Cdx2 positive cells observed during the derivation of EpiSCs could derive from the EpiSCs themselves. However, this ability has never been described within the context of normal EpiSC culture conditions where Fgf2 and Activin A are continuously present. More specific experiments are needed to provide a definitive answer. Furthermore, as Cdx2 is also expressed later during development in the endodermal gut lineages, in order to firmly confirm the trophoblast identity of these cells, it would be important to characterise them with more specific markers expressed solely in trophoblast lineages such as MASH-2, Placental Lactogen 1 (PL-1) and Trophoblast specific protein alpha (Tpbpa/4311) at the protein level.

To clarify the origin of the Cdx2 positive cells, one approach that could be taken is to investigate the lineage segregation occurring during the differentiation by clonal analysis. This approach however, could be accompanied by many difficulties as EpiSCs do not possess high clonogenic capacities as the ESCs [60]. An alternative to this approach, although less stringent, is to use the EpiSCs with Oct4-GFP [78] to separate the GFP positive and negative cells (using stringent gating or double sorting methods) and culture them separately to monitor the emergence of Cdx2 expressing cells. This would certainly be an important question to address in order to understand the identity and differentiation capacities of ESCs and EpiSCs, and to dissect the function of RaLP in balancing the two subpopulations emerging in culture during the derivation of EpiSCs.

ESCs and EpiSCs are pluripotent cells and their self-renewal abilities are sustained by completely different mechanisms. This is an interesting aspect to investigate in terms of mechanisms underlying the regulation of signal transduction. For example, the same pathway that is responsible for triggering the differentiation of ESCs, the FGF/Erk pathway, is crucial for the maintenance of EpiSCs [59,60]. This implies that the pathway must be rewired in EpiSCs in order to be able to generate a different response upon the same stimulation. One possible mechanism to achieve this is by the differential expression of regulators of the pathway. As RaLP is expressed at very low levels in ESCs and is highly upregulated in EpiSCs and in the absence of RaLP we observed a defect in EpiSC commitment of ESCs, we believe that RaLP plays a role in the formation and maintenance of these cells and therefore is involved in the regulation of the pathways determining EpiSC fate and self-renewal. Although we have not yet conclusively dissected the pathway in which RaLP is implicated, our data have shown that the absence of RaLP during EpiSC formation results in an enhanced activation of the MAPK/Erk signalling pathway from passage two of differentiation when RaLP is upregulated. The higher levels of phospho-Erk1/2 seen in the RaLP KO cells during the differentiation could be a direct or indirect

effect. The kinetics of the higher levels of phospho-Erk1/2 was very similar to the timing of the appearance of Cdx2 positive cells in culture. One could argue that the enhanced levels mirrors the composition of the culture, as Cdx2 expression has been demonstrated to be downstream of high Erk1/2 activation, in fact, the overexpression of a constitutive active form of Ras proto-oncogene is sufficient to obtain Cdx2 expressing trophoblast cells from ESCs [118]. Furthermore, we observed by immunofluorescence that the large flattened cells growing in isolation show intense nuclear localisation signal of phospho-Erk1/2, suggesting that the non-EpiSC differentiated cells have higher levels of phospho-Erk1/2 than the EpiSCs. In addition, we showed that also in this *in vitro* context of the commitment of ESCs to EpiSC identity, Cdx2 levels were correlated to Erk activation since its attenuation by the inhibition of MEK, resulted in a downregulation of overall Cdx2 levels during the differentiation. Taken together, the data suggests that the enhanced Erk1/2 activation in the RaLP KO cultures could be due to the presence of more differentiated cells in the population compared to the HT. This indirect effect of higher MAPK/Erk activation could be due to the deregulation of a signalling pathway in which RaLP is involved that cross-talks with the MAPK/Erk. However, the possiblity that higher phospho-Erk1/2 levels could be a direct effect of the absence of RaLP cannot be excluded. In this case, RaLP would function as a negative regulator of this pathway and it could be responsible for fine-tuning the final levels of Erk1/2 signalling during the differentiation to promote epiblast fate and shield the cell from taking on an extraembryonic fate. Such inhibitory role of signal transduction has been described for many adaptor proteins, such as Ruk for PI3K signalling [130], Grb10 for PI3K and MAPK signalling [131] and as well as p66ShcA for Ras and MAPK activation [132,133]. One possible mechanism that could be envisioned to achieve the attenuation of MAPK signalling by RaLP, is the competitive sequestration of one of the positive transducers of this pathway such as the Grb2 adaptor protein. It has been reported that RaLP possesses an extra Grb2 binding site, compared to

the three binding sites present in the other Shc family members [22]. A dramatic increase in RaLP protein levels, as was seen by western blot during the formation of the EpiSC stage, together with its higher capacity to bind to Grb2, could result in the attenuation or inhibition of this signalling pathway by sequestering it from transducing the signal. This possibility would certainly be worth investigating, for example by the first testing the interaction of RaLP with Grb2 by immunoprecipitation and then to assess the importance of RaLP in the negative regulation of MAPK by knocking down Grb2 in the RaLP KO background.

Further studies are needed in order to assign the role of RaLP within a signalling pathway. To address this aspect, the postimplantation derived EpiSCs Oct4-GFP would be a valuable tool as it would allow us to directly investigate the immediate effects of the knockdown of RaLP on this pathway. Together with more detailed studies of the possible role of RaLP in MAPK/Erk1/2 signalling, there are two other candidate signalling pathways worth examining; the E-cadherin/β-catenin signaling and the BMP4/Smad pathway. The opposing effects of Ras-MAPK and the β-catenin signalling has been well studied for determining polarity in epithelial cells [134]. This study has demonstrated that prohibitin is necessary for MAPK/Erk activation and modulates cell adhesion and migration of epithelial cells. In the absence of prohibitin, more β-catenin is localized to the cell membrane at the level of the adherens junctions, resulting in less activation of its target genes. Interestingly, prohibitin has come up in our mass spectometry studies as a potential binding partner of RaLP (data not shown). Furthermore, our initial studies in the comparison of the glycogen synthase kinase 3β (GSK3β) activation, β-catenin and its target gene levels during the neural commitment of ESCs have shown that there is an upregulation of this signalling in the absence of RaLP during the time window corresponding to its expression (data not shown). It would be worth investigating whether RaLP could regulate the MAPK/Erk pathway by binding to and inhibiting prohibitin. The

absence of RaLP would result in an enhanced activation of Erk1/2, loss cell to cell contact and higher levels of β-catenin target genes, which would explain the phenotype we have observed.

The BMP4/Smad pathway is another example of a signalling pathway that plays opposing roles in ESCs and EpiSCs. In ESCs, it is important for promoting pluripotency together with the LIF/STAT pathway by repressing non-neural differentiation [68]. A recent study using embryoid bodies as a model system to study epiblast commitment of ESCs have shown that in the two day window of epiblast formation (corresponding to when RaLP is expressed) BMP4 switches its function from maintaining pluripotency to promoting non neural differentiation [47]. The possible involvement of RaLP in this pathway should also be investigated.

In the light of the studies using the ESC to EpiSC differentiation system, we obtained more information to better interpret previous experiments that did not allow us to understand the effects of the absence of RaLP. For example, the gene expression profiles during RaLP HT and KO ESCs during the EB differentation showed consistent differences on day two and three, of Oct4, Nanog and early germ layer marker levels between the genotypes. However, providing an explanation of the differential behavior of the markers was difficult in this context. The EB differentiation has recently been convincingly demonstrated to transit through the epiblast phase as it is possible to derive EpiSCs from day two of the differentiation [47]. If we apply our findings of the defect of proliferation of the pluripotent epiblast population that was observed in the absence of RaLP, we could speculate that perhaps in the context of the EB differentiation there is a similar defect. If this were true, it would mean that the pluripotent population cannot be sustained and proliferate as efficiently as in the HT and therefore result in the premature differentiation of the cells and hence the appearance of differentiated markers in anticipation and an immediate decrease in their expression (see Oct4, FGF5 and Brachyury expression). This is also in line with

what was observed with the neural commitment of ESCs, a protocol that has also just recently been shown to go through an epiblast stage and from which it is possible to derive EpiSCs (again, corresponding to the time-window of RaLP upregulation) [51]. Also in this context we observed a faster differentiation of cells depleted of RaLP starting from day two when RaLP is expressed.

The *in vivo* assay of the differentiation potential, the teratoma assay, showed similar observations as for the EB and NSCs differentiation of ESCs. We found that in the absence of RaLP, the teratomas are reduced in size and the tumours contained a higher proportion of differentiated cells compared to the nondifferentiated proliferative part of the tumour compared to the HT. This seems to suggest that the absence of RaLP confers a proliferative disadvantage to the pluripotent intermediate population and faster differentiation.

Despite the early expression of RaLP during development and the dramatic effects of its absence in the *in vitro* model of ESCs to EpiSCs transition, the RaLP KO mice are viable. This suggests that there are biochemical and/or functional compensatory mechanisms that enter to take part in the process in which RaLP is implicated. There are several possible scenarios that could be envisioned. The first more immediate one is the functional redundancy of a family member or its isoforms. For the latter, we checked carefully the expression of the two putative isoforms of RaLP by qRT-PCR during all the protocols that we have used for our studies and found that the levels of expression were very low that they can be considered not expressed (data not shown). Furthermore, we did not see any compensatory upregulation of both isoforms in the RaLP KO cells. The possible redundancy by another family member leaves us with only ShcA as the possible candidate, as the other two members ShcB and ShcC are not expressed during RaLP upregulation in epiblast formation. P66ShcA is an interesting member of the family to investigate, as in terms of protein structure and homology of sequence, it is the closest to RaLP.

Furthermore, the overexpression of p66ShcA was seen to result in the anticipation of neural differentiation of ESCs [119]. To explore this in more detail, it would be necessary to knockdown this Shc protein in the RaLP null background and perform the differentiation and analyse its effects. If the phenotype is even more striking, it might be worthwhile to consider generating a double KO mutant for p66ShcA and RaLP.

Functional compensation mechanisms confer, to a certain extent, plasticity and adaptability to the organism. Especially during embryogenesis, the embryo is surprisingly compliant to adversities, such as the removal of blastomeres or exposure to various environmental stressors. They have evolved adaptive mechanisms that allow them to override unfavourable condition in order to be able to continue development [135]. If the RaLP null embryos have a smaller epiblast that is not below the threshold that threatens the viability of the embryo, such functional compensation mechanisms could permit such embryos to develop to term. It would be interesting to examine the RaLP KO embryos at the blastocyst stage to investigate whether there is a higher ratio of trophoectoderm cells versus the epiblast.

In addition to these future studies, it would be important to confirm the results by the rescue of the RaLP KO phenotype. One approach would be to re-express RaLP in the RaLP KO ESCs and perform the ESC to EpiSC differentiation. However, considering that RaLP is not expressed in ESCs, its overexpression at this stage would result in a non-physiological reconstitution of this protein as it would be expressed precociously and this might not yield clear-cut results. Furthermore, as RaLP is a regulator of signal transduction, besides the timing of expression, physiological protein levels must also be achieved. The ideal system for the phenotype rescue would be to mimic correctly both the level and timing of expression and this could be achieved by introducing the BAC containing RaLP cDNA together with its regulatory elements into ESCs.

RaLP showed a characteristic bi-phasic pattern of expression during embryogenesis, as it is transiently expressed in the early epiblast then re-expressed during the formation of the neural tube and the development of the central and peripheral nervous system. This pattern of expression was recapitulated in the *in vitro* neurogenesis system, strongly suggesting that RaLP may also play a role in this process. In parallel to the characterisation of RaLP in EpiSC formation and maintenance, we also began to investigate its function in neurogenesis using our RaLP HT and KO ESCs and adult neural stem cells isolated directly from the brain. Both systems evidenced a specific defect in neuronal differentiation of the NSCs, in the absence of RaLP. The ESC derived NSCs however show some restrictions in their neuronal differentiation ability, as they have been shown to preferentially generate inhibitory GABAergic neurons *in vitro* [136]. Preliminary studies of brain sections by immunohistochemistry of our WT and KO mice however, did not show significant differences in the neuronal population in the brain (data not shown). We think that RaLP is probably involved in early onset of neuronal differentiation. Further studies are currently being investigated to clarify the role of RaLP in this context.

In summary, this study showed for the first time the involvement of the newest member of the Shc family of proteins, RaLP, in EpiSC formation and maintenance. Furthermore, we have described in detail the process of ESC commitment to EpiSC fate, which was not characterised before. We think that RaLP plays an important role in the switch of a key pathway/s involved in determining EpiSC identity and that the absence of RaLP perturbs the commitment process, resulting in an enrichment of the population of Oct4 negative and Cdx2 positive cells. This role is unique for this family member and provides an interesting insight in the mechanisms provided by an adaptor protein, that the cell has evolved to regulate signalling pathways in a cell specific manner.

Bibliography

1. Koch CA, Anderson D, Moran MF, Ellis C, Pawson T (1991) SH2 and SH3 domains: elements that control interactions of cytoplasmic signaling proteins. Science 252: 668-674.
2. Rossman MG (1981) Evolution of glycolytic enzymes. Philos Trans R Soc Lond B Biol Sci 293: 191-203.
3. Liu X, Brodeur SR, Gish G, Songyang Z, Cantley LC, et al. (1993) Regulation of c-Src tyrosine kinase activity by the Src SH2 domain. Oncogene 8: 1119-1126.
4. Sadowski I, Stone JC, Pawson T (1986) A noncatalytic domain conserved among cytoplasmic protein-tyrosine kinases modifies the kinase function and transforming activity of Fujinami sarcoma virus P130gag-fps. Mol Cell Biol 6: 4396-4408.
5. Haslam RJ, Koide HB, Hemmings BA (1993) Pleckstrin domain homology. Nature 363: 309-310.
6. Blaikie P, Immanuel D, Wu J, Li N, Yajnik V, et al. (1994) A region in Shc distinct from the SH2 domain can bind tyrosine-phosphorylated growth factor receptors. J Biol Chem 269: 32031-32034.
7. Seet BT, Dikic I, Zhou MM, Pawson T (2006) Reading protein modifications with interaction domains. Nat Rev Mol Cell Biol 7: 473-483.
8. Pelicci G, Lanfrancone L, Grignani F, McGlade J, Cavallo F, et al. (1992) A novel transforming protein (SHC) with an SH2 domain is implicated in mitogenic signal transduction. Cell 70: 93-104.
9. Migliaccio E, Mele S, Salcini AE, Pelicci G, Lai KM, et al. (1997) Opposite effects of the p52shc/p46shc and p66shc splicing isoforms on the EGF receptor-MAP kinase-fos signalling pathway. EMBO J 16: 706-716.
10. Pelicci G, Dente L, De Giuseppe A, Verducci-Galletti B, Giuli S, et al. (1996) A family of Shc related proteins with conserved PTB, CH1 and SH2 regions. Oncogene 13: 633-641.
11. Luzi L, Confalonieri S, Di Fiore PP, Pelicci PG (2000) Evolution of Shc functions from nematode to human. Curr Opin Genet Dev 10: 668-674.
12. Fagiani E, Giardina G, Luzi L, Cesaroni M, Quarto M, et al. (2007) RaLP, a new member of the Src homology and collagen family, regulates cell migration and tumor growth of metastatic melanomas. Cancer Res 67: 3064-3073.
13. Migliaccio E, Giorgio M, Mele S, Pelicci G, Reboldi P, et al. (1999) The p66shc adaptor protein controls oxidative stress response and life span in mammals. Nature 402: 309-313.
14. O'Bryan JP, Songyang Z, Cantley L, Der CJ, Pawson T (1996) A mammalian adaptor protein with conserved Src homology 2 and phosphotyrosine-binding domains is related to Shc and is specifically expressed in the brain. Proc Natl Acad Sci U S A 93: 2729-2734.
15. van der Geer P, Wiley S, Lai VK, Olivier JP, Gish GD, et al. (1995) A conserved amino-terminal Shc domain binds to phosphotyrosine motifs in activated receptors and phosphopeptides. Curr Biol 5: 404-412.
16. Schlessinger J, Lemmon MA (2003) SH2 and PTB domains in tyrosine kinase signaling. Sci STKE 2003: RE12.
17. Songyang Z, Shoelson SE, Chaudhuri M, Gish G, Pawson T, et al. (1993) SH2 domains recognize specific phosphopeptide sequences. Cell 72: 767-778.
18. Thomas D, Bradshaw RA (1997) Differential utilization of ShcA tyrosine residues and functional domains in the transduction of epidermal growth factor-induced mitogen-activated protein kinase activation in 293T cells and nerve growth factor-induced neurite outgrowth in PC12 cells. Identification of a new Grb2.Sos1 binding site. J Biol Chem 272: 22293-22299.

19. Okabayashi Y, Sugimoto Y, Totty NF, Hsuan J, Kido Y, et al. (1996) Interaction of Shc with adaptor protein adaptins. J Biol Chem 271: 5265-5269.
20. Conti L, De Fraja C, Gulisano M, Migliaccio E, Govoni S, et al. (1997) Expression and activation of SH2/PTB-containing ShcA adaptor protein reflects the pattern of neurogenesis in the mammalian brain. Proc Natl Acad Sci U S A 94: 8185-8190.
21. Sakai R, Henderson JT, O'Bryan JP, Elia AJ, Saxton TM, et al. (2000) The mammalian ShcB and ShcC phosphotyrosine docking proteins function in the maturation of sensory and sympathetic neurons. Neuron 28: 819-833.
22. Jones N, Hardy WR, Friese MB, Jorgensen C, Smith MJ, et al. (2007) Analysis of a Shc family adaptor protein, ShcD/Shc4, that associates with muscle-specific kinase. Mol Cell Biol 27: 4759-4773.
23. Yokote K, Mori S, Hansen K, McGlade J, Pawson T, et al. (1994) Direct interaction between Shc and the platelet-derived growth factor beta-receptor. J Biol Chem 269: 15337-15343.
24. Pelicci G, Giordano S, Zhen Z, Salcini AE, Lanfrancone L, et al. (1995) The motogenic and mitogenic responses to HGF are amplified by the Shc adaptor protein. Oncogene 10: 1631-1638.
25. Pronk GJ, McGlade J, Pelicci G, Pawson T, Bos JL (1993) Insulin-induced phosphorylation of the 46- and 52-kDa Shc proteins. J Biol Chem 268: 5748-5753.
26. Vainikka S, Joukov V, Wennstrom S, Bergman M, Pelicci PG, et al. (1994) Signal transduction by fibroblast growth factor receptor-4 (FGFR-4). Comparison with FGFR-1. J Biol Chem 269: 18320-18326.
27. Borrello MG, Pelicci G, Arighi E, De Filippis L, Greco A, et al. (1994) The oncogenic versions of the Ret and Trk tyrosine kinases bind Shc and Grb2 adaptor proteins. Oncogene 9: 1661-1668.
28. Lee MK, Pardoux C, Hall MC, Lee PS, Warburton D, et al. (2007) TGF-beta activates Erk MAP kinase signalling through direct phosphorylation of ShcA. EMBO J 26: 3957-3967.
29. Baldari CT, Telford JL (1999) Lymphocyte antigen receptor signal integration and regulation by the SHC adaptor. Biol Chem 380: 129-134.
30. Wary KK, Mainiero F, Isakoff SJ, Marcantonio EE, Giancotti FG (1996) The adaptor protein Shc couples a class of integrins to the control of cell cycle progression. Cell 87: 733-743.
31. Orsini F, Migliaccio E, Moroni M, Contursi C, Raker VA, et al. (2004) The life span determinant p66Shc localizes to mitochondria where it associates with mitochondrial heat shock protein 70 and regulates trans-membrane potential. J Biol Chem 279: 25689-25695.
32. Giorgio M, Migliaccio E, Orsini F, Paolucci D, Moroni M, et al. (2005) Electron transfer between cytochrome c and p66Shc generates reactive oxygen species that trigger mitochondrial apoptosis. Cell 122: 221-233.
33. Pelicci G, Troglio F, Bodini A, Melillo RM, Pettirossi V, et al. (2002) The neuron-specific Rai (ShcC) adaptor protein inhibits apoptosis by coupling Ret to the phosphatidylinositol 3-kinase/Akt signaling pathway. Mol Cell Biol 22: 7351-7363.
34. Troglio F, Echart C, Gobbi A, Pawson T, Pelicci PG, et al. (2004) The Rai (Shc C) adaptor protein regulates the neuronal stress response and protects against cerebral ischemia. Proc Natl Acad Sci U S A 101: 15476-15481.
35. Zhu Y, Parada LF (2002) The Molecular and Genetic Basis of Neurological Tumours. Nat Rev Cancer 2: 616-626.
36. Lai KM, Pawson T (2000) The ShcA phosphotyrosine docking protein sensitizes cardiovascular signaling in the mouse embryo. Genes Dev 14: 1132-1145.
37. Evans MJ, Kaufman MH (1981) Establishment in culture of pluripotential cells from mouse embryos. Nature 292: 154-156.

38. Martin GR (1981) Isolation of a pluripotent cell line from early mouse embryos cultured in medium conditioned by teratocarcinoma stem cells. Proc Natl Acad Sci U S A 78: 7634-7638.
39. Brinster RL (1974) The effect of cells transferred into the mouse blastocyst on subsequent development. J Exp Med 140: 1049-1056.
40. Martin GR, Evans MJ (1975) Differentiation of clonal lines of teratocarcinoma cells: formation of embryoid bodies in vitro. Proc Natl Acad Sci U S A 72: 1441-1445.
41. Bradley A, Evans M, Kaufman MH, Robertson E (1984) Formation of germ-line chimaeras from embryo-derived teratocarcinoma cell lines. Nature 309: 255-256.
42. Beddington RS, Robertson EJ (1989) An assessment of the developmental potential of embryonic stem cells in the midgestation mouse embryo. Development 105: 733-737.
43. Thomson JA, Itskovitz-Eldor J, Shapiro SS, Waknitz MA, Swiergiel JJ, et al. (1998) Embryonic stem cell lines derived from human blastocysts. Science 282: 1145-1147.
44. Doetschman TC, Eistetter H, Katz M, Schmidt W, Kemler R (1985) The in vitro development of blastocyst-derived embryonic stem cell lines: formation of visceral yolk sac, blood islands and myocardium. J Embryol Exp Morphol 87: 27-45.
45. ten Berge D, Koole W, Fuerer C, Fish M, Eroglu E, et al. (2008) Wnt signaling mediates self-organization and axis formation in embryoid bodies. Cell Stem Cell 3: 508-518.
46. Rathjen J, Rathjen PD (2001) Mouse ES cells: experimental exploitation of pluripotent differentiation potential. Curr Opin Genet Dev 11: 587-594.
47. Zhang K, Li L, Huang C, Shen C, Tan F, et al. (2010) Distinct funtions of BMP4 during different stages of mouse ES cell neural commitment. Development 137: 2095-2105.
48. Ying QL, Smith AG (2003) Defined conditions for neural commitment and differentiation. Methods Enzymol 365: 327-341.
49. Conti L, Pollard SM, Gorba T, Reitano E, Toselli M, et al. (2005) Niche-independent symmetrical self-renewal of a mammalian tissue stem cell. PLoS Biol 3: e283.
50. Abranches E, Silva M, Pradier L, Schulz H, Hummel O, et al. (2009) Neural differentiation of embryonic stem cells in vitro: a road map to neurogenesis in the embryo. PLoS One 4: e6286.
51. Sterneckert J, Stehling M, Bernemann C, Arauzo-Bravo MJ, Greber B, et al. (2010) Neural Induction Intermediates Exhibit Distinct Roles of Fgf Signaling. Stem Cells.
52. Gardner RL (1983) Origin and differentiation of extraembryonic tissues in the mouse. Int Rev Exp Pathol 24: 63-133.
53. Gardner RL, Beddington RS (1988) Multi-lineage 'stem' cells in the mammalian embryo. J Cell Sci Suppl 10: 11-27.
54. Tam PPL, Behringer RR (1997) Mouse gastrulation: the formation of a mammalian body plan. Mechanisms of Development 68: 3-25.
55. Rossant J, Tam PP (2009) Blastocyst lineage formation, early embryonic asymmetries and axis patterning in the mouse. Development 136: 701-713.
56. Tanaka S, Kunath T, Hadjantonakis AK, Nagy A, Rossant J (1998) Promotion of trophoblast stem cell proliferation by FGF4. Science 282: 2072-2075.
57. Kunath T, Arnaud D, Uy GD, Okamoto I, Chureau C, et al. (2005) Imprinted X-inactivation in extra-embryonic endoderm cell lines from mouse blastocysts. Development 132: 1649-1661.
58. Tesar PJ (2005) Derivation of germ-line-competent embryonic stem cell lines from preblastocyst mouse embryos. Proc Natl Acad Sci U S A 102: 8239-8244.
59. Tesar PJ, Chenoweth JG, Brook FA, Davies TJ, Evans EP, et al. (2007) New cell lines from mouse epiblast share defining features with human embryonic stem cells. Nature 448: 196-199.

60. Brons IG, Smithers LE, Trotter MW, Rugg-Gunn P, Sun B, et al. (2007) Derivation of pluripotent epiblast stem cells from mammalian embryos. Nature 448: 191-195.
61. Yan J, Tanaka S, Oda M, Makino T, Ohgane J, et al. (2001) Retinoic acid promotes differentiation of trophoblast stem cells to a giant cell fate. Dev Biol 235: 422-432.
62. Pera MF, Tam PPL (2010) Extrinsic regulation of pluripotent stem cells. Nature 465: 713-720.
63. Chou YF, Chen HH, Eijpe M, Yabuuchi A, Chenoweth JG, et al. (2008) The growth factor environment defines distinct pluripotent ground states in novel blastocyst-derived stem cells. Cell 135: 449-461.
64. Smith AG, Heath JK, Donaldson DD, Wong GG, Moreau J, et al. (1988) Inhibition of pluripotential embryonic stem cell differentiation by purified polypeptides. Nature 336: 688-690.
65. Niwa H, Burdon T, Chambers I, Smith A (1998) Self-renewal of pluripotent embryonic stem cells is mediated via activation of STAT3. Genes Dev 12: 2048-2060.
66. Mishina Y, Suzuki A, Ueno N, Behringer RR (1995) Bmpr encodes a type I bone morphogenetic protein receptor that is essential for gastrulation during mouse embryogenesis. Genes Dev 9: 3027-3037.
67. Winnier G, Blessing M, Labosky PA, Hogan BL (1995) Bone morphogenetic protein-4 is required for mesoderm formation and patterning in the mouse. Genes Dev 9: 2105-2116.
68. Ying QL, Nichols J, Chambers I, Smith A (2003) BMP induction of Id proteins suppresses differentiation and sustains embryonic stem cell self-renewal in collaboration with STAT3. Cell 115: 281-292.
69. Ying QL, Wray J, Nichols J, Batlle-Morera L, Doble B, et al. (2008) The ground state of embryonic stem cell self-renewal. Nature 453: 519-523.
70. Xu RH, Chen X, Li DS, Li R, Addicks GC, et al. (2002) BMP4 initiates human embryonic stem cell differentiation to trophoblast. Nat Biotechnol 20: 1261-1264.
71. Vallier L, Mendjan S, Brown S, Chng Z, Teo A, et al. (2009) Activin/Nodal signalling maintains pluripotency by controlling Nanog expression. Development 136: 1339-1349.
72. Xu RH, Sampsell-Barron TL, Gu F, Root S, Peck RM, et al. (2008) NANOG is a direct target of TGFbeta/activin-mediated SMAD signaling in human ESCs. Cell Stem Cell 3: 196-206.
73. Liu P, Wakamiya M, Shea MJ, Albrecht U, Behringer RR, et al. (1999) Requirement for Wnt3 in vertebrate axis formation. Nat Genet 22: 361-365.
74. Kunath T, Saba-El-Leil MK, Almousailleakh M, Wray J, Meloche S, et al. (2007) FGF stimulation of the Erk1/2 signalling cascade triggers transition of pluripotent embryonic stem cells from self-renewal to lineage commitment. Development 134: 2895-2902.
75. Greber B, Wu G, Bernemann C, Joo JY, Han DW, et al. (2010) Conserved and Divergent Roles of FGF Signaling in Mouse Epiblast Stem Cells and Human Embryonic Stem Cells. Cell Stem Cell 6: 215-226.
76. Stavridis MP, Collins BJ, Storey KG (2010) Retinoic acid orchestrates fibroblast growth factor signalling to drive embryonic stem cell differentiation. Development 137: 881-890.
77. Wakioka T, Sasaki A, Kato R, Shouda T, Matsumoto A, et al. (2001) Spred is a Sprouty-related suppressor of Ras signalling. Nature 412: 647-651.
78. Guo G, Yang J, Nichols J, Hall JS, Eyres I, et al. (2009) Klf4 reverts developmentally programmed restriction of ground state pluripotency. Development 136: 1063-1069.
79. Bao S, Tang F, Li X, Hayashi K, Gillich A, et al. (2009) Epigenetic reversion of post-implantation epiblast to pluripotent embryonic stem cells. Nature 461: 1292-1295.

80. Takahashi K, Yamanaka S (2006) Induction of pluripotent stem cells from mouse embryonic and adult fibroblast cultures by defined factors. Cell 126: 663-676.
81. Pera MF, Tam PP (2010) Extrinsic regulation of pluripotent stem cells. Nature 465: 713-720.
82. Nichols J, Smith A (2009) Naive and primed pluripotent states. Cell Stem Cell 4: 487-492.
83. Burdon T, Chambers I, Stracey C, Niwa H, Smith A (1999) Signaling mechanisms regulating self-renewal and differentiation of pluripotent embryonic stem cells. Cells Tissues Organs 165: 131-143.
84. Buehr M, Smith A (2003) Genesis of embryonic stem cells. Philos Trans R Soc Lond B Biol Sci 358: 1397-1402; discussion 1402.
85. Ying QL, Stavridis M, Griffiths D, Li M, Smith A (2003) Conversion of embryonic stem cells into neuroectodermal precursors in adherent monoculture. Nat Biotechnol 21: 183-186.
86. Papaioannou V. BR (2005) Mouse Phenotypes. A handbook of mutation analysis. New York: Cold Spring Harbor Laboratory Press.
87. Masui S, Nakatake Y, Toyooka Y, Shimosato D, Yagi R, et al. (2007) Pluripotency governed by Sox2 via regulation of Oct3/4 expression in mouse embryonic stem cells. Nat Cell Biol 9: 625-635.
88. Lu CC, Brennan J, Robertson EJ (2001) From fertilization to gastrulation: axis formation in the mouse embryo. Curr Opin Genet Dev 11: 384-392.
89. Longo L, Bygrave A, Grosveld FG, Pandolfi PP (1997) The chromosome make-up of mouse embryonic stem cells is predictive of somatic and germ cell chimaerism. Transgenic Res 6: 321-328.
90. Rebuzzini P, Neri T, Zuccotti M, Redi CA, Garagna S (2008) Chromosome number variation in three mouse embryonic stem cell lines during culture. Cytotechnology 58: 17-23.
91. Chambers I, Smith A (2004) Self-renewal of teratocarcinoma and embryonic stem cells. Oncogene 23: 7150-7160.
92. Niwa H (2007) How is pluripotency determined and maintained? Development 134: 635-646.
93. He Z, Li JJ, Zhen CH, Feng LY, Ding XY (2006) Effect of leukemia inhibitory factor on embryonic stem cell differentiation: implications for supporting neuronal differentiation. Acta Pharmacol Sin 27: 80-90.
94. Dang SM, Gerecht-Nir S, Chen J, Itskovitz-Eldor J, Zandstra PW (2004) Controlled, scalable embryonic stem cell differentiation culture. Stem Cells 22: 275-282.
95. Takahashi T, Lord B, Schulze PC, Fryer RM, Sarang SS, et al. (2003) Ascorbic acid enhances differentiation of embryonic stem cells into cardiac myocytes. Circulation 107: 1912-1916.
96. Yamada T, Yoshikawa M, Kanda S, Kato Y, Nakajima Y, et al. (2002) In vitro differentiation of embryonic stem cells into hepatocyte-like cells identified by cellular uptake of indocyanine green. Stem Cells 20: 146-154.
97. Wiles MV, Keller G (1991) Multiple hematopoietic lineages develop from embryonic stem (ES) cells in culture. Development 111: 259-267.
98. Ikeda W, Nakanishi H, Miyoshi J, Mandai K, Ishizaki H, et al. (1999) Afadin: A key molecule essential for structural organization of cell-cell junctions of polarized epithelia during embryogenesis. J Cell Biol 146: 1117-1132.
99. Wood HB, Episkopou V (1999) Comparative expression of the mouse Sox1, Sox2 and Sox3 genes from pre-gastrulation to early somite stages. Mech Dev 86: 197-201.
100. Nakamura T, Muraoka S, Sanokawa R, Mori N (1998) N-Shc and Sck, two neuronally expressed Shc adapter homologs. Their differential regional expression in the brain and roles in neurotrophin and Src signaling. J Biol Chem 273: 6960-6967.

101. Conti L, Sipione S, Magrassi L, Bonfanti L, Rigamonti D, et al. (2001) Shc signaling in differentiating neural progenitor cells. Nat Neurosci 4: 579-586.
102. Ying QL, Nichols J, Evans EP, Smith AG (2002) Changing potency by spontaneous fusion. Nature 416: 545-548.
103. Yang J, van Oosten AL, Theunissen TW, Guo G, Silva JC, et al. (2010) Stat3 activation is limiting for reprogramming to ground state pluripotency. Cell Stem Cell 7: 319-328.
104. Pease S, Braghetta P, Gearing D, Grail D, Williams RL (1990) Isolation of embryonic stem (ES) cells in media supplemented with recombinant leukemia inhibitory factor (LIF). Dev Biol 141: 344-352.
105. De Felici M, McLaren A (1982) Isolation of mouse primordial germ cells. Exp Cell Res 142: 476-482.
106. Saitou M, Barton SC, Surani MA (2002) A molecular programme for the specification of germ cell fate in mice. Nature 418: 293-300.
107. Payer B, Saitou M, Barton SC, Thresher R, Dixon JP, et al. (2003) Stella is a maternal effect gene required for normal early development in mice. Curr Biol 13: 2110-2117.
108. Lee KH, Li M, Michalowski AM, Zhang X, Liao H, et al. (2010) A genomewide study identifies the Wnt signaling pathway as a major target of p53 in murine embryonic stem cells. Proc Natl Acad Sci U S A 107: 69-74.
109. Strumpf D, Mao CA, Yamanaka Y, Ralston A, Chawengsaksophak K, et al. (2005) Cdx2 is required for correct cell fate specification and differentiation of trophectoderm in the mouse blastocyst. Development 132: 2093-2102.
110. Ralston A, Cox BJ, Nishioka N, Sasaki H, Chea E, et al. (2010) Gata3 regulates trophoblast development downstream of Tead4 and in parallel to Cdx2. Development 137: 395-403.
111. Yagi R, Kohn MJ, Karavanova I, Kaneko KJ, Vullhorst D, et al. (2007) Transcription factor TEAD4 specifies the trophectoderm lineage at the beginning of mammalian development. Development 134: 3827-3836.
112. Sood R, Kalloway S, Mast AE, Hillard CJ, Weiler H (2006) Fetomaternal cross talk in the placental vascular bed: control of coagulation by trophoblast cells. Blood 107: 3173-3180.
113. Niwa H, Miyazaki J, Smith AG (2000) Quantitative expression of Oct-3/4 defines differentiation, dedifferentiation or self-renewal of ES cells. Nat Genet 24: 372-376.
114. Niwa H, Toyooka Y, Shimosato D, Strumpf D, Takahashi K, et al. (2005) Interaction between Oct3/4 and Cdx2 determines trophectoderm differentiation. Cell 123: 917-929.
115. He S, Pant D, Schiffmacher A, Meece A, Keefer CL (2008) Lymphoid enhancer factor 1-mediated Wnt signaling promotes the initiation of trophoblast lineage differentiation in mouse embryonic stem cells. Stem Cells 26: 842-849.
116. Schenke-Layland K, Angelis E, Rhodes KE, Heydarkhan-Hagvall S, Mikkola HK, et al. (2007) Collagen IV induces trophoectoderm differentiation of mouse embryonic stem cells. Stem Cells 25: 1529-1538.
117. Ng RK, Dean W, Dawson C, Lucifero D, Madeja Z, et al. (2008) Epigenetic restriction of embryonic cell lineage fate by methylation of Elf5. Nat Cell Biol 10: 1280-1290.
118. Lu CW, Yabuuchi A, Chen L, Viswanathan S, Kim K, et al. (2008) Ras-MAPK signaling promotes trophectoderm formation from embryonic stem cells and mouse embryos. Nat Genet 40: 921-926.
119. Papadimou E, Moiana A, Goffredo D, Koch P, Bertuzzi S, et al. (2009) p66(ShcA) adaptor molecule accelerates ES cell neural induction. Mol Cell Neurosci 41: 74-84.
120. Chenoweth JG, McKay RD, Tesar PJ (2010) Epiblast stem cells contribute new insight into pluripotency and gastrulation. Dev Growth Differ 52: 293-301.

121. Yeom YI, Fuhrmann G, Ovitt CE, Brehm A, Ohbo K, et al. (1996) Germline regulatory element of Oct-4 specific for the totipotent cycle of embryonal cells. Development 122: 881-894.
122. Savatier P, Huang S, Szekely L, Wiman KG, Samarut J (1994) Contrasting patterns of retinoblastoma protein expression in mouse embryonic stem cells and embryonic fibroblasts. Oncogene 9: 809-818.
123. Till JE, McCulloch EA, Siminovitch L (1964) A Stochastic Model of Stem Cell Proliferation, Based on the Growth of Spleen Colony-Forming Cells. Proc Natl Acad Sci U S A 51: 29-36.
124. Chambers I, Silva J, Colby D, Nichols J, Nijmeijer B, et al. (2007) Nanog safeguards pluripotency and mediates germline development. Nature 450: 1230-1234.
125. Singh AM, Hamazaki T, Hankowski KE, Terada N (2007) A heterogeneous expression pattern for Nanog in embryonic stem cells. Stem Cells 25: 2534-2542.
126. Chazaud C, Yamanaka Y, Pawson T, Rossant J (2006) Early Lineage Segregation between Epiblast and Primitive Endoderm in Mouse Blastocysts through the Grb2-MAPK Pathway. Developmental cell 10: 615-624.
127. Hayashi K, Surani MA (2009) Self-renewing epiblast stem cells exhibit continual delineation of germ cells with epigenetic reprogramming in vitro. Development 136: 3549-3556.
128. Avilion AA, Nicolis SK, Pevny LH, Perez L, Vivian N, et al. (2003) Multipotent cell lineages in early mouse development depend on SOX2 function. Genes Dev 17: 126-140.
129. Bendall SC, Stewart MH, Menendez P, George D, Vijayaragavan K, et al. (2007) IGF and FGF cooperatively establish the regulatory stem cell niche of pluripotent human cells in vitro. Nature 448: 1015-1021.
130. Gout I, Middleton G, Adu J, Ninkina NN, Drobot LB, et al. (2000) Negative regulation of PI 3-kinase by Ruk, a novel adaptor protein. EMBO J 19: 4015-4025.
131. Dufresne AM, Smith RJ (2005) The adapter protein GRB10 is an endogenous negative regulator of insulin-like growth factor signaling. Endocrinology 146: 4399-4409.
132. Galandrini R, Tassi I, Morrone S, Lanfrancone L, Pelicci P, et al. (2001) The adaptor protein shc is involved in the negative regulation of NK cell-mediated cytotoxicity. Eur J Immunol 31: 2016-2025.
133. Ma Z, Liu Z, Wu RF, Terada LS (2010) p66(Shc) restrains Ras hyperactivation and suppresses metastatic behavior. Oncogene 29: 5559-5567.
134. Rajalingam K, Wunder C, Brinkmann V, Churin Y, Hekman M, et al. (2005) Prohibitin is required for Ras-induced Raf-MEK-ERK activation and epithelial cell migration. Nat Cell Biol 7: 837-843.
135. Power MA, Tam PP (1993) Onset of gastrulation, morphogenesis and somitogenesis in mouse embryos displaying compensatory growth. Anat Embryol (Berl) 187: 493-504.
136. Spiliotopoulos D, Goffredo D, Conti L, Di Febo F, Biella G, et al. (2009) An optimized experimental strategy for efficient conversion of embryonic stem (ES)-derived mouse neural stem (NS) cells into a nearly homogeneous mature neuronal population. Neurobiol Dis 34: 320-331.

Acknowledgements

First and foremost, I would like to thank Lusia Lanfrancone for giving me the opportunity to explore the intriguing world of stem cells and pluripotency. Thank you for your warm support and understanding throughout my PhD years.

Thank you to my co-supervisors, Giuseppe Testa and Friedrich Beerman for their advice. Thanks to our collaborators, Daniel Constam and Anja Dietze (EPFL) and Antonio Simeone (TIGEM) for their expertise.

A huge thank you to Mario Faretta, who joined us on this project that faced us with numerous challenges and provided an important helping hand. Thank you for your support and for all those interesting and fruitful discussions through which I really learned a lot.

Thank you to PierGiusppe Pelicci for the challenging discussions and insightful advice on the project and for sometimes turning things upside down to make me look at things from a different perspective.

Thank you to the Imaging Facility staff Dario Parazzoli, Simona Ronzoni and Anna Sciullo for their help. Thanks to the Real Time PCR Unit, especially Valentina for her work and for the fun chats. Thanks to Giovanni Mazzarol for his expertise immunohistochemistry analysis.

I want to thank a bunch of people at the IFOM-IEO Campus, who during the years became from colleagues to dear friends and who always had a smile and kind words to share: Ewa, Guenda, Lucy, Serena, Mirko, Cristina, Rodrigo, Rachel and Arianna.

Thanks to Laura for always being there for me and to Giancarlo for believing in me and convincing me to move to Milan to start this whole PhD adventure.

And Teo for being Teo and for providing the hilarious and much needed moments of “pause” as well as the shoulder to lean on in difficult moments. Things just wouldn’t have been the same without you here.

And to Thomas… words will not be enough to describe how important you are to me. So here, I just want to simply say thank you for everything, I am so lucky to have you. A huge hug and いろいろ本当にありがとう、to my family: my parents, Valentina and Guglielmo for supporting me and always cheering me on throughout these years.

Margherita.